BASIC AND APPLIED ASPECTS OF CHICKEN MACROPHAGE BIOLOGY

A Dissertation

by

WEN-KO CHOU

Submitted to the Office of Graduate and Professional Studies of
Texas A&M University
in partial fulfillment of the requirements for the degree of

DOCTOR OF PHILOSOPHY

Chair of Committee,	Luc R. Berghman
Committee Members,	Ciro A. Ruiz-Feria
	Morgan B. Farnell
	Nancy Ing
	Rosemary L. Walzem
	Waithaka Mwangi
Head of Department,	David Caldwell

December 2013

Major Subject: Poultry Science

ABSTRACT

The best way to prevent infectious disease is to directly establish mucosal immunity and also induce circulatory immunity to avoid pathogen invasion and spread. In our first study, we tested the hypothesis that a single mucosal or subcutaneous administration of antigen immunotargeted to chicken CD40 can effectively target antigen-presenting cells (APCs) of the mucosal associated lymphoid tissue (MALT) and induce specific mucosal sIgA and circulatory IgG. Levels of peptide-specific tracheal mucosa sIgA and circulatory IgG were measured on day 7 and 14 post-injection (p.i.) by ELISA. The results indicated that a single subcutaneous (s.c.) injection of anti-chCD40 guided 2C5-peptide complex not only induced a rapid and strong *systemic* peptide-specific IgG immune response, but also established a significant *mucosal sIgA* immune response.

Currently, only a few APC-specific markers and monoclonal antibodies (Mabs) are available in chicken. In mice, peritoneal exudate macrophages (PEMs) have been demonstrated to express the M1 phenotype and display CD62L on their cell surface, which allows them to migrate to lymph nodes as functional APCs. This makes chicken inflammatory-type PEMs a potential target for generating Mabs. However, the functional phenotype of chicken PEMs has yet to be elucidated. In the second and third study, we defined the functional phenotypes of two chicken macrophage models (Sephadex- and egg yolk-PEMs, S- and Y-PEMs) and generated Mabs against S-PEMs. The results suggest that arginase activity, the gene expression of the SOCS1/STAT3 axis, and the SOCS1/SOCS3 ΔCt ratio, cannot be used as markers for phenotyping in chickens as in mice. Our results demonstrate that S-PEMs skew the phenotype to the M1

side and Y-PEMs shift the phenotype towards M2. In the final study, three new Mabs against S-PEMs were generated. Two candidate antigens, CD110 and Fat 1, were recognized by 3F6 Mab using a 7-mer peptide phage display library. In mice, the expression of CXCR4 mRNA (a homing receptor) was shown to be up-regulated in the presence of thrombopoietin-CD110 ligation, which suggests that S-PEMs may have the potential to migrate to peripheral lymphoid tissues to function as APCs in the chicken.

The poultry industry needs a new generation of vaccines to induce both mucosal and systemic immunity in a single immunization. The antibody-guided CD40-targeting concept described in this dissertation provides a new platform that can fit this need.

TABLE OF CONTENTS

Page

LIST OF FIGURES

Page

LIST OF TABLES

Page

CHAPTER I

INTRODUCTION

Antigen-presenting cells [APCs; including dendritic cells (DCs), B-cells and macrophages] are the bridge between innate and adaptive immunity. Recently, a study from our lab described that an anti-CD40 Mab complexed with a synthetic peptide targeted to APCs can induce a rapid (as early as 4 days post-immunization) and robust systemic IgG response after a single subcutaneous (s.c.) injection (Chen *et al.*, 2012). The results demonstrate the capacity of a CD40-targeted vaccine to induce a rapid and strong immune response, and most importantly, the capability to induce an immunoglobulin class switch from IgM to IgG. Theoretically, via the interconnected common mucosal immune system, mucosal immunity can be established at the effector sites of the mucosal associated lymphoid tissue (MALT) by immunization at the MALT inductive sites through different routes of administration (Barr et al., 2005). **The first goal of this project** was to test the hypothesis that a single mucosal administration of antigens immunotargeted to chicken CD40 can effectively target APCs of the MALT and induce a specific sIgA response.

Given the success of targeting APCs via CD40 as a new vaccination strategy, extending our repertoire of new monoclonal antibodies (Mabs) against APCs is a topic that is of considerable interest to our laboratory (lab). Currently, only a few APC specific markers and Mabs are available in chicken, including CD40 and our anti-chCD40 monoclonal antibody (Mab). Ideally, our next target for Mab production would use recombinant DNA technology expressed chicken CD11c or CD205 as immunogen,

because in mammals, both receptors have been reported as useful targets for *in vivo* immunogen targeting (Cheong *et al*., 2010). However, the chicken CD11c ortholog has not been identified in the chicken genome, and repeated efforts to make antibodies against CD205 have failed due to a lack of a suitable immunogen. Therefore, we decided to use primary chicken macrophages as our immunogen and attempt to identify the cognate antigens of any resulting Mabs *post facto*. In chicken, peritoneal exudate macrophage (PEM) is the major (perhaps the only) source of obtaining relatively abundant of primary macrophage.

In mice, PEMs in the murine macrophage model have recently been shown to preferentially express M1 functional phenotypic characteristics by use of functional assays and gene expression profiling (Corna *et al*., 2010; Sica and Mantovani, 2012; Tenbusch *et al*., 2013). More importantly, mouse PEMs expressed CD62L (L-Selectin), supporting the idea that upon appropriate stimulation, PEMs may migrate to lymph nodes and serve as APCs (Ghosn et al., 2010; Idoyaga et al., 2011). These features make PEMs an ideal alternative antigen source (next to recombinant DNA technology), for the development of Mabs to explore the receptors expressed on APCs.

Chicken PEMs are the major source of macrophages for the study of chicken macrophage biology (Sabet *et al*., 1977). Currently, two chicken PEM models are available, *i.e.* those induced by i.p. injection of either Sephadex G-50 or by injection of yolk particles, and apparently these stimuli elicit cells with different features (Cornax *et al*., 2013; Golemboski *et al*., 1990). Sephadex-elicited PEMs (S-PEMs) display characteristics of an increasingly activated state over time and can effectively bind,

internalize, and degrade bacteria by lysosomal acid hydrolysis (Golemboski *et al*., 1990). Upon i.p. injection with egg yolk, chicken blood monocyte-derived macrophages express anti-inflammatory and scavenger properties (Cornax *et al*., 2013). However, it is still unclear if egg yolk skews the phenotype of macrophages towards M2, and the details of the functional phenotype and mechanism of macrophage polarization under the influence of egg yolk remains to be elucidated. Based on preliminary evidence, we hypothesize that S-PEMs display a phenotype skewed towards M1, the inflammatory phenotype, and that egg yolk-PEMs (Y-PEMs) display an M2 macrophage, anti-inflammatory (scavenger) phenotype. Since our ultimate goal is to verify the cell markers recognized by new Mabs produced against S-PEMs, it become important to gain information about the functional phenotypes of S-PEMs. At the same time, we also investigated the functional phenotypes of other primary chicken macrophage model, Y-PEMs. **Therefore as the second goal of this project**, we propose to evaluate the phenotypes of S- and Y-PEMs by use of functional assays (arginase and NOS activity assays) and through gene expression profiling. The plasticity of macrophage polarization was evaluated by exposing both sources of macrophages to LPS (a strong M1 inducing stimulant). The results were used as reference for the third part of this project: development and characterization of new Mabs against chicken peritoneal exudate macrophages.

In the **third and final goal of this study**, we tested the hypothesis that S-PEMs are a good source of antigen for Mab development against APCs, more specifically M1 macrophages. Cell surface markers are the mainstay for macrophage phenotyping

research. However, identifying chicken macrophage phenotypes remains a challenge because only a few Mabs against chicken macrophage cell surface markers are commercially available, and many well-identified murine cell markers, like F4/80 and CD11b, are not yet available in for use in the chicken.

CHAPTER II

REVIEW OF LITERATURE

Mucosal associated lymphoid tissue (MALT)

Mucosal surfaces are the major portal of pathogens entering the host and represent the largest surface area in contact with the external environment. Collectively, they can also be considered the largest organ system in vertebrates. Animal pathogens enter the host by breaching the mucosal barrier, which consists of specialized tissues characterized by an externally located epithelium and underlying connective tissue. Due to a continuous challenge by new materials and microorganisms, including pathogenic microorganisms, the immunological activity at the mucosal interface is intense. A wide variety of protective mechanisms are involved in mucosal immunity, ranging from barrier functions to highly specialized immune cells and organized lymphoid structures, in order to prevent the entry of pathogens through the mucosal tissues. In particular, the mucosal immune systems of the respiratory, digestive, and reproductive tract have highly developed lymphoid tissues called mucosal associated lymphoid tissue (MALT). MALT is stretched out from the gut [**g**ut-associated lymphoid tissue (GALT)] and respiratory [**n**asal (NALT) and **b**ronchus- (BALT) associated lymphoid tissues] tracts, to eyelids [**c**onjunctiva-associated lymphoid tissue (CALT)] in chickens.

The MALT represents a highly compartmentalized immunological system and functions essentially independently from the systemic immune apparatus (Holmgren and Czerkinsky, 2005). MALT is comprised of 1) *inductive* sites such as the Peyer's patches,

the appendix, and solitary follicles in the intestine (such as the cecal tonsils) where the immune response is initiated, and 2) diffuse *effector* sites such as the lamina propria of the gut where mucosal immune effector mechanisms (such as secretory IgA) are at work. The mucosal sites are interconnected by a *common mucosal immune system* (CMIS) enabling the induction and regulation of host-protective immunity against an invading pathogenic microorganism (Barr *et al.*, 2005; Holmgren and Czerkinsky, 2005). Secretory IgA is one of the critical components in mucosal effector function. It is largely protease resistant and can therefore bind and neutralize pathogens or toxins in the mucosal sites.

The Common Mucosal Immune System (CMIS)

The CMIS is an integrated pathway that allows communication between the *inductive* sites at the MALT and the diffuse mucosal *effector* sites, enabling the induction and regulation of host-protective immunity against pathogenic microorganisms. The CMIS has been well defined in mammals, and an overview of the system is presented in Fig. 1. The mechanism of CMIS starts with antigen transportation. Luminal antigens are transcytosed to the MALT *inductive* sites by adsorptive epithelial cells or microfold (M-) cells that are present in the epithelium overlaying the lymphoid follicles at the *inductive* sites. Upon transcytosis, those antigens are directly captured by antigen-presenting cells [APCs; including dendritic cells (DCs), B-cells, and macrophages]. M-cells have special properties for the transportation of antigens across the epithelial barrier (epithelial cells held together by tight junctions) (Neutra and Kozlowski, 2006). APCs (a DC in Fig. 1)

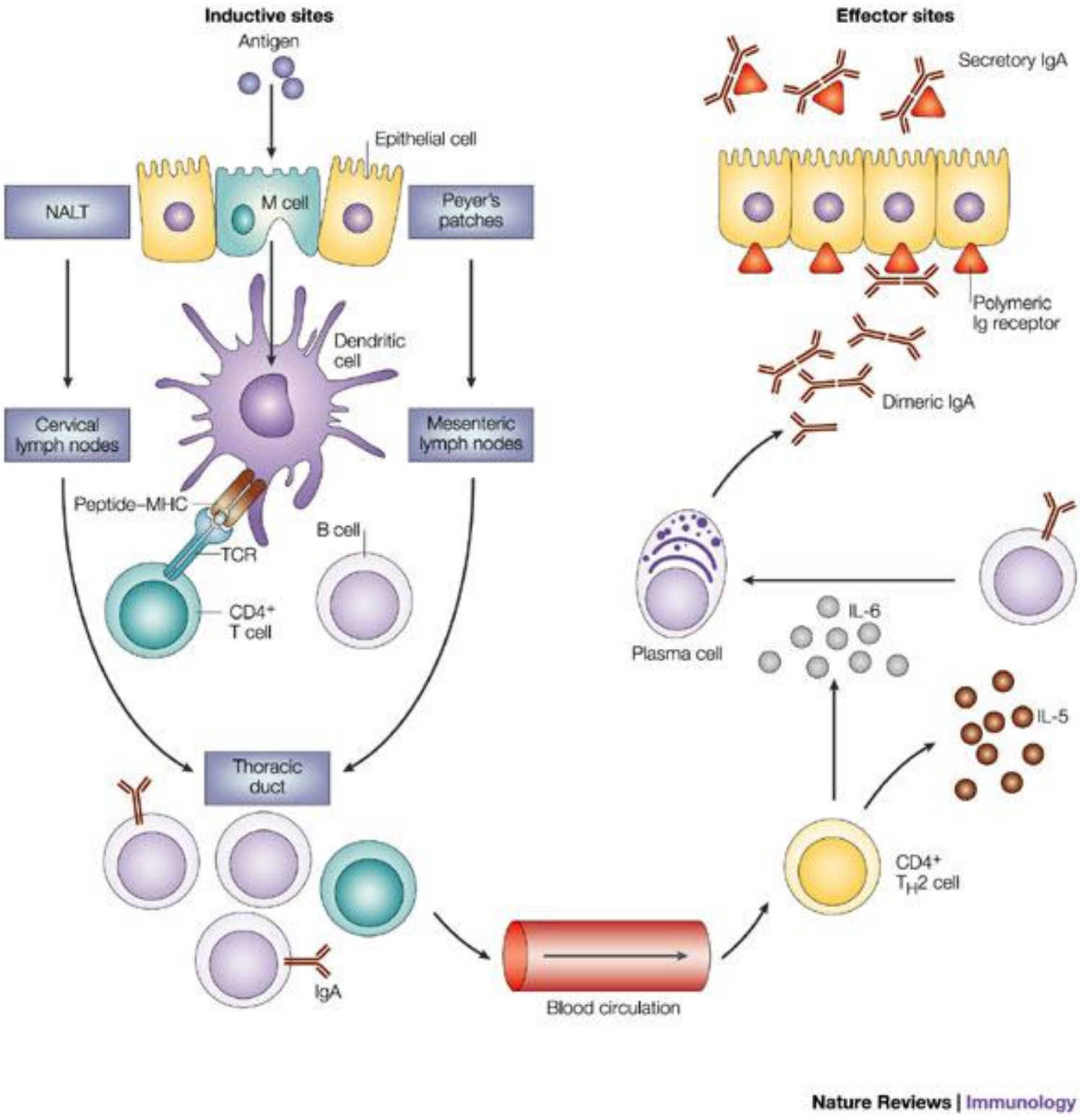

Figure 1. The common mucosal immune system (Barr *et al*., 2005). The common mucosal immune system is an integrated pathway that connects the mucosal *inductive* sites (*e.g.* Peyer's patches) and *effector* sites in MALT (*e.g.* intestinal lamina propria). Luminal antigens are transcytosed to the MALT *inductive* sites by adsorptive epithelial cells or microfold (M) cells. Upon transcytosis, those antigens are directly captured by antigen-presenting cells [APCs; including dendritic cells (DCs), B-cells, and macrophages]. Dendritic cells process and present antigen to $CD4^+$ T-cells. Activated $CD4^+$ T-cells temporally express CD154 on their cell surface allowing them to engage with CD40 expressing B-cells. CD40-CD154 ligation stimulates B-cell differentiation and class-switching from IgM- to IgA-committed B-cells. IgA^+ B-cells rapidly migrate from *inductive* sites to peripheral lymph nodes through the efferent lymphatics. Finally, under the influence of chemokines produced in the local microenvironment, antigen-specific $CD4^+$ T-cells and IgA^+ B-cells start to express homing receptors, such as CCR10, and migrate to *effector* sites through the thoracic duct and the blood circulation. IgA^+ B-cells and plasmablasts then differentiate into IgA-producing plasma cells in the presence of interleukin-5 (IL-5) and IL-6, which are produced by T helper 2 (T_H2) cells, and they subsequently produce dimeric forms of IgA. These dimeric forms of IgA then become secretory IgA (sIgA) by binding to polymeric Ig receptors, becoming the secretory component in the process of secretory IgA formation. Secretory IgA are displayed on the monolayer of epithelial cells lining the mucosa.

process and present antigens to conventional $CD4^+$ and $CD8^+$ αβ T-cells in the follicles located at the *inductive* sites. Certain antigens may also be processed and presented directly to neighboring intra-epithelial T-cells and natural killer (NK) cells with limited repertoire diversity, which then results in the suppression of a specific immune response (Holmgren and Czerkinsky, 2005). $CD4^+$ T cells are activated by pathogens harboring motifs that are sensed as danger signals (danger-associated molecular patterns, or DAMPS) delivered by DCs. Activated $CD4^+$ T cells then temporally express CD154 on their cell surface and engage with CD40 expressed on B-cells. The engagement of CD154 and CD40 induces class-switching, affinity maturation, and proliferation of B-cells, thereby enhancing the terminal differentiation process from IgM-producing B-cells to IgA- or IgG-committed B-cells in the germinal center (GC) of the lymphoid follicle (Iwasaki, 2007). B-cells rapidly migrate from *inductive* sites to the regional peripheral lymph nodes through the efferent lymphatics.

B-cell homing to mucosal and peripheral tissues is mediated by specific combinations of chemokine receptors and adhesion molecules. After encountering antigen in the mucosal inductive sites, the B-cell is activated. This results in the up-regulation of CCR10 and expression of α4β1 integrin, which mediates attraction to CCL28 and VCAM-1 respectively, on various effector sites of BALT, NALT, and GALT (Fig. 2) (Macpherson *et al*., 2008). Within the GALT, the activation of B- cells additionally induces strong expression of CCR9 and α4β7, directing homing back to the effector sites in GALT, which express CCL25 and MAdCAM-1 (Fig. 2). Shared paring of homing receptors and addressins explain how activated IgA-producing lymphocytes from one

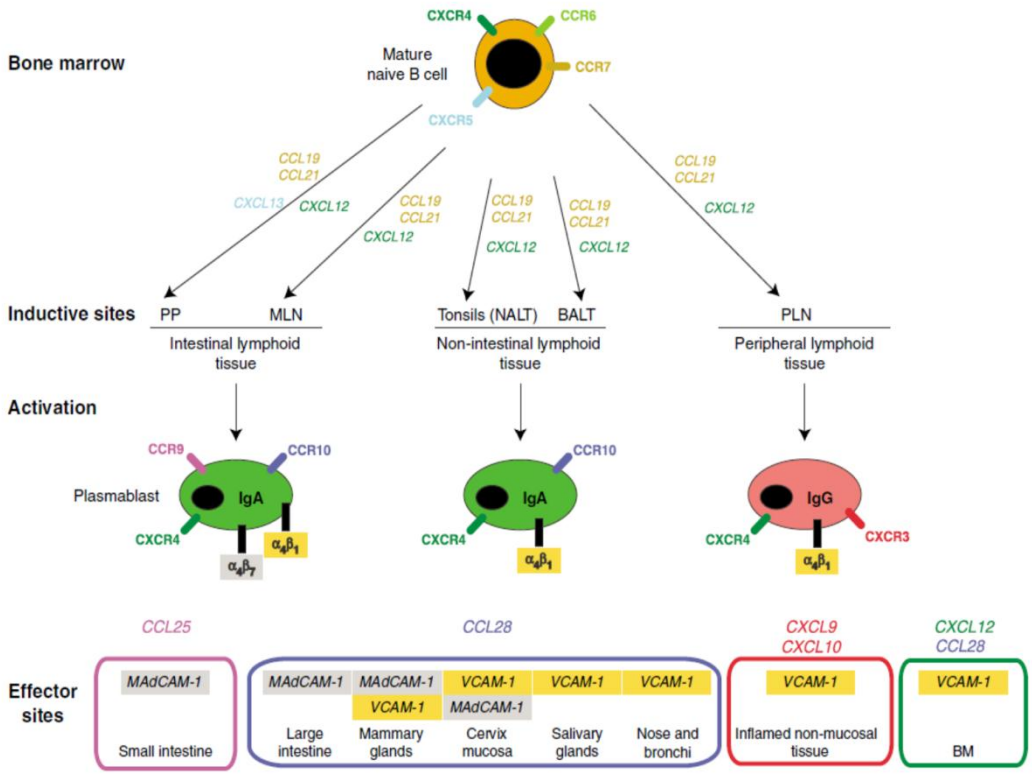

Figure 2. Mechanism of B-cell homing (Macpherson *et al*., 2008). B-cell homing to mucosal and peripheral tissues is mediated by specific chemokine receptors (homing receptors) and adhesion molecules (addressins). In general, IgA^+ B-cells induce CCR10 and α4β1 integrin expression, mediating attraction to CCL28 and VCAM-1 that are expressed in specific target tissues (*effector* sites), respectively.

mucosal inductive site can populate other effector sites with IgA-producing cells. It is this phenomenon that gave rise to the concept and terminology of a "**common mucosal immune system**."

Finally, under the influence of chemokines produced in the local microenvironment as mentioned above, antigen-specific $CD4^+$ T-cells and IgA^+ B-cells start to express homing receptors and migrate to *effector* sites (such as the lamina propria in the intestine) through the thoracic duct and blood circulation. IgA^+ B-cells and plasmablasts then differentiate into IgA-producing plasma cells in the presence of interleukin-5 (IL-5) and IL-6, which are produced by T helper 2 (T_H2) cells, and they subsequently produce dimeric forms of IgA. These dimeric forms of IgA then become secretory IgA (sIgA) by binding to polymeric Ig receptors, becoming the secretory component in the process of secretory IgA formation. Secretory IgA are displayed on the monolayer of epithelial cells lining the mucosa (Barr et al., 2005; Holmgren and Czerkinsky, 2005).

Compared to mammals, chickens lack well-organized, encapsulated lymphoid nodes; however, they developed diffuse lymphoid aggregations (nodules) instead (Muir *et al*., 2000). Despite the anatomical and organizational differences, a similar gateway has been reported (Muir *et al*., 2000; Smialek *et al*., 2011). The structure of mucosal *inductive* sites in chicken (*e.g.* Peyer's patches) is similar to those in mammals (Befus *et al*., 1980). IgA^+ B-cell trafficking through the circulation between mucosal *inductive* and *effector* sites in GALT or between the Harderian gland and ceca tonsils has also been observed (Akaki *et al*., 1997; Muir *et al*., 2000). The cellular traffic between GALT and systemic sites, including bone marrow and spleen, has also been reported

CD40

CD40, an integral membrane glycoprotein belonging to the TNF-receptor super family, is a co-stimulatory molecule and found on all the professional APCs, including B-cells, macrophages, and dendritic cells (van Kooten and Banchereau, 2000). CD40 and its immunomodulating ligand, CD154 (CD40L), play essential roles in the cell immune response. CD154 is transiently expressed on activated $CD4^+$ T-cells and the ligation of CD154 to the CD40 receptor on APCs provides the critical signal required for downstream events, such as APC activation. The activation of APCs results in up-regulation of MHC-II and CD40 expression, increased expression of CD80/86, enhanced production of cytokines (mostly IL-12), and increased cross-priming of exogenous antigens to cytotoxic T-cells (Grewal and Flavell, 1996; Hernandez et al., 2007; Noelle, 1996). These outcomes are critical for optimal priming and expansion of antigen-specific effector and memory T-cells, B-cell responses, and immunoglobulin class switching (Gordon and Pound, 2000). It has been clearly demonstrated that a primary defect in CD40-CD154 engagement is associated with human hyper-IgM syndrome, also known as immunoglobulin class switch recognition (CSR) deficiencies, and immune deficiencies found in CD4 knockout mice (Callard et al., 1993; Monson et al., 2001). CD40-CD154 deficient mice also exhibit defects in both humoral and the cellular immune responses, such as an impaired ability of APCs to deliver enhanced antigen presentation to cytotoxic T-cell (Carlring *et al*., 2011).

In mammals and chicken, anti-CD40 Mabs and recombinant CD154 have been successfully used to mimic T-cell help (*i.e.* to exert “agonistic” biological activities), and

to thus manipulate the activity of APCs, both *in vitro* and *in vivo* (Bennett et al., 1998; Chen et al., 2010a; Kothlow et al., 2008). In mice, agonistic monoclonal antibodies (Mabs) against (mouse) CD40 have also been shown to directly mimic T-cell help *in vivo*, in response to both T-cell dependent and independent antigens (Barr and Heath, 1999; French *et al*., 1999). Direct mimicking of T-cell help to B-cells by agonistic anti-CD40 Mabs may have therapeutic value in T-cell deficiency syndromes such as AIDS and hyper-IgM syndrome (Barr *et al*., 2003). Recently, agonistic CD40 Mabs were reported to offer new therapeutic opportunities against cancer by activating APCs and promoting anti-tumor T-cell responses, and by fostering cytotoxic myeloid cells with the potential to control cancer in the absence of T-cell immunity (Khong *et al*., 2012; Vonderheide and Glennie, 2013). The role of CD40 in lymphocyte migration has been discussed in the murine model by (von Bergwelt-Baildon et al., 2006). CD40-activated B-cells can be cellular adjuvants: they can prime naïve T-cells, expand memory T-cells, and stimulate their migration toward secondary lymphoid tissues. B-cells displaying activated CD40 signaling have been reported to express homing receptors such as CD62L, CCR7/CXCR4, and CD11a/CD18, which are crucial for homing to secondary lymphoid tissues. Moreover, soluble polyclonal anti-CD40 has been described to induce CCR10 expression on memory B-cells *in vitro* in mammals (Bernasconi *et al*., 2002). This is important because CCR10 is a homing receptor on IgA-secreting B-cells.

Agonistic anti-CD40 Mabs can be immuno-potentiators when chemically conjugated with antigen, and the adjuvant effect can be attained against any physically attached antigen, inducing antigen-specific immune responses in both mammals and chickens

(Barr *et al.*, 2006; Barr *et al.*, 2003; Chen *et al.*, 2012; Hatzifoti and Heath, 2007). Recently, a study from our lab described that an APC-targeting anti-CD40 Mab complexed with a synthetic peptide can induce a rapid and robust systemic IgG response after a single subcutaneous (s.c.) injection (Chen *et al.*, 2012). The result demonstrates the capacity of a CD40-targeted immunogen to induce a rapid and strong immune response, and most importantly, the capability to induce immunoglobulin class switching from IgM to IgG.

Antibody-guided vaccination targeting CD40

While there is great potential for novel vaccines based on recombinant proteins and synthetic peptides, such antigens often lack the immunogenicity of whole, killed pathogens used in traditional vaccines. Therefore, development of potent immunological adjuvants with low reactogenicity and high potential to enhance humoral immune responses are needed (Barr *et al.*, 2003). Arguably one of the most successful strategies to attain this goal consists of attaching the antigen to an antibody against a co-stimulatory cell surface receptor expressed by APCs, such as CD40 (Barr et al., 2005). A novel strategy of vaccine development using agonistic anti-CD40 antibody Mabs, was reported to act directly on APCs, resulting in this desired combination of low reactogenicity and high immunogenicity. This strategy was reportedly able to enhance humoral immune responses 1,000-fold compared with the use of an aluminum based adjuvant, and avoided the inflammatory side effects induced by most adjuvants (Barr et al., 2005; Hamzah et al., 2008). Agonistic anti-CD40 antibodies not only target antigen

delivery and activate B-cells, but also induce antibody class-switching. Murine and human naïve B-cells can be activated with anti-CD40 Mabs or CD40L (CD154) to undergo class switch recombination *in vitro* (Peterson et al., 2006). This is crucial, because IgA is readily transported across the intestinal mucosa and is endowed with effector properties that are critical for the local humoral immune response (Ravn et al., 2007).

Macrophages

Macrophages belong to the mononuclear phagocyte system and play a crucial role in both the innate and adaptive immune system. Moreover, macrophages fulfill homeostatic functions beyond their role in defense, such as tissue remodeling during ontogenesis and orchestration of metabolic functions (Sica and Mantovani, 2012). Macrophages originate from myeloid (MP) committed precursors derived from bone marrow hematopoietic stem cells. Under the influence of granulocyte macrophage colony stimulating factor (GM-CSF), MPs differentiate into monocyte precursors first, which will then further differentiate into monocytes. Finally, monocytes leave the bone marrow and enter the blood circulation. After about one day (in humans) or three days (in chickens and mice) of patrolling in the blood circulation, monocytes migrate and seed various tissues and organs; upon migration, they subsequently differentiate into macrophages (Geissmann *et al*., 2010; Qureshi *et al*., 2003; Tacke and Randolph, 2006).

Macrophage activation and polarization

Phenotyping cells in the mononuclear phagocyte system, which includes macrophages and dendritic cells (based on the expression of cell surface markers such as CD11b, CD68, and F4/80), has been the mainstay of macrophage characterization in the murine model (Murray and Wynn, 2011a). In contrast to the progress in the murine model, corresponding avian subsets are yet to be elucidated due to the fact that very few monoclonal antibodies (Mabs) against markers expressed by avian mononuclear phagocytes are available. M1 macrophage refers to macrophages that have been exposed to Toll-like receptor (TLR) ligands/interferon-γ (IFN-γ). They not only possess potent microbicidal properties through the production of NO and reactive oxygen intermediates, but also promote strong interleukin-1 (IL-1), IFN-γ, and IL-12-mediated Th1 responses through secretion of pro-inflammatory cytokines. In contrast, M2 macrophages produce anti-inflammatory cytokines, such as IL-4/IL13 and IL-10, and are mainly associated with Th2 effector functions, such as anti-parasitic activity and tissue repair through production of polyamines and proline (Sica and Mantovani, 2012).

In the mouse, M2 macrophages can be further divided into three subpopulations: M2a, (after exposure to IL-4/13), M2b (after exposure to immune complexes in combination with IL-1β or LPS), and M2c (induced by IL-10, tumor growth factor- β (TGF-β) or glucocorticoids) (Martinez *et al*., 2009). M2 macrophages also synthesize arginase, an enzyme that inhibits NO production and allows the cells to produce ornithine, a precursor of polyamines and proline, instead (Chang *et al*., 1998). Interestingly, although M1 and M2 macrophages display distinct phenotypes, the essential metabolic substrate

that drives M1 and M2 macrophages through different pathways is the same amino acid L-arginine (Stempin *et al*., 2010). Chicken HD11 cells produce abundant NO and secrete pro-inflammatory cytokines upon exposure to Toll-like receptor (TLR) ligands, or pathogens such as *Campylobacter jejuni* (Smith *et al*., 2005). However, the polarization of avian primary macrophages has yet to be addressed in detail (He *et al*., 2011).

Gene markers in macrophage phenotyping

Recently, various genes have been reported as being preferentially expressed in either M1 or M2 macrophages (Table 1). These observations would be particularly useful if they could be extended to chicken macrophages, as the equivalent of some reliable mammalian macrophage markers does not exist in chicken.

SOCS3 *vs.* SOCS1

Suppressor of cytokine signaling (SOCS) molecules are a family of intracellular proteins, several of which have emerged as feedback inhibitors of the Janus kinase (JAK)/Signal Transducer and Activator Transcription (STAT) pathway and play key roles as the physiological regulators of cytokine responses (Qin *et al*., 2012). Recently, the role of SOCSs has been investigated in murine macrophages. SOCS1, but not SOCS3, was induced rapidly in macrophages in response to stimulation with the anti-inflammatory cytokines IL-4 and IL-13 *in vitro*. A similar induction was observed in

Table 1 Gene markers used in macrophage phenotyping in mammalian species

Pro-inflammatory	Anti-inflammatory ("scavenger")
M1 macrophage	M2 macrophage
SOCS3	SOCS1
iNOS	Arginase
STAT1	STAT3
FtH	TfR
Ratio	
SOCS1/SOCS3 (the higher the ratio, the more "M1 like"**)** **Arg/iNOS** (the higher the ratio, the more "M1-like")	

peritoneal macrophages following i.p. infection of mice with the parasitic nematode *Brugia malayi (Briken and Mosser, 2011)*.

In SOCS1-knocked down mice, IL-4 failed to induce robust induction of arginase expression (Dickensheets *et al*., 2007). In addition macrophages from SOCS1 knockout mice also produced increased levels of TNF, IL-12, IFN-γ, and NO in response to stimulation with TLR-ligands (Briken and Mosser, 2011). Resting macrophages express low to undetectable levels of SOCS1, but the gene is induced rapidly following stimulation with IL-4/IL-13. SOCS-1 is also involved in the induction of arginase in M2 macrophages. SOCS3 plays a crucial role in inhibiting STAT3 activation, cytokine signaling, and inflammatory gene expression in macrophages (Qin *et al*., 2012). Increased SOCS3 expression has been observed in LPS-and TNF-α-activated RAW 264.7 mouse macrophages (Bode *et al*., 1999). Combined, these observations led to a key conclusion: that *the ratio of SOCS1:SOCS3 is high in M2 macrophages* and lower in M1 macrophages. SOCS1:SOCS3 ratio is therefore suggested to be a new *indicator to identify M2* macrophages (Briken and Mosser, 2011).

STAT1 *vs.* STAT3

In response to different stimuli, a network of signaling molecules, especially the STAT/SOCS signaling pathway, outline the different types of macrophage activation in the murine model. In macrophages displaying the M1 phenotype, expression of STAT1 and IRF5 is up-regulated after exposure to IFNs and TLRs. The activation of STAT1 is crucial for inducing the production of cytokines [IL-12, IL-23, tumor necrosis factor

(TNF)] from M1 macrophages, which is involved in eliciting Th1 and Th17 responses (Krausgruber *et al*., 2011). In contrast, a predominance of STAT3 and STAT6 up-regulation results in polarization to the M2 macrophage phenotype. STAT-mediated activation in macrophages is regulated by members of the SOCS family (Sica and Mantovani, 2012).

iNOS / nitric oxide *vs.* arg / arginase

Nitric oxide (NO), an important regulator and mediator in many physiological and pathophysiological events, is produced by the oxidation of one of the guanidine nitrogens of L-arginine by a family of nitric oxide synthase (NOS) isoforms (Morris *et al*., 1998). When inducible nitric oxide synthase (iNOS) is induced in M1 macrophages, L-arginine will be converted into OH-arginine and then into NO. In contrast, M2 macrophages express higher levels of arginase, which degrades L-arginine into urea and ornithine, which is then metabolized subsequently into proline and polyamines; these molecules contribute to collagen production and tissue repair (Classen *et al*., 2009). Both iNOS and arginase use intracellular L-arginine as substrate. As a consequence, arginase can compete with iNOS and diminish NO production by reducing the availability of L-arginine to iNOS (Chang *et al*., 1998).

The NOS expressed in macrophages can be induced by various pro-inflammatory cytokines, such as tumor necrosis-α (TNF-α), IL-1β, and IFN-γ, and by microbes or microbial membrane components such as lipopolysaccharide (LPS) and lipid A. Upon induction of iNOS, NO is produced continuously at a high rate in the presence of

adequate L-arginine supply. The availability of L-arginine is one of the rate-limiting factors in macrophage NO production (Chang *et al*., 1998). Production of NO has been implicated in several cytostatic and cytotoxic actions mediated by macrophages.

Arginase, another L-arginine consuming enzyme, coexists with iNOS in macrophages and is found to have high activity in the IL-4/IL-13- (anti-inflammatory cytokine) induced M2 phenotype (Mantovani *et al*., 2013). Arginase metabolizes arginine into urea and ornithine. Arginase can be found in two isoforms, liver-type arginase I (Arg I) and non-hepatic type II (Arg II). Arginase I is located in the cytosol; while arginase II is located in the mitochondria. Both arginase isozymes can compete with iNOS and diminish NO production by reducing the availability of L-arginine to iNOS (Cecilio *et al*., 2011). Arg II and iNOS are upregulated early in LPS-induced mouse macrophages, while the Arg I isoenzyme is induced much later. In the mouse, Arg I and II mediate the production of L-ornithine, which can be decarboxylated by the enzyme L-ornithine aminodecarboxylase (ODC) to produce polyamines and contribute to regulation of cell growth. On the other hand, L-ornithine can also be converted into proline by L-ornithine amino-transferase (OAT), implicating Arg I and II in collagen production (Gordon, 2003). Recently, Arg I, but not iNOS, was shown to be expressed in bone marrow-derived macrophages submitted to M2 polarizing conditions. In contrast, M1 macrophages expressed Arg II in addition to iNOS, but did not express Arg I (Khallou-Laschet et al., 2010). The functions of Arg II include the production of ornithine and thus the production of proline and polyamines that are necessary for wound healing and

the formation of granulomas (Ash *et al*., 2000). Despite the progress in mammals, Arg I has unfortunately, not yet been identified or characterized in the chicken genome.

Transferrin receptor *vs.* ferritin heavy chain

Iron is a key nutrient and a limiting factor of bacterial growth. Macrophages play a crucial role in body iron homeostasis by recovering iron from old red blood cells and returning it to circulation to bound to transferrin. Transferrin then delivers the metal to cells which require iron for various functions, thus contributing to more than 80% of the daily iron turnover (Recalcati *et al*., 2010). Iron handling by macrophages has been shown to happen in opposite directions by M1 and M2 phenotypes. Iron *retention* in the reticulo-endoepithelial system is the main response to inflammation in terms of body iron homeostasis (Recalcati *et al*., 2010). Iron handling was recently suggested as one of the indicators of functional polarization of macrophages in mammals (Recalcati *et al*., 2010). Ferritin heavy chain (FtH, an iron storage protein) and transferrin receptor (TfR, a mediator of iron uptake) both play important roles in the handling of iron by macrophages in mice. In M1 macrophages, the iron retention is *increased* by expanding the intracellular iron pool. The expansion is a means of increasing the iron uptake and delaying the iron export through expression of high levels of FtH and low levels of TfR (Corna *et al*., 2010). M1 macrophages also have limited ability to act as scavengers because they express lower levels of CD163 (Canton *et al*., 2013). Thus, M1 macrophages limit the availability of iron in the circulation that could favor invading pathogens. By increasing expression of FtH and expanding their intracellular iron pool,

macrophages can protect themselves from oxidative damage (Kakhlon and Cabantchik, 2002). In contrast, M2 macrophages lack the typical iron-withholding mechanism that is present in M1 macrophages. Macrophages, which phagocytose senescent red blood cells, are the major contributors of iron required for erythropoiesis (Corna *et al.*, 2010). M2 macrophages, by contrast, are professional scavengers that express high levels of CD163 (hemoglobin/haptoglobin receptor), enabling efficient iron re-uptake and recycling, a characteristic of M2 macrophages to promote iron release into the microenviroment (Gaetano et al., 2010).

Ex vivo experimental model of macrophages: the peritoneal macrophage

The current fundamental knowledge regarding macrophage biology relies on the analysis of peritoneal macrophages, which have been widely used as a source of primary macrophages (Turchyn *et al.*, 2007). In the murine model, the most commonly used technique for obtaining peritoneal macrophages is injecting mice with sterile Brewer's thioglycolate broth (a mixture of salts, proteins, and growth factors used as bacterial growth medium), or with sterile 7.5% casein solution. A single injection of Brewer's thioglycolate broth results in a mild inflammatory response, which is characterized by an influx of neutrophils during the first 4 to 12 hours, followed by increased numbers of elicited macrophages 24 to 90 hours post-injection (Turchyn *et al.*, 2007). A growing body of evidence suggests that two functionally and phenotypically distinct subsets of macrophages (resident and elicited) co-exist in the abdominal cavity of mice upon

stimulation with inflammatory stimuli. Moreover, resident and elicited macrophages can be clearly distinguished by a series of different surface markers (Idoyaga et al., 2011).

Recent studies in mice indicate that resident peritoneal macrophages expressing M2 phenotype scavenger receptors, such as SR-A1, act as scavengers for recognizing and taking up modified lipoproteins and apoptotic cells (Canton *et al*., 2013; Platt and Gordon, 2001; Selvarajan *et al*., 2011). Elicited peritoneal macrophages express high levels of M1 phenotype receptors, such as MHC-II and co-stimulatory molecules including CD40, CD80, CD86, and CD54, upon inflammatory stimulation (Liu *et al*., 2006; Liu *et al*., 2012). These cells also play a role in growth promotion by secreting growth factors such as vascular endothelial growth factor (VEGF), platelet-derived growth factor (PDGF), and transforming growth factor (TGF-β), able to rescue early apoptotic cells (Selvarajan *et al*., 2011).

In contrast to mice, chickens lack resident macrophages in their abdominal cavity. However, chicken macrophages can be recruited rapidly and extensively into the abdominal cavity if appropriate stimuli are applied (Klasing, 1998; Sabet *et al*., 1977). The most commonly used stimulus and technique for the avian model consists of injecting the bird intraperitoneally with 8 ml 3% (w/v) Sephadex G-50 in PBS and then harvesting elicited macrophages 42 hours post-injection by peritoneal lavage (Qureshi *et al*., 2000; Sabet *et al*., 1977). Chicken PEMs undergo functional maturation over time and can effectively bind, internalize, and degrade bacteria by lysosomal acid hydrolysis (Golemboski *et al*., 1990). Although Sephadex-elicited macrophages are considered to

be activated macrophages, they however require additional activation signals in order to acquire more specialized effector functions (Qureshi and Miller, 1991).

Chicken PEMs are the most commonly used macrophage subpopulation for studying avian macrophage biology; however, the features of macrophage polarization remain unclear in birds. Next to the injection of Sephadex G-50, a biologically relevant event, internal ovulation, also elicits macrophage influx into the abdominal cavity for the purpose of clearing yolk particles (Nili and Kelly, 1996). Recently, the effects of intraperitoneally injected egg yolk on chicken blood monocyte-derived macrophages were investigated *in vitro* (Cornax *et al*., 2013). Egg yolk decreased the expression of pro-inflammatory cytokines and the production of NO by chicken macrophages (Cornax *et al*., 2013). This evidence suggests that exposure to egg yolk skews the macrophage phenotype towards M2, the functional phenotype of egg yolk-elicited macrophages and mechanism of their polarization is not entirely clear.

Monoclonal antibodies against chicken macrophages

Few Mabs have been developed and used to study avian macrophage heterogeneity. (Trembicki et al., 1986) developed two Mabs (CMTD-1 and -2) which selectively reacted with chicken peritoneal exudate macrophages and splenic myeloid cells. Jeurissen *et al*. (1988) reported two Mabs, CVI-ChNL-68.1 and CVI-ChNL-74.2, reactive with chicken monocytes, macrophages, and interdigitating cells in tissue sections. Kaspers *et al*. (1993) described a Mab (K1) which detected chicken macrophages and thrombocytes. More recently, Mast *et al*. (1998) partially characterized

a Mab (KUL01) that positively cross-reacted with macrophage subpopulations in monocytes, macrophages, and interdigitating cells. However, the exact epitope recognized by any of these Mabs remains unknown. Despite its cross-reactivity with other APCs, the anti-chCD40 Mab developed by our lab was shown to recognize and activate primary macrophages and cells from the chicken HD11 macrophage cell line (Chen et al., 2010b).

CHAPTER III

A SINGLE DOSE OF A CD40-TARGETED IMMUNOGEN DELIVERED AT VARIOUS MUCOSAL INDUCTION SITES RESULTS IN ANTIGEN-SPECIFIC MUCOSAL SIGA AND CIRCULATING IGG PRODUCTION IN THE CHICKEN

Introduction

Mucosal surfaces are vast surface areas that are the major portal of entrance of a wide range of pathogens. Therefore, the mediation of adaptive immunity at the mucosal sites is a key objective for improving avian health. Although the consequence of phylogenetic separation of chickens from the reptile ancestor of mammals was about 300 million years ago, chickens are also endowed with a sophisticated mucosal immune system including a series of redundant protective mechanisms (Smialek *et al*., 2011) Chickens lack encapsulated lymph nodes such as are found in mammals, but rather possess diffuse lymphoid tissues (Muir *et al*., 2000). Mucosal immune responses are most efficiently induced when the antigen is delivered directly onto mucosal sites through mucosal routes (Woodrow *et al*., 2012). Mucosal immune sites are interconnected by a common mucosal immune system (CMIS) whereby stimulation of an *inductive* site (where the immune response initiated), the resulting immune response can be disseminated to the distal *effector* sites of the mucosa (Iwasaki, 2007). Vaccination has the great potential to be a vehicle to deliver antigen and induce an antigen-specific adaptive immune response in mucosal sites. However, direct mucosal immunization has been found to be difficult due to several factors including dilution of mucosal vaccines in the bulk of mucosal fluid

that limits absorption of antigen by the mucosal epithelium. Due to the complexity of mucosal surfaces, mucosal vaccines frequently fail to transverse the mucosal gel and are subsequently degraded by proteases (Neutra and Kozlowski, 2006; Woodrow *et al*., 2012).

Several mucosal vaccines are universally used in poultry industry. However, most of these mucosal vaccines can only induce a local IgA immune response, and they are unable to react against the pathogen once it spreads through the circulation (Rauw *et al*., 2010). Thus, a new formulation of vaccines that is capable of inducing *both* local mucosal and systemic immune responses is desired. The goal of any mucosal vaccine design is to increase immunogenicity (useful effector mechanisms) without leading to reactogenicity (inflammation, hypersensitivity, *etc*.). Among the various strategies under development, there is great potential for novel vaccines based on recombinant proteins and synthetic peptides. However, such antigens often lack the immunogenicity of live attenuated or whole killed pathogens used in traditional vaccines. There is, therefore, an urgent need to develop immunological adjuvants with a high potential to enhance immune responses (Barr *et al*., 2003) while simultaneously possessing a low potential of negative side effects.

A number of mucosal adjuvants for co-administration with live attenuated vaccines through the oculo-nasal or oral routes have been reported in chickens (Fingerut *et al*., 2005; Girard *et al*., 1999; Linghua *et al*., 2007; Rauw *et al*., 2010). Despite the fact that these adjuvants do enhance mucosal sIgA and systemic IgG responses, they are still

considered time- and antigen-consuming since repeated injections of a large amount of antigen are still required.

In several studies, antigen-presenting cell (APC) targeting by antibodies directed against a co-stimulatory cell surface receptor, such as CD40, has been proposed as a promising strategy to induce specific systemic immunity in mammals (Barr *et al*., 2003; Hatzifoti and Heath, 2007). Recently, a study from our laboratory described that an anti-chCD40 Mab-peptide complex targeted to APCs induces a rapid and robust systemic IgG response after a single subcutaneous (s.c.) injection (Chen *et al*., 2012). This result demonstrates the capacity of a CD40-targeted vaccine to rapidly induce a strong immune response, and, most importantly, the capability to induce a fast immunoglobulin class switch from IgM to IgG.

Complexes of anti-chCD40 and immunogen seem to show great potential as a potential vaccine platform in chickens, we were interested in assessing the effect of an anti-chCD40-peptide complex on mucosal immunogenicity. In this chapter, we test the hypothesis that a short synthetic peptide immuno-targeted to chCD40 can effectively target APCs of the MALT *in vivo* and induce an immunogen-specific sIgA response in the trachea *and* a specific IgG response in the circulation. We assessed mucosal and systemic antibody responses after a single administration via different mucosal routes, as compared to a classic s.c. injection. Each time, the cCD40-specific peptide complex was compared to a "blind", non-specific MIgG-peptide complex.

Materials and methods

Anti-chCD40 monoclonal antibody (designated as 2C5)

Our lab has previous reported the development of an agonistic anti-chCD40 Mab, designated as 2C5 (Chen et al., 2010b). Mab 2C5 was made against the recombinant extracellular domain of chCD40 ($chCD40_{ED}$), produced in collaboration with the lab of Dr. Mwangi (CVM-VTPB). This Mab recognized CD40 as expressed on primary chicken B-cells and macrophages, DT40 B-cells, and HD11 macrophages. Mab 2C5 also induced NO production in HD11 macrophages, and stimulated DT40 B-cell proliferation (Chen et al., 2010b). These results demonstrated that 2C5 induces downstream CD40 signaling after binding to CD40 and is thus agonistic. Mab 2C5 mimicked at the very least partially the functions of the chicken's natural CD40 ligand, CD154. Chen *et al.* (2012) also reported that targeting an antigen to chicken $CD40^+$ APCs can significantly enhance antigen-specific circulatory IgG responses and thus induce fast immunoglobulin isotype-switching (Chen *et al*., 2012).

Streptavidin-mediated complexing of peptide to mouse antibody

The anti-CD40 Mab-peptide complex (designated as "Mab 2C5-peptide complex") and control complexes (where non-specific MIgG was substituted for anti-cCD40 Mab 2C5) were prepared essentially as described previously (Chen *et al*., 2012). Briefly, anti-chicken CD40 Mab 2C5 and non-specific control mouse immunoglobulin (MIg) were directionally biotinylated by derivatization of the carbohydrate moieties on the Fc fragment. Biotinylation and retention of chCD40-binding capacity were verified by

enzyme-linked immunosorbent assay (ELISA; results not shown). A synthetic amino-terminally biotinylated peptide (b-NAWSKEYARGFAKTGK) and streptavidin (SA) were used in a stoichiometrically controlled complexing reaction of the biotinylated peptide with biotinylated 2C5 (or MIg) in a ratio of 1 SA molecule to 2 peptide molecules and 2 immunoglobulin molecules (Fig. 3).

However, because an immunoglobulin-peptide complex is likely susceptible to the enzymatic and acidic pH environment of the gastrointestinal tract, protective encapsulation of the immunoglobulin-peptide complex in an alginate matrix was considered a logical precaution when oral administration was required. Alginate encapsulation is a viable approach for oral delivery of antigens, and the entrapped functional immunoglobulin-peptide complex in fine alginate spheres can be safely delivered to the appropriate site, (such as the Peyer's patches), despite the harsh gastrointestinal environment that would likely degrade any non-protected protein (Desai and Schwendeman, 2013). For this study, encapsulation of Mab 2C5-peptide complex and MIg-peptide complex in alginate spheres was performed essentially as reported by Park and colleagues (Bowersock *et al.*, 1999) with minor modifications. To prepare Mab 2C5-peptide or non-specific MIg-peptide complex in the form of alginate-protected particles, the molecular complex was freshly produced and then gently mixed with 3% (w/v) sodium alginate (Sigma-Aldrich, St Louis, MO) in phosphate buffered saline (PBS), pH 7.4, to obtain a homogeneous solution. The resulting solution was then extruded drop-wise through a 23-gauge needle attached to a 1mL plastic syringe into 3%

(w/v) $CaCl_2$ solution with gentle stirring for 30 minutes at room temperature. Gelified alginate spheres were separated from the $CaCl_2$ solution by centrifugation at 3,000g for

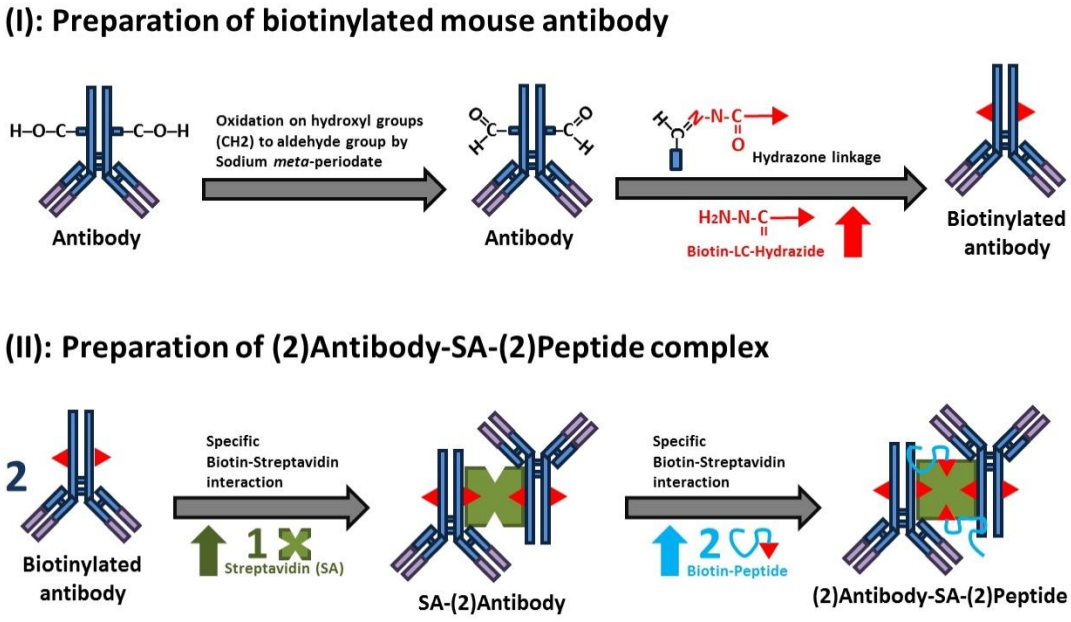

Figure 3 Preparation of antibody-peptide complex based on biotin-streptavidin interaction (Chen *et al*., 2012). Preparation of antibody-peptide complex based on biotin-streptavidin interaction. (I): Biotinylation was limited to the carbohydrate groups on the Fc region of MIg, hence did not interfere with antigen-antibody interaction. (II): Streptavidin (SA) was used for controlled complexing of biotinylated peptide with biotinylated MIg. Mab 2C5 in the 2C5-SA-peptide complex retained its biological function as demonstrated by ELISA (results not shown).

10 minutes at 4°C and were further washed three times with PBS, pH 7.4. To reduce the porosity of the alginate spheres, they were stabilized by coating them in 0.3% (w/v) poly-L-lysine solution with gentle stirring for 30 minutes at room temperature. Poly-L-lysine coated alginate spheres were then washed three times with PBS, pH 7.4. These alginate spheres could be stored at 4^{o}C until use. On the day of use, the alginate spheres were mechanically fragmented using an IKA® T10 basic ultra turrax homogenizer (Sigma-Aldrich) to form a suspension of smaller microspheres prior to oral administration of the suspension. The morphological characteristics of the alginate spheres were microscopically verified using a hemocytometer. The mean size of the alginate spheres prior to fragmentation was around 1.5mm in diameter, and the diameter of (fragmented) alginate microspheres in suspension ranged from 10 to 100µm.

Immunization of chickens with Mab 2C5-peptide complex in solution or as alginate-encapsulated Mab 2C5-peptide complex microsphere suspension

Four-week old male Leghorns were randomly assigned to different groups (n=16/group). Non-encapsulated Mab 2C5-peptide complex (or "blind", non-specific MIg-peptide complex, used as negative control) solution in PBS (pH=7.4), was used for immunization via subcutaneous (s.c.) injection, via cloacal drinking (bursal route), and via intraocular drop (oculo-nasal route) administration. For s.c. injection, 50µg Mab 2C5-peptide / MIg-peptide complex in a volume of 0.5mL emulsified PBS (containing 5% (v/v) squalene and 0.4% (v/v) Tween 80 (Sigma-Aldrich), pH=7.4) was injected in the nape of the neck of each chicken. For cloacal drinking, 50µg Mab 2C5-peptide /

MIg-peptide complex in a volume of 150μL PBS was administrated by dropping the immunogen solution onto the cloacal lips of chickens using a P200 pipette. For intraocular immunization, 50μg 2C5-peptide / MIg-peptide complex in a volume of 40μL PBS was administrated as eye drops in both eyes of the chickens. For oral immunization with alginate sphere suspension, the immunogen was gently dropped into the oral cavity of the restrained chickens until they spontaneously swallowed it. Alginate suspension containing 50μg 2C5-peptide complex in a volume of 2mL PBS, pH 7.4, using a pasteur pipette was administered to each of the 16 chickens. Chickens that received the immunogen through cloacal or oral administration were fasted 24 hour prior immunization to prevent the immunogen from being regurgitated or expelled. The conditions for animal use in this study were approved by the Institutional Animal Care and Use Committee of Texas A&M University, in accordance with the guidelines of the American Association for Laboratory Animal Science.

Quantification of peptide-specific serum IgG in by ELISA

Levels of peptide-specific IgG in circulation were determined by ELISA essentially as described previously (Chen *et al*., 2012). Briefly, biotin-peptide was first complexed with goat anti-biotin antibody (Thermo Scientific) on a rotator at 37^{o}C for one hour in equimolar ratios. Next, the peptide-goat antibody complex (5μg/mL) was coated overnight on flat-bottom, 96-well microtiter plates (Thermo Scientific) in 0.05M carbonate-bicarbonate buffer, pH 9.6, at 4^{o}C. Excess unadsorbed peptide-goat antibody complex was removed by rinsing the plates, and then they were blocked with PBS

containing 5% (w/v) bovine serum albumin (BSA) (Rockland Immunochemicals Inc., Gilbertsville, PA) for one hour at 37^{o}C. Peptide coated wells were washed with PBS containing 0.2% (v/v) Tween 20 (SIGMA) (PBST) and then incubated with chicken serum samples diluted (1:100) in PBST containing 3% (w/v) BSA overnight at 4^{o}C. The plates were then washed as described above and incubated with horseradish peroxidase-conjugated rabbit anti-chicken IgY (H+L) (Thermo Scientific) diluted (1:12,000) in PBST containing 3% (w/v) BSA for one hour at room temperature. Isotype-specific rabbit anti-chicken IgY was used to avoid potential cross-reactions with IgM. The color reaction was developed using OptEIA™ TMB substrate (BD) according to manufacturer's instructions. The reaction was terminated by addition of 1N sulfuric acid. Absorbances at 450 nm (A_{450}) were measured in a Wallac plate reader (PerkinElmer Inc., Waltham, MA). The presence of peptide-specific IgG was determined by relating the mean A_{450} value of each serum sample to that of a positive control serum sample (diluted at 1:100), which was used as the internal standard on all plates, to allow comparison of titers across plates and experiments, but within isotype. The relative levels of peptide-specific IgG in all serum samples were determined and normalized by calculating the sample to positive (S/P) ratio as follows: S/P value = (Sample mean - negative control mean)/(Positive control serum mean - negative control mean). The effect of specifically targeting the peptide to cCD40 (as opposed to incorporating it in a non-specific antibody complex) was estimated by using the following calculation: Mab 2C5 (S/P) *minus* MIg (S/P). Student's t-test was used to determine significant differences in means of S/P values between treatments across all groups, and S/P values

of the MIg-peptide complex group were used as baseline. All data were analyzed and generated using JMP® version 9 software (SAS Institute Inc., Cary, NC). Statistical significance was determined at $P < 0.05$.

Quantification of peptide-specific tracheal sIgA by ELISA

Levels of peptide-specific sIgA in tracheal mucosa samples were determined by ELISA. Eight chickens from each group were sacrificed at either seven or 14 days post immunization (p.i.), and the tracheal mucosa sample from each chick was collected by preparing a tracheal wash as follows. In order to avoid blood contamination of the trachea, every chicken was euthanized using a CO_2 chamber. The trachea was exposed aseptically at the pharyngeal region, and a 1-cm segment of trachea was collected, weighed, and then transferred to a 2-mL microcentrifuge tube. The trachea was suspended in cold PBST [137mM NaCl, 2.7mM KCl, 10mM Na_2HPO_4, 2mM KH_2PO_4, and 0.5% Tween 20 (v/v)] containing Halt® Protease and Phosphatase Inhibitor (Thermo Fisher Scientific Inc., Barrington, IL), 0.1% (w/v) thimerosal, and 3% (w/v) BSA. To maximize the extraction efficiency of tracheal IgA, 1mL PBST was added per 100mg trachea sample weight. The tracheal mucosa was sloughed off from the inner liner of the trachea by vigorously vortexing for 30 seconds. The tube was centrifuged at 5,000*x*g for 30 minutes at 4°C, and the supernatant was collected and frozen at -20°C until use.

The detection of sIgA in the mucosal extracts was performed as follows. Biotinylated peptide (b-NAWSKEYARGFAKTGK) was incubated with goat anti-biotin antibody (Thermo Fisher Scientific Inc.) on a rotator at 37°C for one hour. Flat-bottom, 96-well

microtiter plates (Thermo Fisher Scientific Inc.) were coated with peptide-goat antibody complex (5μg/mL) in 0.05M carbonate-bicarbonate buffer, pH 9.6 (SIGMA), overnight at 4^{o}C. Excess peptide-goat antibody complex was removed, and plates were blocked with PBS, pH 7.4 containing 5% (w/v) bovine serum albumin (BSA) (Rockland Immunochemicals Inc., Gilbertsville, PA) overnight at 4^{o}C. Peptide- coated wells were washed with PBST and then incubated with chicken tracheal IgA samples (diluted to 1:100) in PBST containing 3% (w/v) BSA overnight at 4^{o}C. The plates were then washed as described above and incubated with horseradish peroxidase-conjugated goat anti-chicken IgA (Thermo Fisher Scientific Inc.) diluted (1:10,000) in PBST containing 3% (w/v) BSA for one hour at room temperature. Isotype-specific goat anti-chicken IgA was used to avoid the cross-reaction with other antibody isotypes. The color reaction was developed using OptEIA™ TMB substrate (BD, Lakes, NJ) per the manufacturer's instructions, and terminated by addition of 1N sulfuric acid. Absorbances at 450nm (A_{450}) were measured in a Wallac plate reader (PerkinElmer Inc., Waltham, MA). The presence of peptide-specific IgA was determined by relating the mean (A_{450})value of each tracheal IgA sample to that of a positive control IgA sample used as internal standard (1:100). The relative levels of peptide-specific IgA in all tracheal samples were determined and normalized by calculating the sample to positive (S/P) ratio as explained above for IgG. Student's t-test was used to determine significant differences in means of S/P values between treatments across all groups, and S/P values of the MIg-peptide complex group were used as baseline. All data were analyzed and generated using JMP®

version 9 software (SAS Institute Inc., Cary, NC). Statistical significance was determined at $P < 0.05$.

Results

Antibody responses after a single parenteral (s.c.) immunization with anti-CD40-guided peptide complex vs. non-specific, "blind" peptide complex

To evaluate the effect of parenteral immunization of anti-CD40-guided Mab 2C5-peptide complex on specific systemic and mucosal antibody responses, groups of five-week old male Leghorns received a single s.c. immunization with 50 μg Mab 2C5-peptide complex, and their responses were compared to those obtained with a "blind" non-specific MIg-peptide complex that served as the negative control. Trachea and plasma samples were collected from all immunized chickens at day 7 and 14 p.i., and peptide-specific IgA and IgG immune responses were assessed by ELISA. As shown in Fig. 2A, a single s.c. injection of Mab 2C5-peptide complex induced peptide-specific circulatory IgG antibody responses that were significantly higher than those obtained with non-specific MIg-peptide controls at 7 ($P<0.001$) and 14 days ($P<0.001$) p.i.. Peptide-specific sIgA immune responses were also significantly enhanced on day 7 ($P<0.001$) and 14 ($P<0.05$) p.i. by targeting the immunogen to CD40 expressed on the chicken APCs (Fig. 2B). While we observed still statistically significant increased IgG and sIgA immune responses compared to controls on day 14 p.i., the major immune-enhancement was clearly observed on day 7 p.i. The same effect can also be observed on the overview graph of all antibody responses shown in Fig. 4.

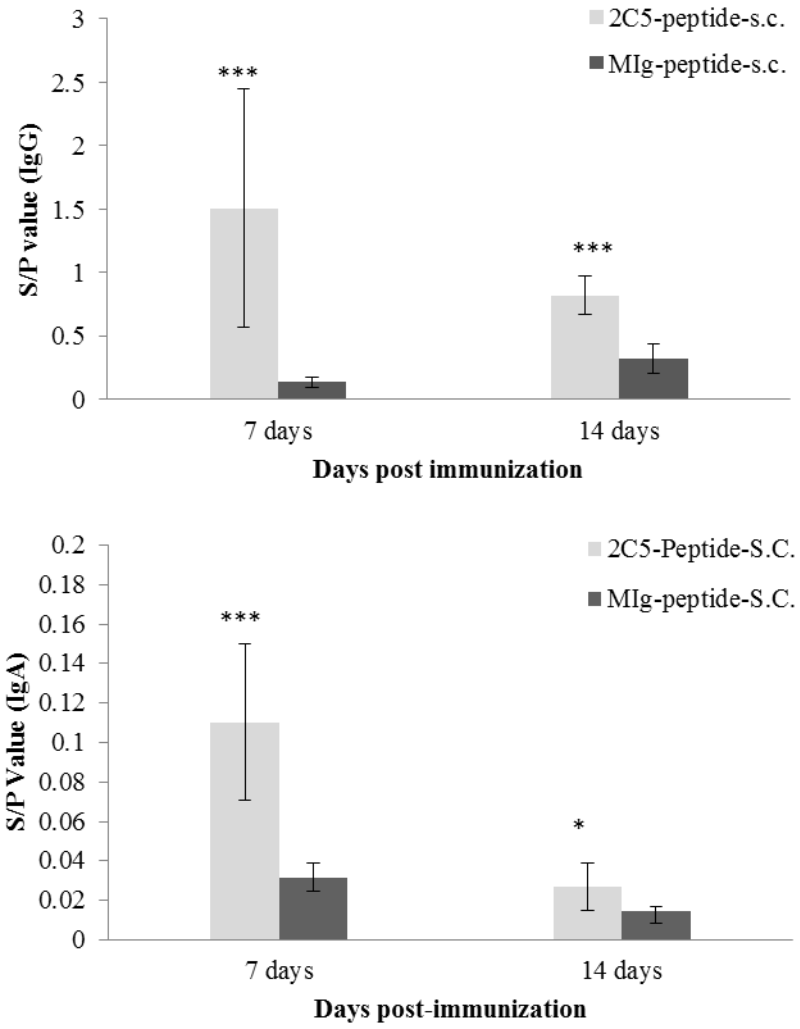

Figure 4. Levels of peptide-specific circulatory IgG in serum and mucosal sIgA in trachea. Levels of peptide-specific circulatory IgG (A) and mucosal IgA in trachea (B) elicited by a single s.c. injection of anti-cCD40-guided peptide complex (grey bars, as compared to non-specific MIgG-peptide complex, black bars) as determined by ELISA. Groups of eight five-week old male Leghorn chickens were subcutaneously immunized once with 50 μg Mab 2C5-peptide complex or negative control complex. In each case, error bars represent standard deviations from the mean and the asterisks represent statistical significance (n=8; *P<0.05; **P<0.01; ***P<0.001) compared with MIg-peptide complex controls as determined by Student's t-test. At both time points, and for both antibody isotypes, a significant immune enhancement caused by CD40 targeting of the peptide cargo to the APCs was observed.

Antibody responses after a single mucosal immunization with anti-CD40-guided peptide complex vs. non-specific MIgG peptide complex

The potential immune-enhancing effect of the anti-CD40 Mab 2C5-peptide complex was also evaluated by administration of the immunogen via three different mucosal induction sites to the birds, each time using "blind" non-specific MIg-peptide complex as the negative control. Groups of five-week old male Leghorns were administrated a single Mab 2C5-peptide complex dose (50 μg) via one of the following mucosal routes: oculo-nasal (eye drops), cloacal-drinking (drops on the lips of the vent), and oral administration. The oral route was not administration by gavage into the stomach (which would bypass the esophagus and the crop) but active drinking of the immunogen solution. Trachea and plasma samples were collected 7 and 14 days p.i. and antibody responses were measured as described previously for the s.c. administration route. The results obtained from different mucosal routes of administration showed that 2C5-peptide complex induced similar antibody response patterns of IgG (Fig. 5) and sIgA (Fig. 6) for each of the different routes. Antigen directly delivered to mucosal *inductive* sites via all three mucosal routes induced significant peptide-specific systemic IgG immune responses from days 7 p.i. ($P<0.001$) onward through day 14 p.i. (oculo-nasal: $P<0.001$; oral: $P<0.01$; cloacal-drinking: $P<0.05$) compared to MIg-peptide control (Fig. 5). Fig. 6 shows that anti-CD40-guided Mab 2C5-peptide complex was also able to induce significant peptide specific sIgA responses through all three tested mucosal routes at days 7 p.i. (oculo-nasal: $P<0.001$; oral: $P<0.01$; cloacal-drinking: $P<0.01$) but those IgA responses clearly declined by day 14 p.i. (oculo-nasal: non-significant; oral:

P<0.01; cloacal-drinking: *P*<0.01) compared with MIg-peptide complex. Notably, mucosal administration of "blind" MIg-peptide complex through different routes also seemed to slightly numerically increase peptide-specific systemic IgG responses, and also the mucosal sIgA response but only after oculo-nasal administration.

Calculation of the net immuno-enhancing effect of anti-CD40- targeting through different routes of administration

The above results allow us to assess the net immuno-enhancing effect of targeting a peptide to $CD40^+$ APCs, as opposed to incorporation of the same peptide in a non-specific, "blind" protein complex. For this purpose, the immuno-enhancing effect was defined as: [average (S/P) value of anti-CD40-guided complex) from which was subtracted [average (S/P) value of administration of"blind" complex]. This adjuvant effect was compared between administration routes (4) and time points (2).

As shown in Fig. 7A, s.c. administration of 2C5-peptide complex generated by far the most robust systemic IgG immune response achieved by CD40 targeting at day 7 p.i.. However, the level of magnitude of this enhancement was not sustained and declined to less than half of the original value by 14 p.i. (1.371 vs. 0.497). Although the net IgG effect of CD40 targeting through s.c. administration had declined by day 14 p.i., the net effect on systemic peptide-specific IgG levels was still higher than that obtained with any of the other mucosal routes, at any other time. The three mucosal administration routes posted similar but low net effect on systemic IgG responses at days 7 p.i. and moderately increased toward day 14 p.i. (Fig. 7A).

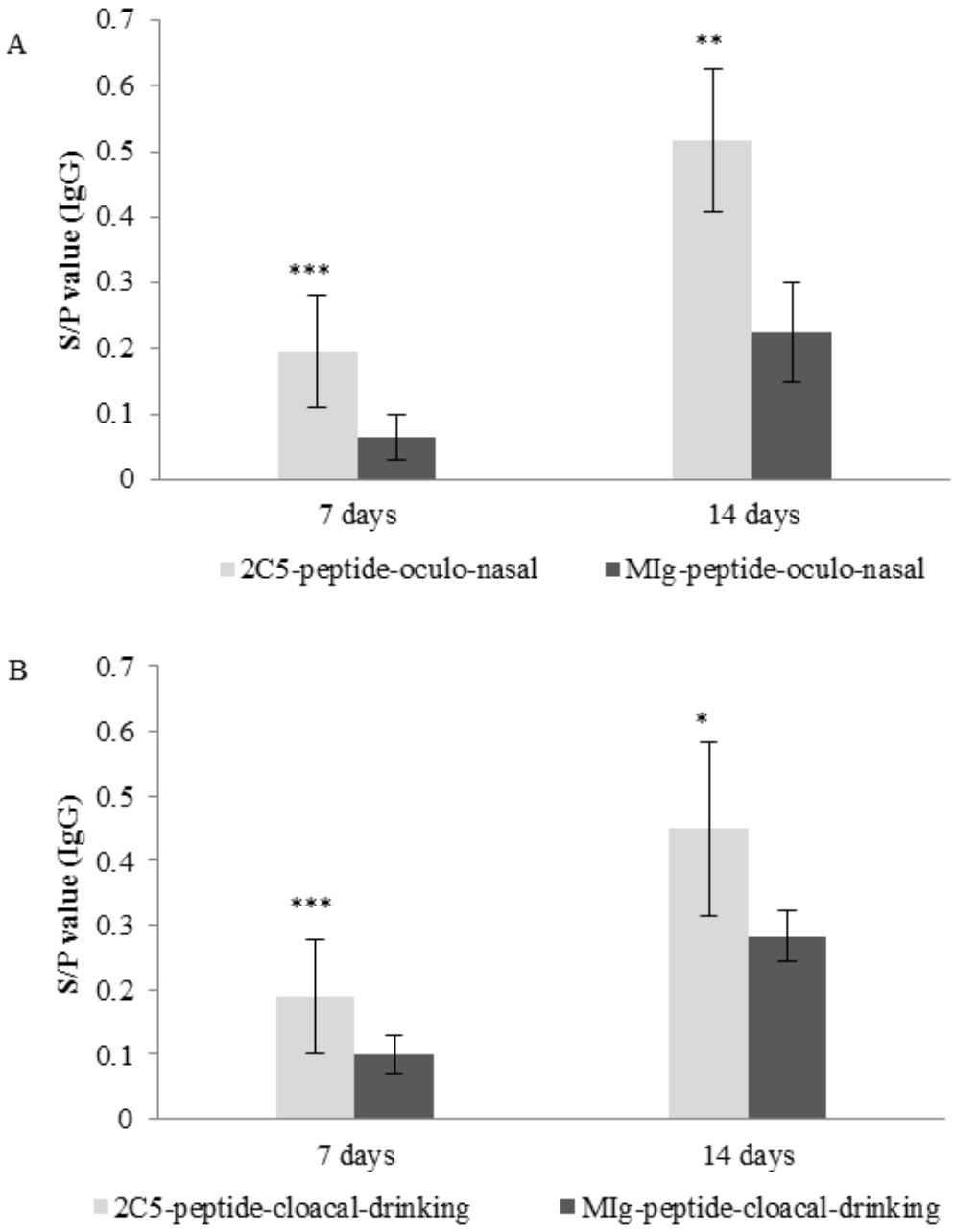

Figure 5. Levels of peptide-specific circulatory IgG in serum. Levels of peptide-specific circulatory IgG elicited by a single administration of anti-chCD40-guided peptide complex (gray bars, as compared to non-specific MIgG peptide complex, black bars) through oculo-nasal (A), cloacal drinking (B), and oral alginate suspension)(C) routes as determined by ELISA. Groups of eight five-week-old male Leghorn chickens were immunized once with either 50 μg anti-CD40-guided Mab 2C5-peptide complex or negative control MIgG-peptide complex via three different mucosal routes. Serum and trachea samples were collected 7 and 14 days p.i. and peptide-specific IgG responses were assessed by ELISA. In each case, error bars represent standard deviations from the mean and the asterisks represent statistical significance (n=8; *P<0.05; **P<0.01; ***P<0.001) compared with MIg-peptide complex controls as determined by Student's t-test.

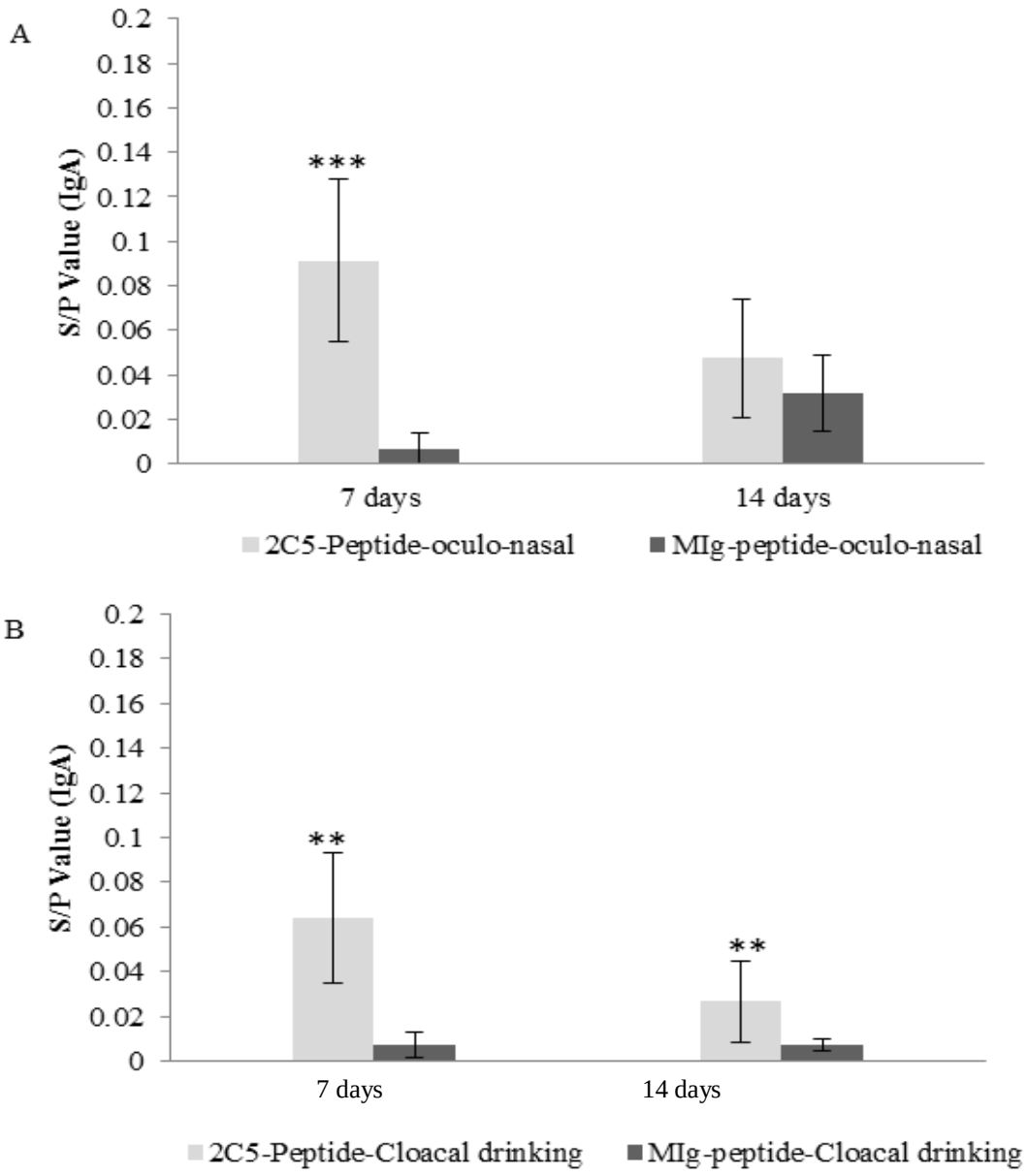

Figure 6. Levels of peptide-specific sIgA in trachea. Levels of peptide-specific mucosal sIgA elicited by a single administration of anti-chCD40-guided peptide complex (gray bars, as compared to non-specific peptide complex, black bars) through oculo-nasal (A), cloacal drinking (B), and alginate suspension (oral)(C) mucosal routes as determined by ELISA. Groups of eight five-week-old male Leghorn chickens were immunized once with 50 μg Mab 2C5-peptide complex or negative control complex via various mucosal routes and serum and trachea samples were collected from chickens at 7 and 14 days p.i. In each case, error bars represent standard deviations from the mean and the asterisks represent statistical significance (n=8; *P<0.05; **P<0.01; ***P<0.001) compared with MIg-peptide complex controls as determined by Student's t-test.

Surprisingly, s.c. immunization with 2C5-peptide complex induced a net effect of CD40 targeting on the secretion of peptide-specific IgA. The effect if the s.c. administration on specific IgA levels was similar in magnitude to that of the three different mucosal routes at day 7 p.i. (Fig. 7B). The net effect of CD40 targeting on peptide-specific IgA production had dropped substantially at day 14 p.i. in all routes of administration. This could be partially the result of the fact that by day 14 p.i., the blind MIg-peptide complex started slowly inducing some peptide-specific sIgA immune response, which detracts from the net CD40-targeting effect of 2C5.

Discussion

Agonistic monoclonal anti-CD40 antibodies have been demonstrated to be an effective immunological adjuvant in inducing specific systemic antibody responses in mammals through parenteral administration (Bartholdy *et al*., 2007; Li and Ravetch, 2011). In our own lab, Chen *et al*, (2012) previously demonstrated that a single s.c. injection of anti-chCD40 Mab complexed with a synthetic peptide induced a specific, rapid and robust systemic IgG immune response, indicating an accelerating effect on immunoglobulin isotype switching of B-cells in chickens. However, for many pathogens, optimal protection seems to require *both systemic and mucosal* immune effectors (Neutra and Kozlowski, 2006).

Most immunization protocols for chickens have traditionally required intramuscular or subcutaneous injections (Dennehy *et al*., 1991; Knuf *et al*., 2010). These mostly induce a circulating IgM or IgG antibody immune response that often does not make any impact on the

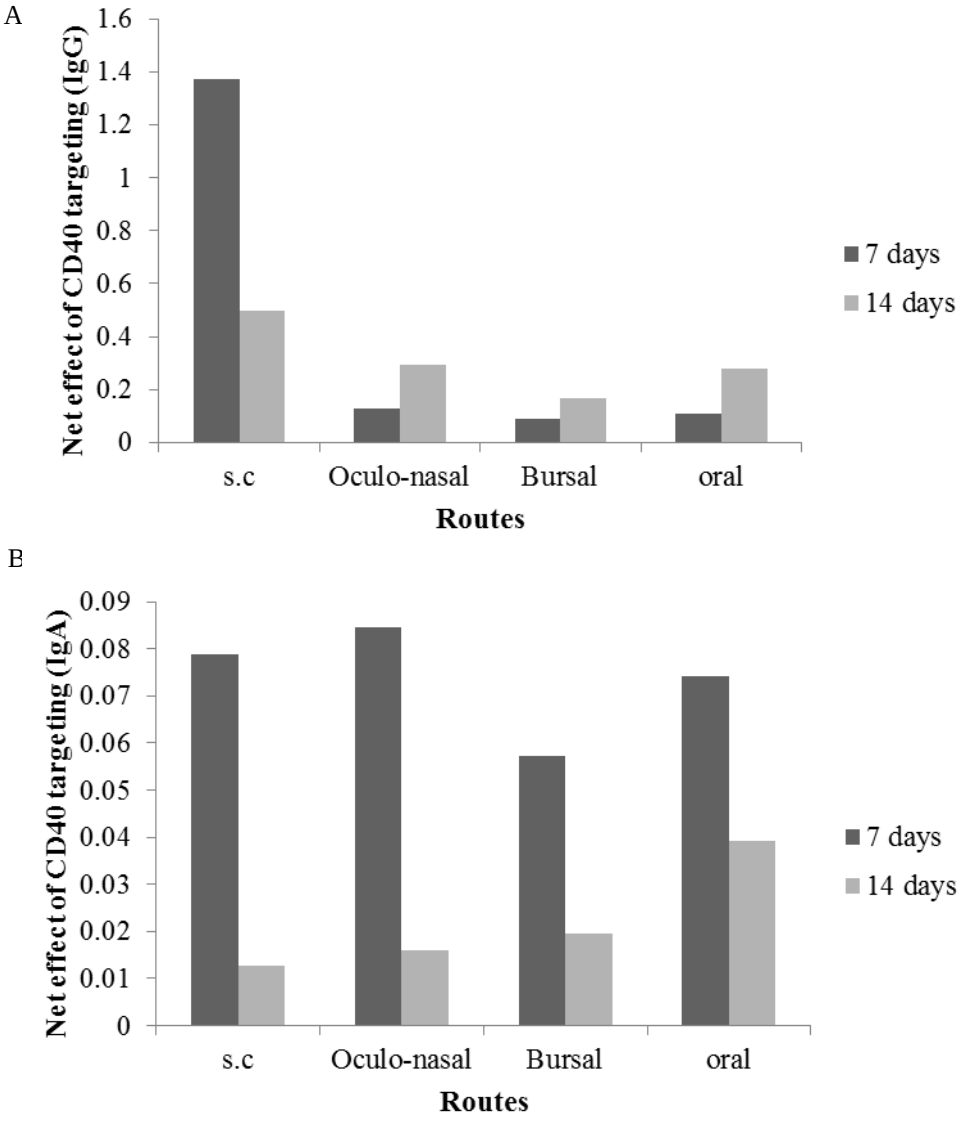

Figure 7. The net effect of 2C5-peptide complex. The net effect of 2C5-peptide complex on induced circulatory IgG (A) and mucosal sIgA (B) immune response through various mucosal and classic s.c. routes. The CD40 targeting induced net effect was calculated as [Average (S/P) value of treatment from each route]-[Average (S/P) value of corresponding MIg control].

mucosal sites to be protected, due to (1) lack of isotype switching (to sIgA), (2) insufficient presence of blood-derived monomeric IgG or IgA on the apical cell surfaces, due to the lack of receptor-mediated transportation, or (3) inability of IgG or IgM to function in the external mucosal environment (Bowersock and Martin, 1999; Czerkinsky and Holmgren, 2012).

In our current study, we have demonstrated that a single s.c. injection of anti-chCD40-guided 2C5-peptide complex not only induces a rapid and strong *systemic* peptide-specific IgG immune response, but also established a significant specific *mucosal sIgA* immune response, as measured in tracheal mucosal extracts. In the current study, the single s.c. injection with Mab 2C5-peptide complex induced significant systemic IgG responses on day 7 and 14 p.i., which is consistent with our previous study (Chen *et al*., 2012), which focused on systemic IgG responses alone. It is tempting to consider that IgG secretion occurred even prior to day 7 p.i., but we did not sample on day 4 p.i., unlike in the previous study. Compared to conventional adjuvants, the anti cCD40 Mab 2C5-peptide complex is able to mimic the biological role of $CD4^+$ T cells by targeting APCs, including B-cells, and further enhancing CD40 downstream signaling and subsequent immunoglobulin class-switching from IgM to IgG.

Interestingly, a single s.c. injection with 2C5-peptiede complex *also* induced a significant *mucosal* peptide-specific sIgA immune response as early as 7 days p.i. as measured by ELISA in mucosal extracts from trachea segments. In the past, the most effective strategy to induce both systemic and mucosal immunity was by using a combination of priming and boosting through the mucosal and systemic routes,

respectively (Holmgren and Czerkinsky, 2005). To the best of our knowledge, past literature states that parenteral immunization alone is unable to prime the specific mucosal immune response in mammals because circulatory resting B-cells in the periphery express different homing receptors compared to the mucosal B-cells in the CMIS (Macpherson *et al*., 2008; Mei *et al*., 2009; Mestecky, 1987; Neutra and Kozlowski, 2006). However, this concept has recently been challenged, and a system similar to the CMIS has been proposed to explain that parenteral immunization might also contribute to antibody-mediated mucosal immunity in humans (Fernandes, 2012). Recently, activated B-cells were shown to express the mucosal homing receptor, chemoattractant cytokine receptor 10 (CCR10). $CCR10^{+}$ B-cells in circulation are considered to be in transit between a systemic (peripheral) lymphoid tissue and mucosal effector tissues, where they are transformed into polymeric IgA-secreting plasma cells (Fernandes and Snider, 2010). Polyclonal anti-CD40 antibodies have been reported to initiate the CCR10 expression on recently activated memory B-cells in mice *in vitro* (Bernasconi *et al*., 2002). On the other hand, CCR10 ligand is expressed in all mucosal *effector* sites (Mora and von Andrian, 2008). In mammals, polyclonal anti-CD40 antibodies were also reported to mediate the expression of CXCR4 on IgG-secreting B cells. CXCR4 is a homing receptor for homing of B-cells to the bone marrow and to secondary lymphoid organs, (Barr et al., 2005; Czerkinsky and Holmgren, 2012; Macpherson *et al*., 2008). We believe this provides a plausible mechanistic explanation for why parenteral immunization with 2C5-peptide complex may indeed be capable of

inducing *both* significant peptide-specific *systemic* IgG and *mucosal* sIgA immune responses.

Taking together, these results suggest that a single parenteral or mucosal immunization with an anti-cCD40 Mab guided antigen complex can induce not only a fast and long-lived systemic IgG immune response, but also a rapid local mucosal sIgA response. Therefore, this new platform may have the potential to be widely used for immunization of chickens through mucosal and/or parenteral administration in cases where both systemic and mucosal immunization is highly desirable. The latter is especially important for vaccination of poultry, in which most pathogens invade through the mucosal surfaces of the respiratory or digestive tract. Even though there are unresolved questions about the mechanism and the microenvironment of the interaction of APCs and anti-chCD40-peptide complex, the results obtained in the current study are encouraging, and there seems to be considerable potential for the development of safe, effective and affordable vaccines. While we have obtained convincing circumstantial evidence pointing towards enhanced clonal expansion of B- and T-cells as well as enhanced class-switching, an important immune parameter that remains to be studied is immunological memory (duration of protection), which, according to mammalian studies is also positively influenced by CD40 signaling.

CHAPTER IV

FUNCTIONAL PHENOTYPING OF CHICKEN PERITONEAL EXUDATE MACROPHAGES ELICITED WITH EITHER SEPHAROSE BEADS OR EGG YOLK PARTICLES

Introduction

Mammalian macrophages are capable of displaying different phenotypes and can be polarized into two distinct phenotypic subtypes in response to microenvironmental queues: the "classical" (pro-inflammatory, M1) and the "alternative" (anti-inflammatory, M2) phenotype (Classen *et al*., 2009). M1 macrophages display antimicrobial activity while M2 macrophages typically act as scavengers. Diversity and plasticity are hallmarks of cells from monocyte-macrophage lineage. Until recently, phenotyping cells in the mononuclear phagocyte system, which includes macrophages and dendritic cells based on expression of cell surface markers such as CD11b, CD68, and F4/80, has been the mainstay of murine macrophage characterization (Murray and Wynn, 2011b). Murine polarized macrophages can be classified into either the M1 phenotype or the alternative M2 phenotype based on two criteria. Those criteria are (1) the specific stimuli that induce a particular phenotype, and (2) the cytokines secreted by the cells upon polarization. "M1 macrophage" refers to macrophages that have been exposed to Toll-like receptor (TLR) ligands or interferon-γ (IFN-γ). These cells not only possess potent microbicidal properties through the production of NO and reactive oxygen intermediates, but also promotes strong Th1 responses through secretion of pro-inflammatory cytokines,

such as interleukin-1 (IL-1), Interferon (IFN)-γ, and IL-12. (Gordon, 2003). In contrast, M2 macrophages produce anti-inflammatory cytokines, such as IL-4/IL13 and IL-10, and are mainly associated with Th2 effector functions, including anti-parasitic activity and tissue repair through the production of polyamines and proline (Sica and Mantovani, 2012). In mice M2 macrophages can be further divided into three functional subpopulations: M2a, (after exposure to IL-4/13), M2b (after exposure to immune complexes in combination with IL-1β or LPS), and M2c (induced by IL-10, tumor growth factor- β (TGF-β), or glucocorticoids) (Martinez *et al*., 2008). M2 also synthesizes arginase, an enzyme that inhibits NO production, allowing M2 macrophages to produce ornithine (a precursor of polyamines and proline) (Chang *et al*., 1998). Interestingly, although M1 and M2 macrophages display distinct phenotypes, the essential metabolic substrate that drives M1 and M2 macrophages through different pathways is identical: the amino acid L-arginine (Stempin *et al*., 2010).

In avian species, the immune-phenotypic polarization of avian primary macrophages has yet to be addressed in detail (He *et al*., 2011). In the past decade, a new way to identify macrophage phenotype based on gene expression profiles has been adopted in the murine model. In that model, M1 macrophage-associated genes have been thoroughly described, but relatively little is known about the functions of individual M2 macrophage-associated genes. Recently, the fundamental knowledge of gene expression in M2 macrophages has rapidly increased due to deletion studies of two M2 macrophage effector genes, *Arg1* and *Retnla* (Murray and Wynn, 2011a). Unfortunately, neither of these genes is known in the chicken.

As shown in Table 1, various other genes appear to be preferentially expressed in either M1 or M2 mouse macrophages (M1 *vs.* M2: SOCS3 *vs.* SOCS1, iNOS *vs.* Arginase, STAT1 *vs.* STAT3, and FtH *vs.* TfR) (Briken and Mosser, 2011; Corna *et al*., 2010; Sica and Mantovani, 2012; Whyte *et al*., 2011). Extension of these gene expression profiles to chicken macrophages would be particularly useful because most reliable markers for mammalian macrophages are not available for chicken macrophages. As a consequence, identifying chicken macrophage phenotypes is a challenge.

The current fundamental knowledge of mammalian macrophage biology relies mostly on the analysis of peritoneal macrophages, which have been widely used as a source of primary macrophages (Turchyn *et al*., 2007). A growing body of evidence suggests that two functionally and phenotypically distinct subsets of macrophages (resident *vs.* elicited) *co-exist* in the abdominal cavity of mice upon stimulation with inflammatory stimuli. Moreover, resident and elicited macrophages can be clearly distinguished by a series of different surface markers (Ghosn et al., 2010; Idoyaga et al., 2011).

In contrast to mice, chickens lack resident macrophages in their abdominal cavity. However, macrophages can be recruited rapidly and extensively into the abdominal cavity if appropriate stimuli are applied (Klasing, 1998; Sabet *et al*., 1977). The most commonly used stimulus and technique for the avian model consists of injecting chickens intraperitoneally with Sephadex G-50 (8 ml of 3% (w/v) Sepharose G-50 suspension in PBS) and then harvesting elicited macrophages 42 hours post-injection by peritoneal lavage (Qureshi *et al.*, 2000; Sabet *et al*., 1977). Chicken PEMs undergo functional maturation over time and can effectively bind, internalize, and degrade

bacteria by lysosomal acid hydrolysis (Golemboski *et al*., 1990). Although Sephadex-elicited macrophages are considered activated, they require additional activation signals in order to acquire further specialized effector functions, such as anti-tumor activity (Qureshi and Miller, 1991).

Chicken elicited PEMs are the only abundant source of macrophages available for the study of avian macrophage biology and detailed features of macrophage polarization remain unclear. Next to the injection of Sephadex G-50, which is obviously an experimental manipulation, a biologically relevant event, *i.e.* internal ovulation, also elicits macrophage influx into the abdominal cavity for the purpose of clearing yolk particles (Nili and Kelly, 1996). Recently, the effects of intraperitoneally injections with egg yolk on chicken peripheral blood monocyte-derived macrophages were investigated *in vitro* (Cornax *et al.*, 2013). Egg yolk was reported to decrease the expression of pro-inflammatory cytokines and the production of NO by chicken monocyte-derived macrophages (Cornax *et al*., 2013). This partial phenotyping provides evidence showing that exposure to egg yolk skews the macrophage phenotype towards M2. However, the details of the functional phenotype and the mechanism of macrophage polarization caused by egg yolk particles require further study.

Since elicited peritoneal macrophages provide the major source of cells for studying chicken macrophage biology, it is crucial to understand and characterize their functions and the mechanism of macrophage polarization following different eliciting stimuli (Sephadex G-50, *vs*. egg yolk). Utilizing functional assays and gene expression profiling

will hopefully help us better understand avian macrophage biology and potentially aid in the characterization of novel Mabs against Sepharose-elicited peritoneal macrophages.

Experimental design

Our experiments were designed to test the hypothesis that avian macrophages can change their functional phenotype in response to micro-environmental influences. To determine the *ex vivo* levels of arginase enzymatic activity in S-PEMs and Y-PEMs, the arginase assay was performed immediately after PEMs were obtained from the peritoneal cavity of the bird and therefore were designated as "*ex vivo"*. Elicited PEMs were purified by plastic adherence (a protocol that takes several hours) were stimulated with LPS (5 μg/ml) for 8 hours. Since this stimulus was introduced several hours *after* the isolation and purification of the cells from the peritoneal cavity, this experimental treatment was designated as "*in vitro".* After *in vitro* LPS stimulation, the functional phenotype of the cells was assessed using iNOS and (again) arginase enzymatic activity assays. Relative gene levels of eight of the most frequently cited genes in the context of macrophage polarization studies in mammals were measured in both *ex vivo* and *in vitro* groups using real-time PCR. The genes characteristic for M1 polarization included SOCS3, iNOS, STAT1, and FtH, while the genes pointing towards the M2 phenotype included SOCS1, arginase, STAT3 and TfR (see Table 1). Relative mRNA levels of arginase *vs.* iNOS ratio frequently used as an indicator of macrophage polarization and relative mRNA levels of SOCS1 to SOCS3 recently proposed as a new readout for macrophage polarization were also evaluated using real-time PCR.

Materials and methods

Peritoneal exudate macrophage preparation

Peritoneal exudate macrophages were prepared according to previous publication with minor modifications (Cornax *et al*., 2013; Sabet *et al*., 1977). Female Leghorns were given a single intraperitoneal injection with 8 ml of 3% (w/v) Sephadex G-50 (Sigma) suspension in PBS or 5 ml of 50% (v/v) egg yolk in PBS with a 23-gauge needle. The optimum injection site was found to be: anatomical lower left, anterior-lateral, abdominal quadrant (i.e. 10 to 15 mm lateral to the mid-sagittal plane and 10 to 20 mm cephalad to the cloacal pore). Forty-two hours (Sephadex) or 30 hours (egg yolk) post injection (p.i.) the chickens were sacrificed, the peritoneal cavity opened, and the PECs were harvested by peritoneal lavage with 25 ml sterile PBS. Usually, 20 to 25 ml of cell suspension was harvested. The suspension was centrifuged at 270 *x g* for 10 min and the supernatant was discarded. The cell pellet was resuspended and carefully layered onto Histopaque-1077 (Sigma) in a 1:1 ratio, followed by centrifugation at 400 *x g* for 30 min at room temperature to separate the mononuclear cells. Peritoneal exudate macrophages (PEMs) were further purified by culture in a plastic flask for 4 h at 37˚C and 5% CO_2. The non-adherent cells were removed by washing with warm RPMI1640 medium (Sigma). The adherent cells were detached and harvested with Accutase (Invitrogen; applied for 10 min at 37^{o}C). The purity of the detached cells was evaluated by Giemsa stain. Over 90% of the plastic-adherent cells were morphologically identified as macrophages. Purified PEMs were then used in functional phenotyping and gene expression profiling assays.

Quantification of arginase enzymatic activity

To detect arginase enzyme activity in macrophages, the arginase assay was carried out according to previous published protocols (Chang *et al*., 1998). To detect arginase activity in both *ex vivo* and *in vitro* groups of S-PEMs and Y-PEMs, 3 x 10^6 PEMs were rinsed with ice-cold DPBS twice, detached by incubation with commercially obtained Accutase solution (Invitrogen) at 37^{o}C for 10 min, and then centrifuged at 250 *x g* for 5 min. Cell pellets were resuspended in 200 µl lysis buffer (1 M Tris-Cl, pH=7.4, 5M NaCl, and 1% Triton X-100) containing 1% (w/v) protease inhibitor (Sigma; P2714) at 4^{o}C for 2 h. Cell lysate was added to 50 µl of Tris-HCl buffer (50 mM, pH=7.5) containing 10 mM $MnCl_2$ and the mixture was incubated for 10 min at 55-60˚C to activate macrophage arginase. The hydrolysis reaction of L-arginine was carried out by incubating the cell lysate with 50 µl L-arginine (0.5M; pH=9.7) at 37 ˚C for 1 h. The reaction was stopped by adding 400 µl of an acid mixture consisting of H_2SO_4, H_3PO_4, and H_2O in the ratio of 1:3:7. α-isonitrosopropiophenone [25 µl, 9%; dissolved in 100% ethanol (w/v)] was then added to the mixture, followed by heating to 100^{o}C for 45 min. After the mixture was incubated in the dark for 10 min at room temperature, the urea concentration was determined spectrophotometrically by measuring the absorbance at 550 nm with a Wallac plate reader (PerkinElmer Inc., Waltham, MA). The rate of urea production was used as an index for arginase enzymatic activity.

Detection of nitric oxide (NO) synthase enzymatic activity with the Griess assay

To detect the concentration of NO synthesized by chicken S-PEMs and Y-PEMs upon stimulation with LPS *in vitro*, chicken S- and Y-PEMs (1×10^6) were cultured in a 24-well cell culture plate in the presence or absence of LPS (5μg/ml; Sigma) in an atmosphere of 5% CO_2 at 37 ^oC for 8 h. Nitrite concentration, a measure of NO synthesis, was assayed in 50 μL of culture supernatant using the Griess reagent essentially as previously described (Bingaman *et al*., 2000; Shoda *et al*., 2000; Shoda *et al*., 2001a; Shoda *et al*., 2001b). Briefly, 100 μL sulfanilamide solution [1% (w/v) sulfanilamide (Sigma) in 2.5% (v/v) phosphoric acid in MQ-water] was added to the supernatants, followed by addition of 100 μL naphthylethylenediamine dihydrochloride solution [0.1% (w/v) naphthylethylenediamine dihydrochloride (Sigma) in 2.5% (v/v) phosphoric acid in MQ-water)]. Absorbance at 550nm (A_{550}) was measured and compared to that of a freshly prepared $NaNO_2$ standard curve constructed to range from 0 to 160 μM. The mean micromolar concentration of nitrite was calculated from triplicate culture wells (± standard deviation). Differences in concentrations of accumulated nitrite were analyzed for statistical significance using the t-test.

RNA extraction and reverse transcription

To determine the gene expression profile in S-PEMs, Y-PEMs, and their respective activated phenotypes, approximately 3×10^6 PEMs were used. Total RNA extraction was performed using Trizol Reagent (Invitrogen, Carlsbad, CA) according to the manufacturer's instructions. RNA yield was measured with a Nanodrop-1000 (Thermo

Scientific). The 260/280 absorption ratio was used as an estimate of RNA quality. Extracted RNA was stored at -80^{o}C until used. Genomic DNA contamination was removed by incubation of the samples with DNase using the TURBO DNase Free kit (Invitrogen Carlsbad, CA). Reverse transcription was carried out on 100 ng of RNA with the SuperScript II reverse transcription kit (Invitrogen, Carlsbad, CA).

Gene expression profile by quantitative Real-time PCR

Quantitative real-time analysis was performed on a 7500 Fast Real-time PCR System (Applied Biosystems). Genes and primers used in qPCR are shown in Table 2, RNA detection was performed using *Power* SYBR Green PCR Mastermix (Applied Bioscience). Most frequently used gene markers in mammals were assessed by quantitative real time PCR (Table 3). The 20 µl reaction mixture contained 10 µl SYBR PCR Mastermix, 1 µl cDNA, and 200 nmol/L of forward and reverse primers. The PCR cycle consisted of an initial 10 min denaturation step at 95˚C, followed by 40 cycles of denaturing (95˚C for 15 seconds) and annealing/extend (60˚C for 60 seconds). All the data were analyzed by Student's t-test. P-values of less than 0.05 were considered significant. Quantification of the relative expression level of the gene of interest was performed according to the Livak method (Livak *et al.*, 2001). All data were normalized to blood monocyte GAPDH Ct values.

Table 2. Primer sequences used in macrophage phenotyping

Primer Name	Direction	Primer sequence	References
SOCS3	Forward	5' – TTCCCCTCGTTCTGGGAGAT – 3'	Primer3/ NM_204600.1
	Reverse	5' – TCCTTTCTCGGGCACAACTC – 3'	
SOCS1	Forward	5' – CAATGCAGTTGCAGCAGACC – 3'	Primer3/ NM_001137648.1
	Reverse	5' – GTAACCTCGAGCCTGAGAGC – 3'	
STAT1	Forward	5' – AGCGGGATGACTCAGTGGTA – 3'	Primer3/ NM_001012314.1
	Forward	5' – GATACGTTGTTGGCTGCGTG – 3'	
STAT3	Forward	5' – AGTGCTTTCGTGGTGGAGAG – 3'	Primer3/ NP_001026102.1
	Reverse	5' – CTTTGGTGGTGAACTGCACG – 3'	
ARG	Forward	5' – CCACTGCTTGGAGCTTCTCA – 3'	Primer3/ NM_001199704..1
	Reverse	5' – GGAGAACTGGGTGTTGGGAG – 3'	
iNOS	Forward	5' – GCATTCTTATTGGCCCAGGA – 3'	(Dusanic *et al*., 2012)
	Reverse	5' – CATAGAGACGCTGCTGCCAG – 3'	
FtH	Forward	5' – TCTCTCTTTCTCTCCCGCCA – 3'	Primer3/ NM-205086.1
	Reverse	5' – GCGTACAGCTCCAGGTTGAT – 3'	
TfR	Forward	5' – TACAAACCGAGGCGAAGCAT – 3'	Primer3/ NM_205256.1
	Reverse	5' – AGAGTACCCCTCCAGCCATT – 3'	
GAPDH	Forward	5' – ACTGTCAAGGCTGAGAACGG – 3'	Primer3/ NM_204305.1
	Reverse	5' – ACCTGCATCTGCCCATTTGA – 3'	

Table 3. Gene markers used in macrophage phenotyping in mammalian species

Pro-inflammatory*	**Anti-inflammatory ("scavenger")***
M1 macrophage	M2 macrophage
SOCS3	SOCS1
iNOS	Arginase
STAT1	STAT3
FtH	TfR
Ratio**	
SOCS1/SOCS3 (the higher the ratio, the more "M1 like")	
Arg/iNOS (the higher the ratio, the more "M1-like")	

* The relative mRNA levels of several genes in S- and Y-PEMs were determined by ΔΔCt method. The fold change of each gene was expressed as a relative increase or decrease compared to blood monocyte control.

** The relative mRNA levels used for ratio calculation were determined by ΔCt value. The Ct value is inversely related to the actual mRNA values. A high Ct means a low mRNA content.

Results and discussion

Arginase activity in S- and Y- PEMs

Because arginase has been historically described as a typical M2 macrophage functional enzyme, we first examined the arginase activity in both sources of PEMs. As shown in Fig. 8, arginase activity is significantly higher in S-PEMs compared to the enzyme activity in Y-PEMs ($P<0.01$). No difference in arginase activity was observed between Y-PEMs and blood monocyte baseline expression control. After stimulation with the M1 stimulant LPS, arginase activity did not change significantly in either cell type (Fig. 8).

In mice, exposure of macrophages to M2-inducing stimuli induced high arginase expression levels (Gordon, 2003). The anti-inflammatory and scavenger properties make Y-PEMs an ideal model for M2 macrophage phenotype research (Cornax *et al*., 2013). Surprisingly, our results showed Y-PEMs contain less arginase activity than inflammatory chicken macrophage S-PEMs.

In mice, several reports indicate arginase activity can not only be up-regulated by Th2 cytokines but also by various inflammation-inducing agents, such as casein and thioglycollate (Munder, 2009). The role of arginase in inflammation has been demonstrated by the fact that TLR-activated M1 macrophages also up-regulated their arginase activity by bypassing the IL-4 or IL-13 receptors and directly activating the arginase enhancer (El Kasmi *et al*., 2008; Louis *et al*., 1998). Djeraba *et al*., (2002) also

reported arginase activity is not only up-regulated by TGF-β and PGE_2, but M2-inducing stimuli. Arginase also appears to be up-regulated in LPS/IFN-γ-activated macrophages

.

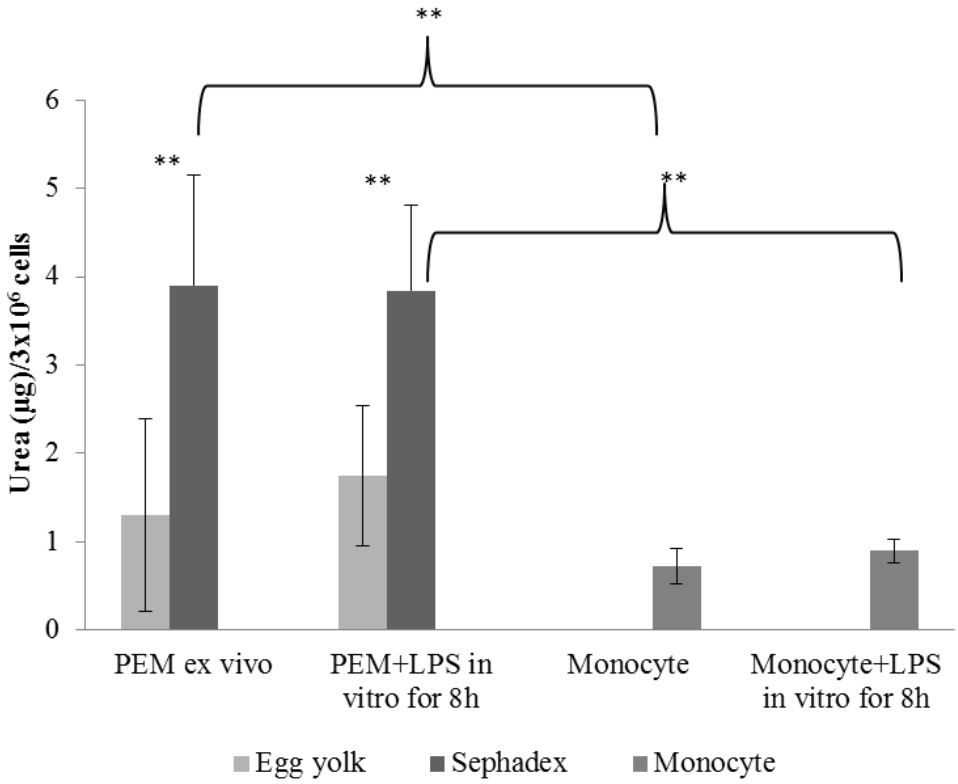

Figure 8. Arginase activity in Sephadex- and egg yolk-elicited PEMs *ex vivo* and after *in vitro* LPS stimulation. Blood monocytes isolated from PBS-injected chicken were used as baseline control. The results are expressed as mean ± SD (n=5; *** $p<0.001$, **$p<0.01$, *$p<0.05$).

in B^{13}/B^{13} chickens, which are highly susceptible to Marek's disease. Thus, in the light of our data, we can conclude that using arginase activity as a "specific" marker for M2 macrophage phenotyping in chicken remains somewhat controversial. Arginase activity is inducible and expressed at higher levels in M1 macrophage *ex vivo* in the chicken.

Evaluation of NO producing capacity of Y- and S-PEMs after stimulation with LPS

As shown in Fig. 9, LPS-activated S-PEMs produced significantly higher levels of NO ($P<0.05$) compared to LPS-activated Y-PEMs. Vigorous production of NO after stimulation with LPS/IFN-γ is the hallmark of M1 macrophages (Classen *et al*., 2009). The formation of NO is also associated with the ability of macrophages to deplete tumor cells of iron-sulfur prosthetic groups (Qureshi *et al*., 2000). This finding is consistent with the previous report by Cornax *et al*. (2013) that exposure to egg yolk limited macrophage NO production. This suggests egg yolk may indeed down-regulate mRNA expression of pro-inflammatory cytokines (such as IL-1, IL-8, and IFN-γ) in chicken macrophages *in vitro* (Cornax *et al*., 2013). Our results (Fig. 9) indicate that both NO production (iNOS activity) and arginase activity were higher in S-PEM inflammatory-type macrophages in the chicken. In our hypothesis, chicken S-PEMs and Y-PEMs polarize towards the M1 and M2 phenotype, respectively

Based on NO production patterns we can still conclude that S-PEMs are M1 macrophages and that Y-PEMs are more likely shifted to the M2 phenotype, despite the apparent conflict on chicken macrophage arginase activity with the murine model. Currently, very little is known about arginase activity in chicken macrophages. The

regulation of arginase in chicken macrophages is still under debate and may indeed be different than in murine macrophages. (Djeraba *et al*., 2002).

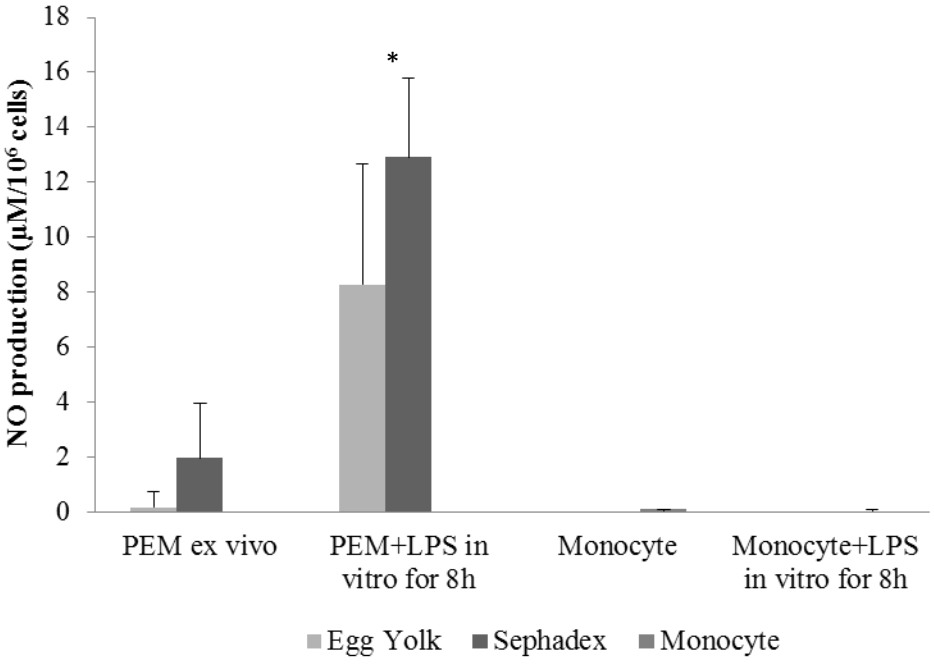

Figure 9. NO production by *ex vivo* and *in vitro* LPS-stimulated Sephadex- and egg yolk-elicited PEMs. Monocytes isolated from PBS-injected chicken used as baseline control. The results are expressed as mean ± SD (n=5; *** $p<0.001$, ** $p<0.01$, * $p<0.05$).

Gene expression profiles in S-PEMs and Y-PEMs, ex vivo or after in vitro LPS stimulation

Comparison of Arg II and iNOS mRNA expression

In *ex vivo* preparations, LPS stimulation down-regulated Arg II and but up-regulated iNOS mRNA expression in S-PEMs, (-2.985 ± 0.409 *vs.* 2.544 ± 1.064 fold change, respectively), both when compared with blood monocytes. In contrast, in *ex vivo* Y-PEMs, the mRNA expression of Arg II and iNOS mRNA expression (-5.258 ± 4.653 *vs.* -7.554 ± 1.994 fold change, respectively) were both down-regulated. Arg II gene expression did not show statistically significant differences between S- and Y-PEMs. However, iNOS mRNA expression was significantly higher in *ex vivo* S-PEMs than in *ex vivo* Y-PEMs ($P<0.05$, Table 4 and 5). *In vitro* LPS stimulation resulted in Arg II mRNA expression being up-regulated in both S- and Y-PEMs. The increased mRNA expression did not reflect the functional enzyme activity levels observed in both types of PEMs, which were not influenced by LPS stimulation (Fig. 8).

Arginase and iNOS mRNA expression are the most commonly used indicators in macrophage functional phenotyping in mice (Chiang *et al.*, 2008). The mRNA expression of Arg II and iNOS in avian S-PEMs is consistent with observations in M1 macrophages in mice (Mullner *et al.*, 2002). The down-regulation of iNOS mRNA levels in *ex vivo* Y-PEMs is expected and consistent with our results of NO production in the previous functional assay. Egg yolk is an anti-inflammatory immunostimulant by nature (Cornax *et al.*, 2013). Walzem *et al.* (1994) and others demonstrated egg yolk is phagocytosed by chicken macrophages (probably through scavenger receptors) and gets

Table 4. Relative mRNA expression of iNOS and Arg II (fold change) in *ex vivo* and *in vitro* LPS-stimulated Sephadex and egg yolk elicited PEMs.

Gene symbol	*Ex vivo* Sephadex (fold change)[a]	*In vitro* LPS-mediated Sephadex (fold change)[a]	*Ex vivo* Egg yolk (fold change)[a]	*In vitro* LPS-mediated Egg yolk (fold change)
iNOS	2.544±1.064	31.783±7.852	-7.554±1.994	42.050±33.120
Arg	-2.985±0.409	5.40±1.590	-5.258±4.653	8.251±6.537

[a]. All data normalized to blood monocyte control Ct values. The results are expressed as mean ± SD (n=3)

Table 5. Comparison of gene expression profiles in *ex vivo* and *in vitro* LPS-stimulated macrophages.

Gene	Sephadex *Ex vivo* vs. *in vitro* LPS stimulated for 8 h[a]	Sephadex vs. Egg yolk *Ex vivo* [a]	Egg yolk *Ex vivo* vs. *in vitro* LPS stimulated for 8 h [a]	Sephadex vs Egg yolk In vitro LPS-stimulated for 8 h[a]
iNOS	*	*	NS	NS
Arg	**	NS	NS	NS

[a]. n=3; NS: non-significant, *** p<0.001, **p<0.01, *p<0.05.

repackaged into novel lipoproteins for secretion into blood stream (Barron *et al*., 1999; Walzem *et al*., 1994). Egg yolk also inhibited LPS-induced mRNA expression of pro-inflammatory cytokines (IL-1, IL-8, and IFN-γ), while leaving IL-10 expression unchanged in chicken macrophages *in vitro*. As previously mentioned, egg yolk inhibited LPS-induced NO production by reducing mRNA expression. The anti-inflammatory effect of yolk was suggested to potentially be mediated by carotenoid (Cornax *et al*., 2013); however, the underlying mechanism is still unclear.

Furthermore, the composition of egg yolk is complicated. One of the components, modified lipoprotein, induced Arg I but not Arg II mRNA expression in mouse macrophages; this effect is mediated by peroxisome proliferator-activated receptor (PPAR) (Gallardo-Soler *et al*., 2008). This indicates the expression of Arg II may not be affected by egg yolk and contribute to the baseline expression of arginase. Arg II mRNA expression can be induced by LPS in the murine model, which is consistent with our results (Morris *et al*., 1998).

The value of the Arg II /iNOS ΔCt ratio as a phenotypic macrophage marker

In this study, the ratio of Arg II to iNOS mRNA levels was determined based on the ΔCt value of each gene as normalized to GAPDH. A higher value for the Arg II/iNOS ΔCt ratio points toward an M1 polarized macrophage phenotype. In this study, the Arg II/iNOS ΔCt ratio was shown to be significantly higher ($P<0.05$) in *ex vivo* S-PEMs compared to both Y-PEMs and blood monocytes (1.661 *vs.* 1.077 and 0.994) with no significant differences between Y-PEMs and blood monocytes (Fig. 10). After LPS

stimulation *in vitro*, the Arg II/iNOS ΔCt ratio significantly increased ($P<0.01$) in Y-PEMs (2.549), and a numerical but statistically non-significant increase was observed in S-PEMs (Fig. 10).

As mentioned above, the Arg II/iNOS ΔCt ratio is often used as a functional indicator for determining macrophage phenotypes. In our experiments, the Arg II/iNOS ΔCt ratio indicates *ex vivo* S-PEM phenotype was shifted towards M1. However, after *in vitro* LPS activation, the Arg II/iNOS ΔCt ratio was no longer different between S-PEMs and Y-PEMs, indicating that chicken macrophages indeed have the capacity to change their phenotype in response to the microenvironmental queues they are exposed to *in vitro*. Therefore, with regard to phenotypic plasticity, avian macrophages are similar to their mammalian counterparts (Stout *et al*., 2005).

Ferritin Heavy chain (FtH) mRNA vs. Transferrin Receptor (TfR) mRNA

In our study, the level of FtH mRNA expression was shown to be significantly higher ($P<0.05$, Table 6) in *ex vivo* S-PEMs than *ex vivo* Y-PEMs (14.597 ± 4.015 vs. 3.101 ± 2.204)(Table 6). On the other hand, TfR mRNA expression was slightly up-regulated in *ex vivo* S-PEMs (compared to blood monocyte controls), but down-regulated in Y-PEMs ($P<0.05$, 1.569 ± 0.368 vs. -3.979 ± 1.84) (Table 6 and 7). After LPS activation *in vitro*, FtH mRNA expression in both sources of PEMs was down-regulated compared to the control blood monocytes (-4.798 ± 1.023 *vs.* -1.728 ± 0.484)(Table 7). TfR mRNA

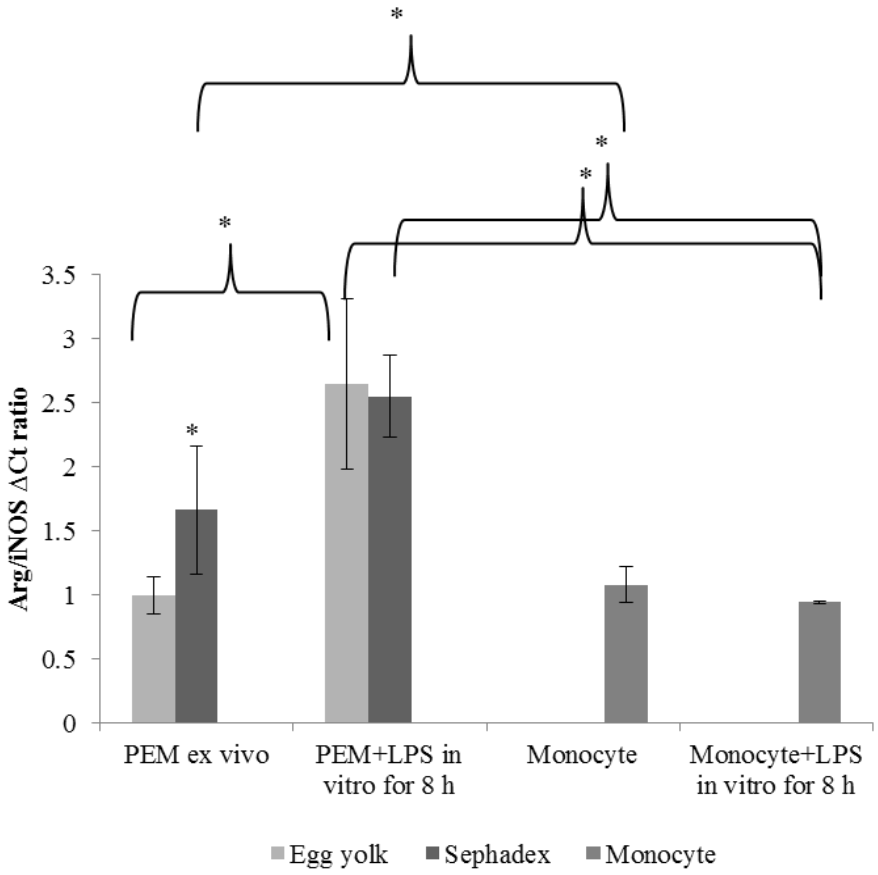

Figure 10. The Arg II/iNOS ΔCt ratio in *ex vivo* and *in vitro* LPS-stimulated Sephadex- and egg yolk-elicited PEMs. Blood monocytes isolated from PBS-injected chicken used as baseline control. The results are expressed as mean ± SD (n=3; *** $p<0.001$, ** $p<0.01$, * $p<0.05$).

Table 6. Relative mRNA expression of FtH and TfR (fold change) in *ex vivo* and *in vitro* LPS-stimulated Sephadex and egg yolk elicited PEMs.

Gene symbol	*Ex vivo* Sephadex (fold change)[a]	*In vitro* LPS-mediated Sephadex (fold change)[a]	*Ex vivo* Egg yolk (fold change)[a]	*In vitro* LPS-mediated Egg yolk (fold change)[a]
FtH	14.597±4.015	-4.798±1.023	3.101±2.204	-1.728±0.484
TfR	1.569±0.368	8.451±1.687	-3.979±1.84	4.470±0.672

[a.] All data normalized to blood monocyte control Ct values. The results are expressed as mean ± SD (n=3)

Table 7. Comparison of gene expression profiles in *ex vivo* and *in vitro* LPS-stimulated macrophages.

Gene	Sephadex *Ex vivo* vs. *in vitro* LPS stimulated for 8 h[a]	Sephadex vs. Egg yolk *Ex vivo* [a]	Egg yolk *Ex vivo* vs. *in vitro* LPS stimulated for 8 h [a]	Sephadex vs Egg yolk In vitro LPS-stimulated for 8 h[a]
FtH	*	*	*	*
TfR	*	*	**	*

[a]. n=3; NS: non-significant, *** p<0.001, **p<0.01, *p<0.05.

expression in both sources of cells was up-regulated (8.451 ± 1.687 vs 4.470 ± 0.672)(Table 7).

Iron is a key nutrient and limiting factor of bacterial growth (Corna *et al*., 2010). Iron handling was recently suggested as one of the indicators of functional polarization of macrophages in mammals (Recalcati *et al*., 2010). FtH and TfR play opposite roles in the handling iron by macrophages and have been described as novel indicators of macrophage polarization in murine models (Corna *et al*., 2010; Recalcati *et al*., 2010). M1 macrophages limit the availability of iron in circulation which could deter invading pathogens. In contrast, M2 macrophages lack the typical iron-withholding mechanism present in M1 macrophages (Kakhlon and Cabantchik, 2002).

The gene expression patterns of FtH and TfR in S-PEMs *ex vivo* are consistent with the M1 phenotype in mice *in vitro* (Corna *et al*., 2010). The results suggest that Sephadex recruits blood monocytes to enter the peritoneal cavity; they become S-PEMs and undergo functional maturation into inflammatory type macrophages. In previous studies, S-PEMs showed an increased expression of TfR on their cell surface throughout the maturation process inside the peritoneal cavity *in vivo* (Golemboski *et al*., 1990). This could explain the slightly increased TfR mRNA expression immediately after purification in S-PEMs (42 hours p.i. of Sepharose). The strongly elevated levels of mRNA expression of FtH (an almost a 15-fold upregulation of FtH mRNA was observed) indicate the S-PEMs harvested in our studies displayed a phenotype skewed towards M1 in order to increase their Fe withholding capacity from the microenvironment. Furthermore, a reduction of iron in the circulation was also shown to activate T-cell-

dependent antimicrobial adaptive immunity, favoring the shift towards Th1 responses (Mencacci *et al*., 1997; Omara and Blakley, 1994).

In the current study, *ex vivo* Y-PEMs expressed high levels of FtH (3-fold up-regulation) but low levels of TfR (3-fold down-regulation). The relatively high *ex vivo* expression of TfR mRNA in Y-PEMs was phenotypically opposite to what was observed in murine M2 gene expression *in vitro* in mammals (Recalcati *et al*., 2010). TfR is a carrier protein needed for transport of iron into macrophages and is regulated by intracellular iron concentration. Low iron concentrations induce increased levels of TfR to increase iron intake into the cells. Cornax *et al.* (2013) observed that egg yolk increased plasma iron concentrations greatly, because of the rich source of phosphoprotein-bound iron (Cornax *et al*., 2013). This could be a reason that TfR mRNA expression levels did not increase in Y-PEMs. The concentration of iron in the milieu could be an important factor controlling the expression of TfR mRNA.

In mice, stimulation of macrophages with IFN-γ/LPS activates the iron regulatory binding proteins (IRP)-1 and -2, which then inhibits translation of the FtH protein (Weiss *et al*., 1997). In the current study, both S- and Y-PEMs may secrete IFN-γ *in vitro,* and may be regulated in an autocrine fashion in response to the plastic adherence, in synergy with the added LPS stimulus which further inhibits FtH mRNA expression.

Gene expression of STAT1 vs. STAT3 and SOCS1 vs. SOCS3

So far, in this comparative analysis of avian and mammalian macrophages, clear parallels between both systems have been observed. However (as shown in Table 8 and

9) in the postulated avian M2 equivalent, *ex vivo* Y-PEMs, SOCS1, and its upstream regulator, STAT3, clearly don't behave as their mammalian (M2) counterparts. The mRNA expression of SOCS1 was down-regulated in both *ex vivo* sources of PEMs, but this effect was dramatic in *ex vivo* Y-PEMs (-22 fold) compared to blood monocytes (Table 10). Similarly, STAT3 was also down-regulated (-7 fold) in *ex vivo* Y-PEMs (Tables 9 and 10). These discrepancies could result from the differences between species, as seems to be the case in our analysis of arginase activity (Fig. 8). The divergence may simply be the consequence of phylogenetic separation of chickens from mammals about 300 million years ago (Furlong, 2005).

Table 8. Diagrammatic comparison of the gene expression of SOCS1, SOCS3, STAT1, and STAT3 in mice and our current *ex vivo* chicken macrophage models.

	M1		**M2**	
	Mice	**Chicken (*ex vivo S-PEMs)***	**Mice**	**Chicken (*ex vivo* Y-PEMs)**
SOCS1	—	—	↑	↓
STAT3	—	—	↑	↓
SOCS3	↓	↑	—	—
STAT1	↑	↑	↓	↓

— : no change; ↓ : down-regulate; ↑: up-regulate. Arrows in red indicate the genes behave differently between mice and chicken.

Table 9. Relative mRNA expression of SOCS1, SOCS3, STAT1, and STAT3 (fold change) in *ex vivo* and *in vitro* LPS-stimulated Sephadex- and egg yolk-elicited PEMs.

Gene symbol	*Ex vivo* Sephadex (fold change)[a]	*In vitro* LPS-mediated Sephadex (fold change)[a]	*Ex vivo* Egg yolk (fold change)[a]	*In vitro* LPS-mediated Egg yolk (fold change)[a]
SOCS1	-1.378±0.332	-1.419±0.826	-22.802±15.342	-2.061±0.708
SOCS3	-3.196±2.228	3.108±0.600	-1.790±1.168	2.570±0.825
STAT1	2.017±0.249	3.692±1.675	1.423±0.870	16.356±3.104
STAT3	-1.406±0.396	-1.112±0.154	-6.973±6.267	1.150±0.124

[a]. All data normalized to blood monocyte control Ct values. The results are expressed as mean ± SD (n=3)

Table 10. Comparison of gene expression profiles in *ex vivo* and *in vitro* LPS-stimulated macrophages.

Gene	Sephadex *Ex vivo* vs. *in vitro* LPS stimulated for 8 h[a]	Sephadex vs. Egg yolk *Ex vivo* [a]	Egg yolk *Ex vivo* vs. *in vitro* LPS stimulated for 8 h [a]	Sephadex vs Egg yolk In vitro LPS-stimulated for 8 h[a]
SOCS1	NS	*	NS	NS
SOCS3	*	NS	**	NS
STAT1	NS	NS	**	NS
STAT3	NS	NS	NS	***

However, methodological aspects may also help explain the contrast. As previously mentioned, the plastic adherence purification process (which lasts 4 hours) may induce macrophage secretion of pro-inflammatory cytokines such as IL-1, IFN-γ, and TNF-α in an autocrine fashion (Chiang *et al*., 2008). This secretion could result in the inhibitory effect on SOCS1/STAT3 signaling (Bode *et al*., 1999). Our results indicate that mRNA expression of SOCS1/STAT3 in avian macrophages does behave differently compared with mouse macrophages.

The value of the SOCS1/SOCS3 ΔCt ratio as a phenotypic macrophage marker

In the previous section, the *ex vivo* SOCS1 and SOCS3 mRNA expression was demonstrated to behave differently in chickens than in mice. In mice, the M1 macrophage expresses a higher SOCS1/SOCS3 ΔCt ratio than M2 macrophages. However, as shown in Fig. 11, the SOCS1/SOCS3 ΔCt ratio was significantly higher in *ex vivo* Y-PEMs ($P<0.05$) than in *ex vivo* S-PEMs and blood monocytes, respectively. S-PEMs showed a similar SOCS1/SOCS3 ΔCt ratio as blood monocytes. After stimulation with LPS for 8 h *in vitro*, SOCS1/SOCS3 ΔCt ratio decreased in Y-PEMs, while the value of this parameter would be expected to increase after an inflammatory stimulus. However, it showed no differences with control blood monocytes.

In murine M2 macrophages, IL-4 induced SOCS1 up-regulation and subsequent expression of arginase. However, we have demonstrated that chicken arginase activity does not behave as in the murine model. In this study, SOCS1/SOCS3 ΔCt ratio

expression in S- and Y-PEMs was also different compared to mammals, indicating the SOCS ratio cannot be used as a marker of avian macrophage phenotype.

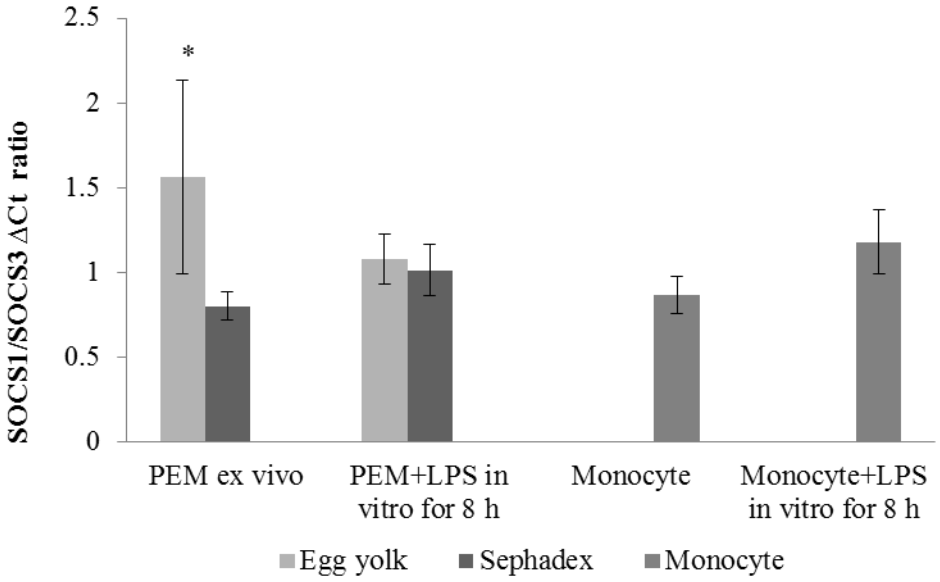

Figure 11. Expression of SOCS1/SOCS3 ΔCt ratio in *ex vivo* and *in vitro* LPS-stimulated Sephadex- and egg yolk-elicited PEMs. Monocytes isolated from PBS-injected chickens were used as baseline control. The results are expressed as mean ± SD (n=3; *** $p<0.001$, **$p<0.01$, *$p<0.05$).

Conclusion

mRNA expression analyses in elicited chicken PEMs *ex vivo* in this study has led to somewhat contradictory conclusions when compared with *in vitro* polarized murine macrophage models. The contradictory gene expression profiles in our two PEMs models, especially in Y-PEMs, may partly result from the methodology used to manipulate the Y-PEMs prior to the mRNA assay procedure, more specifically from the plastic adherence purification step.

Peritoneal exudate cells contain several cell types. In order to enrich the macrophage subpopulation from the exudate, the macrophages were allowed to attach to a plastic surface for several hours, a procedure that is commonly used for this purpose. However, attachment is a priming event for macrophages and thus the gene expression profile could be altered in attached macrophages. This issue has also been reported in the murine models (Krause *et al*., 1996). The mere adherence of monocyte and macrophage to a plastic tissue culture flask could induce expression of a multitude of genes and silence the production of others (Stout *et al*., 2005). Chiang *et al*. (2008) reported peritoneal resident macrophages purified by the adherence method showed significant induction of TNF-α, IL-1α, IL-1β, IL-6, and IFN-γ mRNA expression compared with *in vivo* LPS-activated peritoneal macrophages in murine models.

Chicken Sephadex G-50 elicited peritoneal macrophages represent an inflammatory macrophage population that is highly phagocytic and bactericidal (Qureshi *et al*., 2000). In combination with a strong pro-inflammatory stimulant, S-PEMs can be further activated and are capable of killing tumor cells (Qureshi *et al*., 2003). This priming

effect might not have been very critical for M1 macrophages in our studies. However, the priming effects of plastic adherence may have masked the anti-inflammatory effect of egg yolk, especially with regard to the expression of the SOCS/STAT axis in Y-PEMs. In M2 macrophages, the SOCS1/STAT3 axis is dominantly expressed but can be inhibited by IFN-γ (Sachithanandan *et al*., 2011). The adherence to a plastic surface induces IFN-γ production in macrophages, which then becomes an autocrine pro-inflammatory stimulus. This may have altered the expression of SOCS1/STAT3 pathway in Y-PEMs.

We have demonstrated that some well-defined mammalian macrophage phenotype markers were not recapitulated in chicken macrophages. We found that the arginase activity appeared to be higher than expected in S-PEM inflammatory type macrophages compared to the situation in mammals. In addition, some of the gene expression markers related to cytokine inhibition and activation were likely altered by the adherence purification procedure, especially in the presumed avian M2 equivalent, the Y-PEMs. For example, the SOCS1/SOCS3 mRNA ratio was expected to be high in Y-PEMs, the proposed equivalent of M2 macrophages. However, our results revealed the opposite, suggesting that a simple adhesion purification step may alter or mask responses. This observation suggests that despite the risks of contamination with other cell types, the best way to characterize chicken PEM phenotype might be to directly assay the cells *ex vivo*, immediately following isolation, thus without prior purification.

Taken together, our results clearly suggest Sephadex elicitation skews the phenotype of avian macrophages to the M1 side. In contrast, despite the conflicting gene expression

profiles, we can still conclude that egg yolk elicitation shifts the avian macrophage phenotype towards the M2 pole, especially when taking into account the low level of iNOS mRNA expression.

CHAPTER V

DEVELOPMENT AND CHARACTERIZATION OF NOVEL ANTIBODIES AGAINST CHICKEN PERITONEAL EXUDATE MACROPHAGES

Introduction

The mononuclear phagocyte system (MPS) plays a critical role in host defense and is defined as a group of cells that arises from hematopoietic progenitors in the bone marrow; it consists of circulating blood monocytes and resident tissue macrophages in most of the organs in the body. Macrophages are a heterogeneous group of cells and their subpopulations are polarized depending on the microenvironment from which they were exposed. Until recently, characterization of the differentiation and heterogeneity of macrophages was still defined based on the expression of cell surface markers (such as CD11b, CD68, and F4/80) (Murray and Wynn, 2011a). Specific monoclonal antibodies (Mabs) against cell surface markers have great potential for use in this type of application.

The study of avian macrophages was and still is delayed compared to their mammalian counterparts due to two reasons: (1) relatively few chicken macrophage-specific surface markers have been identified and commercialized, and (2) chickens lack the significant number of harvestable resident macrophages that are commonly used in mammalian species. In 1977, an avian macrophage model system was developed that allowed the isolation of elicited peritoneal macrophages following injection of Sepharose beads (Sabet *et al*., 1977). This avian macrophage model has been used as the

main source of primary chicken macrophages to this day. These elicited chicken peritoneal exudate macrophages (PEMs) are considered to be "primed" macrophages that are already capable of certain activated macrophage functions, such as bacterial killing (Qureshi and Miller, 1991). Sephadex-elicited PEMs (S-PEMs) display characteristics of an increasingly activated state as a function of time after the Sepharose injection into the peritoneal cavity, and can effectively bind, internalize, and degrade bacteria by lysosomal acid hydrolysis (Golemboski *et al*., 1990). Although Sephadex-elicited macrophages are considered activated, they still require additional activation signals in order to acquire more specialized effector functions (Qureshi and Miller, 1991).

In the murine macrophage model, two co-existing but physically, functionally, and developmentally distinct subpopulations of peritoneal macrophages have recently been identified. Furthermore, in the mouse, peritoneal exudate macrophages have been shown to express CD62L (L-Selectin), which supports the idea that peritoneal exudate macrophages may migrate to peripheral lymph nodes and serve as antigen-presenting cells (APCs) if the appropriate stimuli are applied (Idoyaga et al., 2011). Antigen-presenting cells (including dendritic cells [DCs], B-cells, and macrophages) are the bridge between innate and adaptive immunity and are therefore of particular interest to our lab.

Few Mabs have been developed and used to study the heterogeneity of avian macrophages. Trembicki *et al.* (1986) developed two Mabs (CMTD-1 and -2) that selectively reacted with chicken peritoneal exudate macrophages and splenic myeloid

cells, respectively (Trembicki *et al*., 1986). Jeurissen *et al.* (1988) reported a Mab reactive with chicken monocytes, macrophages, and interdigitating cells (Jeurissen *et al*., 1988). Kaspers *et al*. (1993) described a Mab which detected chicken macrophages and thrombocytes (Kaspers *et al*., 1993). More recently, Mast *et al.* (1998) reported a Mab that cross-reacted with chicken macrophage subpopulations of monocytes, macrophages, and interdigitating cells (Mast *et al*., 1998). However, the exact epitope or antigen (Cluster of Differentiation) recognized by these Mabs still remains unknown, and their purported specificity is based on empirical and circumstantial evidence.

Recently, a study from our lab described an anti-chicken CD40 Mab that when complexed with a synthetic peptide, targets APCs and helps induce a rapid and robust systemic IgG response after a single subcutaneous (s.c.) injection (Chen *et al*., 2012). These results indicate Mabs against cell surface receptors can be used to both characterize cell heterogeneity and provide the potential to develop novel immunization strategies.

Ideally, our next target for Mab production would have been chicken CD11c or CD205, because both receptors have been reported as useful targets for *in vivo* immunogen targeting in mammals (Birkholz *et al*., 2010; Tel *et al*., 2011). However, the chicken ortholog for CD11c has not been identified in the chicken genome, and repeated efforts to make antibodies against CD205 have failed due to a lack of a suitable immunogen (results not shown). Therefore, we decided to use primary chicken macrophages as our immunogen and to attempt to identify the cognate antigens of any resulting Mabs *post facto.* In this study, we raised three new Mabs against cell receptors

expressed on Sephadex-elicited chicken peritoneal macrophages and defined the linear epitope recognized by one of these new Mab by using peptide phage display technology.

Materials and methods

Immunogen preparation

Peritoneal exudate macrophages were prepared in essence according to previous publication with minor modifications (Sabet *et al*., 1977). Briefly, female Leghorns were given a single intraperitoneal injection with 8 ml of a 3% Sephadex G-50 suspension in PBS with a 23 gauge needle. The optimum injection site was found to be in the anatomical lower left, anterior-lateral, abdominal quadrant (i.e. 10 to 15 mm lateral to the midsagittal plane and 10 to 20 mm cephalad to the cloacal pore). Forty-two hours post injection chickens were sacrificed, the peritoneal cavity opened, and the peritoneal exudate cells (PECs) were harvested by peritoneal lavage with 25 ml sterile PBS. Usually, 20 to 25 ml of cell suspension was harvested. The suspension was centrifuged at 400 *x g* for 10 min at 4 ˚C and the supernatant was discarded. The cell pellet was resuspended in 3 ml PBS and carefully layered onto Histopaque-1077 (Sigma) in a 1:1 ratio. The cells were then centrifuged at 400 *x g* for 30 min at room temperature to separate mononuclear cells from the PECs. Peritoneal exudate macrophages (PEMs) were further purified using the plastic adherence method described in detail in the previous chapter. The purity of attached cells was evaluated by use of the Giemsa staining method. Based on morphological features, over 90% of the plastic-attached cells were macrophages. Purified PEMs were used for immunizing mice as described below.

Monoclonal antibody production

Monoclonal antibodies against chicken peritoneal macrophages were raised according to previously published protocols used routinely in our lab (Chen et al., 2010b). Three female BALB/c mice received i.p. injections of 5 x 10^6 S-PEMs five times with a three-week interval. The mouse with the best immune response against S-PEMs as judged by immunocytochemistry (ICC) was activated by i.p. injection of 5 x 10^6 PEMs at three and five days prior to splenocyte harvest. The selected donor mouse was sacrificed, a single-cell splenocyte suspension prepared, and splenocytes fused with Sp2/0 myeloma cells (ATCC, Manassas, VA) at a ratio of 2:1 by electrofusion using an Electro Cell Manipulator® ECM 2001 (BTX, Holliston, MA). Hybridomas were plated in 96-well cell culture microplates (Nunc) with addition of cytokines (Berghman et al., 1992) to sustain single parent cell growth and drug selection medium (containing standard concentrations of hypoxanthine, aminopterine, and thymidine (HAT) was applied for seven days. Primary screening was performed by immunocytochemistry (ICC) on day 14 post-fusion using slides coated with S-PEMs or LPS-activated S-PEMs. Briefly, S-PEMs were washed three times with ice-cold PBS, pH 7.4, followed by fixation on poly-L-lysine coated slides using 4% (w/v) paraformaldehyde in PBS, pH 7.4, for 10 minutes. Non-specific binding sites on the cells were blocked for one hour with 10% (v/v) goat serum in TBST [25 mM Tris-HCl, pH 7.6, 0.15 M NaCl, 0.1% Triton X-100 (v/v)] at room temperature. Each slide was then incubated with 3mL hybridoma supernatant at room temperature for four hours, followed by incubation with FITC-conjugated goat anti-mouse IgG (Jackson ImmunoResearch Laboratories, West Grove, PA) diluted 1000-

fold in TBST at room temperature for one hour. Finally, slides were mounted with fluorescence anti-fading reagent containing DAPI (VECTASHIELD). Specific staining on cells was visualized using a Zeiss Axioplan Microscope (Zeiss, Hamburg, Germany) and analyzed using Axio imager software (Zeiss). Fifty-two immunopositive clones were acquired. From the initial 52 observed primary positive clones, the three most promising clones (based on ICC characteristics and hybridoma vigor) were selected for further study in the epitope identification assays described below.

Flow cytometry

In order to identify the antigens corresponding with Mabs 3A8 and 4A5, it would be preferable to perform immunoprecipitation and mass spectrometric analyses. Such studies require a relatively large amount of protein. Therefore, access to alternative sources of the antigen, other than primary macrophages, would be preferable. Therefore, flow cytometric staining was carried out to assess and quantify potential cross-reactivity of our new Mabs with established chicken macrophage cell lines (HD11 and MQ-NCSU) (Beug *et al.*, 1979; Qureshi *et al.*, 1990).

Briefly, Fc receptors on HD11 and MQ-NCSU macrophages were blocked with purified mouse immunoglobulin at 200μg/ml for 30 minutes at 4^{o}C prior to staining, and the Lightening-link labeling kit (Innova Biosciences) was used to directly label Mabs 3A8 and 4A5 (or mouse IgG2b, the negative control) with R-Phycoerythrin according to the manufacturer's instructions. HD11 and MQ-NCSU cells (5×10^{5}) were incubated with various dilutions of R-Phycoerythrin-labeled 3A8 or 4A5 for 30 minutes at 4^{o}C,

followed by fixation with 2% paraformaldehyde in PBS, pH=7.4. Flow cytometric analysis was performed using the FACSCalibur system (BD), and data were analyzed using FlowJo version 8.8.4 software (Tree Star, Inc., Ashland, OR). Data were expressed as percentage of total cells stained specifically by the new Mabs. The levels of staining were shown as median fluorescence intensity (MFI) ratios. Student's t-test was be used to determine significant differences between treatments. The results were expressed as mean ± SD. All data were analyzed using JMP® version 9 software (SAS Institute Inc., Cary, NC).

Epitope mapping by screening with a commercial peptide phage display library

A peptide phage display library (New England Biolabs, Ipswich, MA) was used for epitope mapping in an attempt to directly identify the epitopes recognized by immunopositive hybridoma clones. This filamentous phage library displays linear 7-residue peptides with random sequences on the surface of the M13 phage. The random heptapeptides are fused to the N-terminal end of the phage's minor coat protein (pIII) via a 4-amino acid spacer (GGGS) (New England Biolabs, Ipswich, MA). The library was used according to manufacturer's instructions for screening Mabs 3A8, 3F6, and 4A5. The 7-mer phage display library provides the complexity on the order of 10^9 independent clones, which makes it sufficient to encode 1.28×10^9 possible 7-mer linear amino acid sequences for epitope mapping.

Briefly, purified Mabs 3A8, 3F6, or 4A5 (10μg/ml) were first coated onto 96-wells polystyrene plates in an alkaline bicarbonate buffer (0.1 M $NaHCO_3$, pH=8.6) overnight

at 4˚C. The Mab-coated wells were then blocked with blocking buffer (0.1 M $NaHCO_3$, pH=8.6) containing 5 mg/ml BSA and 0.02% (w/v) NaN_3) for 1 hour at 4˚C. The ELISA plate was washed 6 times with TBST [TBS containing 0.1% (v/v) Tween-20] while avoiding that the wells would dry out.

The phage library was prepared by diluting it 100-fold with TBST (to a working solution of ~2 x 10^9 clones/100 µl), applied to each well, and then incubated for one hour at room temperature. The supernatant was discarded and the wells were washed 10 times with TBST. Bound phages were eluted with 100 µl elution buffer (0.1 M glycine-HCl, pH=2.2) and immediately neutralized by addition of 150 µl neutralizing buffer (1 M Tris-HCl, pH=9.1). An early log phase (OD_{600} = 0.01-0.05) suspension of *Escherichia coli* (ER2783) in LB media containing tetracycline was prepared and the eluted phages were added to 20 ml ER2783 culture and incubated with vigorous shaking for 4.5 hours at 37˚C. The amplified phages obtained from this first panning round were then used as input phages for the next round of biopanning. The same procedures were repeated during two more rounds of screening while increasing the stringency of the washing conditions by increasing Triton X-100 concentration from 0.1%to 0.5% TBST. Phage clones were harvested after the third round of biopanning and individual clones were selected for the extraction of single-stranded phage DNA with iodide buffer (10 mM Tris-HCl, pH=8.0, containing 4 M NaI and 1 mM EDTA). The inserted portions of the phage DNA were sequenced with the -96 gIII sequencing primer 5'-CCCTCATAGTTAGCGTAACG-3' provided by the manufacturer and the nucleotide sequences were used to deduce the amino acid sequence of the encoded 7-mer peptides.

Alignment of the resulting sequences was carried out by use of the BLASTp database on NCBI, ensemble BLAST/BLAT, and UCSC BLAT search genome. The parameters of alignment search were adjusted for short peptide. The window size and the expected value cutoff were adjusted to 2 and 200, respectively. Moreover, the BLOSUM62 scoring matrix was replaced by a more stringent PAM30, as an adaptation to work with short peptides.

The identified epitopes were located in the primary protein sequences and relevant domains were further analyzed using the Kolaskar and Tongaonkar antigenicity scale and Parker hydrophilicity prediction (Kolaskar and Tongaonkar, 1990; Parker *et al*., 1986).

Epitope specificity analysis by ELISA

In order to determine the specificity of the 7-mer peptide (GTHVQAT) acquired after phage display library biopanning, an ELISA binding assay with the synthetic 7-mer biotinylated peptide was carried out. Biotinylated peptide (GTHVQAT) was obtained from Genscript (Piscataway, NJ). Peptide was incubated with goat anti-biotin antibody (Thermo Fisher Scientific Inc.) on a rotator at 37˚C for one hour. A 96-well plate was coated with peptide-goat-antibody complex (10 µg/ml) at 4 ˚C overnight. After washing, 100 µl of 3F6 Mab (10 µg/ml) was added and incubated for 4 hours at room temperature using a different Mab, 3A8, as the negative control. The 7-mer peptide-3F6 complex was then incubated with HRP-conjugated goat anti-mouse secondary antibody (Jackson ImmunoResearch) diluted 1:3000 with 3% (w/v) BSA in PBST for 30 min at room

temperature and washed prior to enzymatic color development. The color reaction was then developed using OptEIA™ TMB substrate (BD) according to manufacturer's instructions. The reaction was terminated by addition of 1N sulfuric acid after incubation at room temperature for 1 min. Absorbances at 450 nm were measured in a Wallac plate reader (PerkinElmer Inc., Waltham, MA).

Results

Primary screening of new Mabs against S-PEMs by ICC

A primary screening of Mabs prepared by hybridoma technology was carried out by ICC against S-PEMs and LPS-activated S-PEMs. As shown in Fig. 12, three (3A8, 3F6, and 4A5) out of 52 clones reacted positively with S-PEM and LPS-activated S-PEMs. The staining patterns strongly suggested that the antigens recognized by the three new Mabs were located on the cell membrane. No positive staining was observed in the negative control (results not shown).

Flow cytometric analysis of chicken macrophage cell lines, HD11 and MQ-NCSU, with Mabs 3A8 and 4A5

As shown in Figs. 13 and 14, Mabs designated 3A8 and 4A5 cross-reacted with 10 to 20% of resting HD-11 and MQ-NCSU cells. Unfortunately, stimulation of the cells with LPS did not increase the percentage of cells reacting with either Mab; actually, the opposite happened. After incubation with LPS, the population of HD11 cells stained with Mab 3A8 significantly decreased from 18.30% to 5.68% ($P<0.01$), with mean

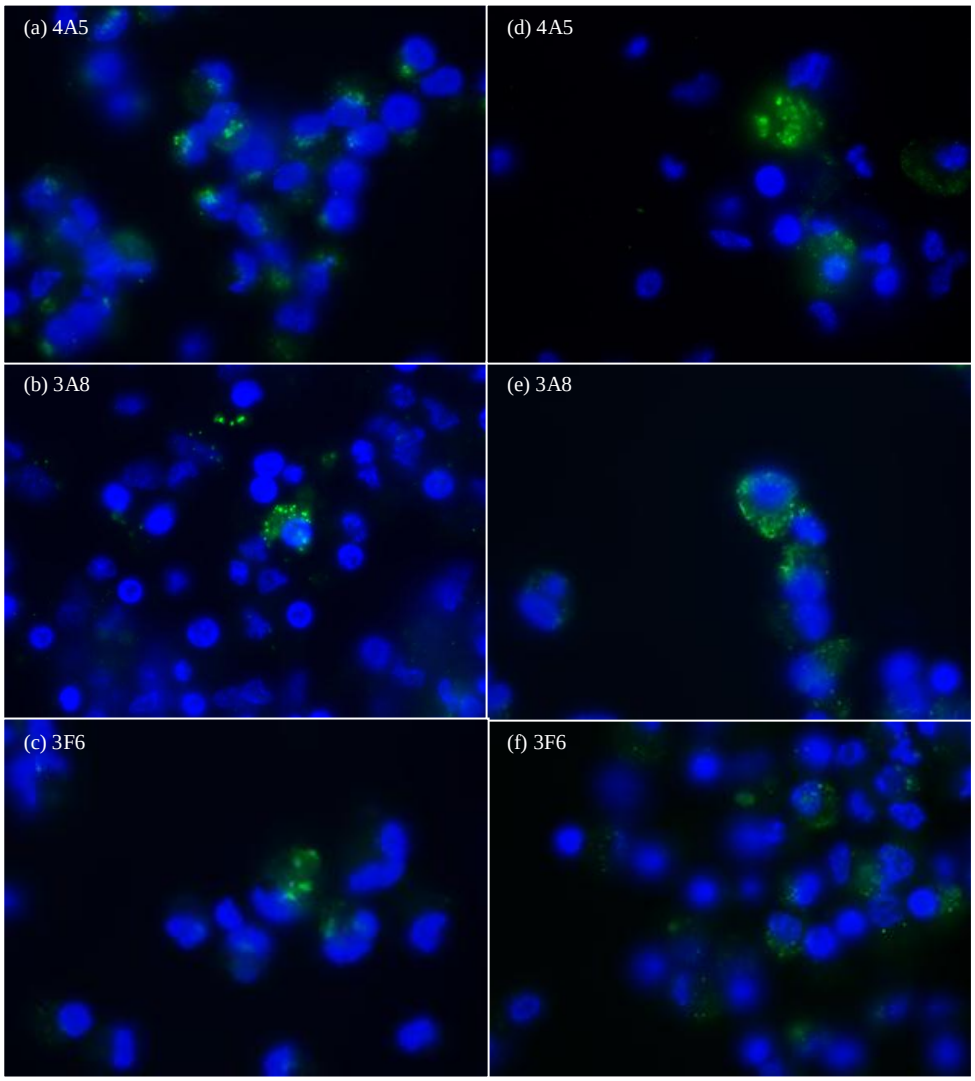

Figure 12. Primary screening of hybridomas raised against S-PEMs by immuno-cytochemical staining of the chicken PEMs. Primary screening of hybridomas raised against S-PEMs by immuno-cytochemical staining of the primary cells used for immunization [(a) 4A5, (b) 3A8, and (c) 3F6] and of LPS-activated S-PEMs [(d) 4A5, (e) 3A8, and (f) 3F6]. Three out of 52 clones reacted positively with S-PEMs. Cells were fixed on poly-L-lysine coated slides using 4% paraformaldehyde in PBS, pH 7.4. FITC-conjugated goat anti-mouse IgG was used for detection. Specific staining on cells was visualized using a Zeiss Axioplan Microscope (Zeiss, Hamburg, Germany) and analyzed using Axio imager software (Zeiss).

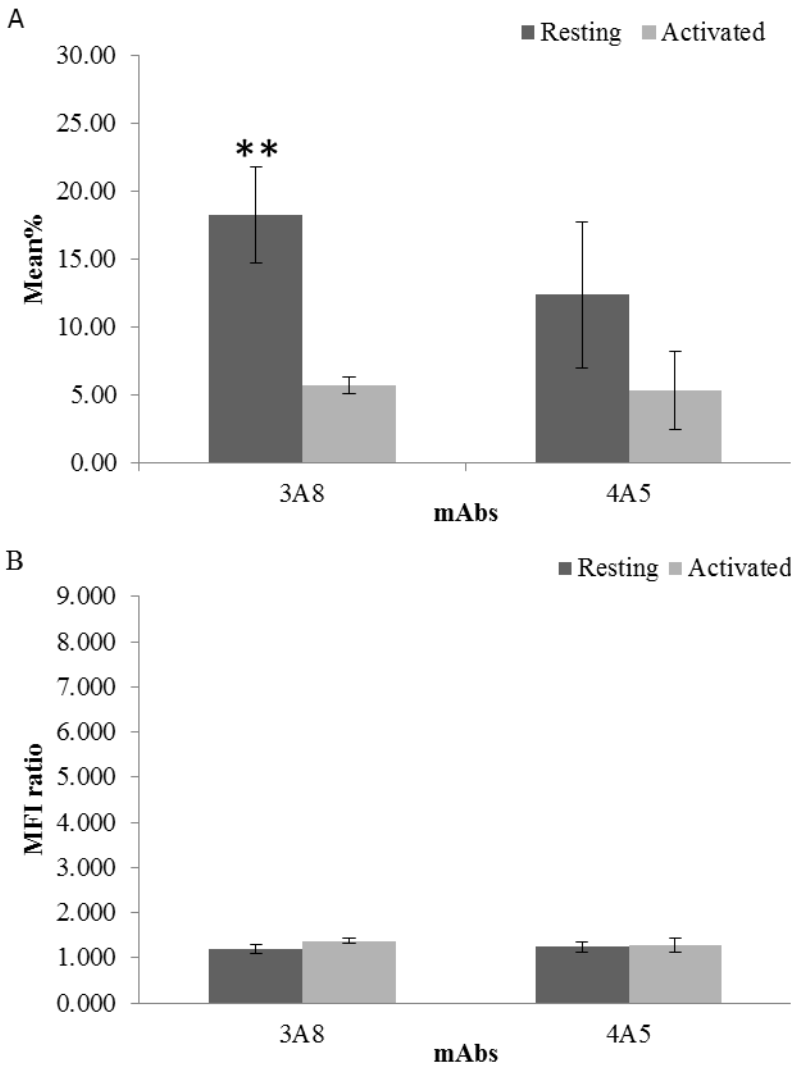

Figure 13. Flow cytometric analysis of HD11 cells using Mabs 3A8 and 4A5. The black bars represent resting HD11 cells and the gray bars represent LPS-activated cells (A) Percentage of HD11 macrophages stained with 3A8 and 4A5. (B) Mean fluorescence intensity (MFI) ratios under resting and stimulated conditions. HD11 macrophages were stained with 5 μg/mL R-Phycoerythrin-labeled 3A8 or 4A5.

fluorescence intensity (MFI) remaining unchanged. Similarly, Mab 4A5 staining on HD11 cells also declined from 12.39% to 5.32% after stimulation with LPS with unchanged MFI (Fig. 13).

The reaction patterns of 3A8 and 4A5 with MQ-NCSU cells were somewhat different; 19.70% and 16.15% of resting MQ-NCSU cells were positively stained with Mabs 3A8 and 4A5, respectively (Fig. 14). After treatment with LPS *in vitro* for 8 hours, the fraction of MQ-NCSU stained with both Mabs slightly decreased; however, the expression levels of antigens (as judged by the MFI values) recognized by Mabs 3A8 and 4A5 on MQ-NCSU cells slightly increased (Fig. 14; $P<0.05$).

One of three Mabs (3F6) recognized a 7-mer peptide displayed by the peptide library after three rounds of biopanning. After sequencing, we found that eleven out of 20 clones displayed a consensus 7-mer motif, Gly-Thr-His-Val-Gln-Ala-Thr (GTHVQAT) (Table 11). The specific interaction of this heptapeptide with Mab 3F6 was further validated by ELISA (Fig. 15). Despite adjusting the parameters of the searching algorithms to improve searching for a 7-mer overlap, no hits were found without mismatches or gaps in the publicly available chicken databases. Nevertheless, several proteins with only a one or two amino acid mismatches or gaps were identified.

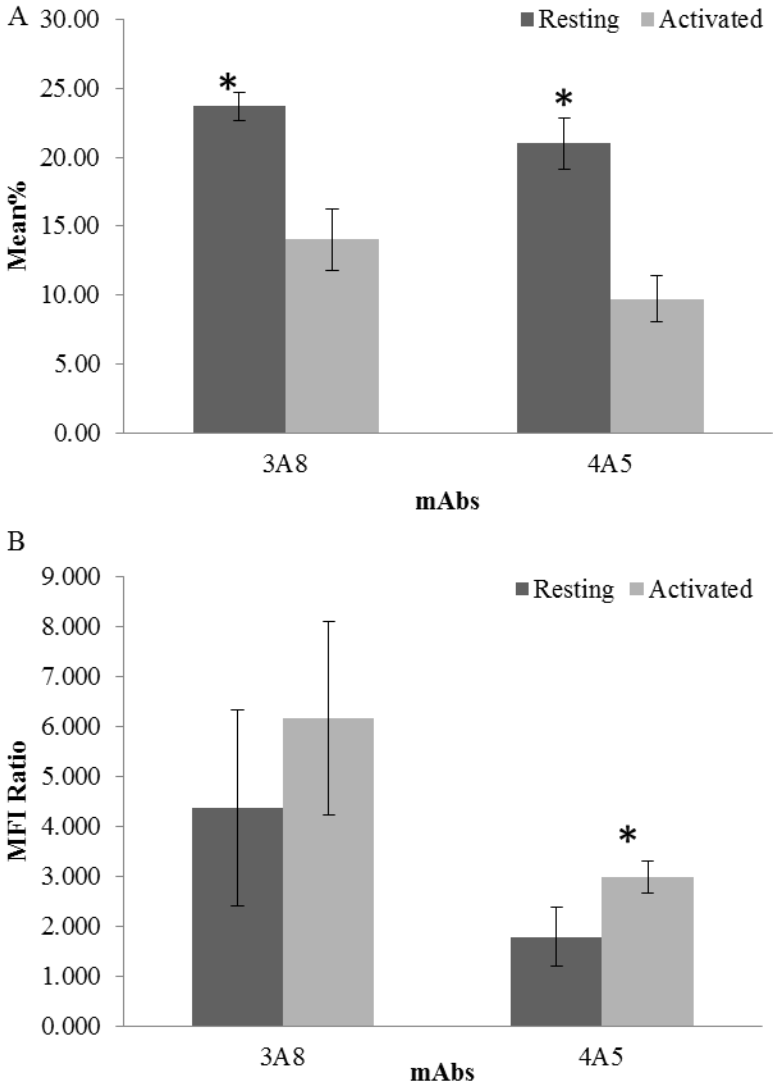

Figure 14. Flow cytometric analysis of MQ-NCSU cells using mAbs 3A8 and 4A5. The black bars represent resting cells and the gray bars represent LPS-activated cells (A) Percentage of MQ-NCSU macrophages stained with 3A8 and 4A5. (B) Mean fluorescence intensity (MFI) ratios under resting and stimulated conditions. MQ-NCSU macrophages were stained with 5 μg/mL R-Phycoerythrin-labeled 3A8 or 4A5.

Table 11. Phage display library screening with Mab 3F6. After three rounds of biopanning with Mab 3F6, 20 phage clones were isolated and sequenced. The phage sequences were aligned using databases available on NCBI, Ensemble, and UCSC.

Antibody	Clones	Epitope Sequence*
3F6	3F6/1	**GTHVQAT**
	3F6/2	GETRAPL
	3F6/3	**GTHVQAT**
	3F6/4	GETLAPL
	3F6/5	**GTHVQAT**
	3F6/6	**GTHVQAT**
	3F6/7	LASVTGQ
	3F6/8	**GTHVQAT**
	3F6/9	**GTHVQAT**
	3F6/10	**GTHVQAT**
	3F6/11	**GTHVQAT**
	3F6/12	VNSAWTY
	3F6/13	NPWIPST
	3F6/14	GFRMCLL
	3F6/15	RASVTGQ
	3F6/17	**GTHVQAT**
	3F6/18	**GTHVQAT**
	3F6/19	GESGGAH
	3F6/20	GETRAPL

*Consensus amino acid residues are highlighted in yellow.

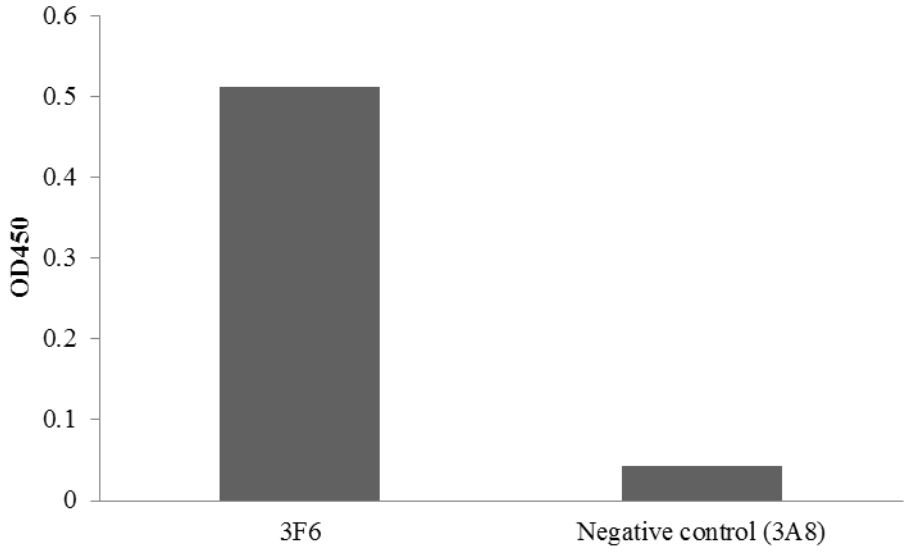

Figure 15. Analysis of peptide binding specificity by ELISA. The 96-well plate was coated with biotinylated 7-mer peptide-goat anti-biotin antibody (10 µg/ml; GTHVQAT) at 4˚C overnight. After washing, 100 µl of 3F6 Mab (10 µg/ml) was added and incubated for 4 hours at room temperature. The 7-mer peptide-3F6 complex was then incubated with goat anti-mouse polyclonal antibody conjugated with HRP (Jackson ImmunoResearch) diluted (1:3000) with 3% BSA in PBST for 30 min at room temperature. MAb 3A8 (an irrelevant Mab at the same concentration) was used as negative control.

Epitope mapping with phage display library technology

The search results of the bioinformatics algorithms were further narrowed down based on the following considerations. First, the staining patterns shown in Fig.12 indicate that the antigen recognized by Mab 3F6 is distributed on the cell surface of S-PEMs. Second, the typical length of a linear B-cell epitope is considered to be in the range of 4 to 20 amino acids (Singh *et al.*, 2013). Based on these premises, the candidate antigens were narrowed down by filtering with the following criteria: 1) classification as a cell surface receptor expressed on APCs and located in an extracellular domain, 2) use of an E-value smaller than 50 as significance threshold, and 3) acceptance of a matched motif at least four amino acid in length. The candidate antigen structure was further analyzed by SMART software (figure not shown; http://smart.embl-heidelberg.de/).

After further adjustment of the E-value to 200, the alignment algorithms revealed two candidate antigens as possible 3F6-binding antigens (Table 12 and 13): CD110 (^{379}HVQAT^{383}) and protocadherin Fat1 (^{3146}TrVQAT^{3151}). The antigenicity and hydrophilicity of the domains matching with the recognized antigens were analyzed by application of the Kolaskar and Tongaonkar antigenicity scale and the Parker hydrophilicity prediction. (http://tools.immuneepitope.org/tools/bcell/iedb_input) (Kolaskar and Tongaonkar, 1990; Parker et al., 1986). Both algorithms indicated that epitopes ^{379}HVQAT^{383}and ^{3146}TrVQAT^{3151} were located within antigenic and hydrophilic regions (Table 13, Fig. 16, and Fig. 17).

Table 12. Sequences producing significant alignments with GTHVQAT (candidate antigens). Eleven out of 20 sequenced phage clones revealed consensus sequences.

Antigen name	Accession number	Identity (%)	Alignment length (aa)	Mismatches	Gaps	E-value
CD110	NP_001001782.1	100	5	0	0	52
Protocadherin Fat 1	XP_420680.2	83	6	1	1	178

Table 13. Motifs and domains recognized by Mab 3F6 in candidate antigens.

Antigen name	3F6 recognized motif*	Domain
CD110	^{379}**HVQAT**^{383}	Type III fibronectin
Protocadherin Fat 1	^{3152}**TrVQA**^{3156}	Cadherin repeats

*Bold letters denote an exact match to the residues of candidate antigens.

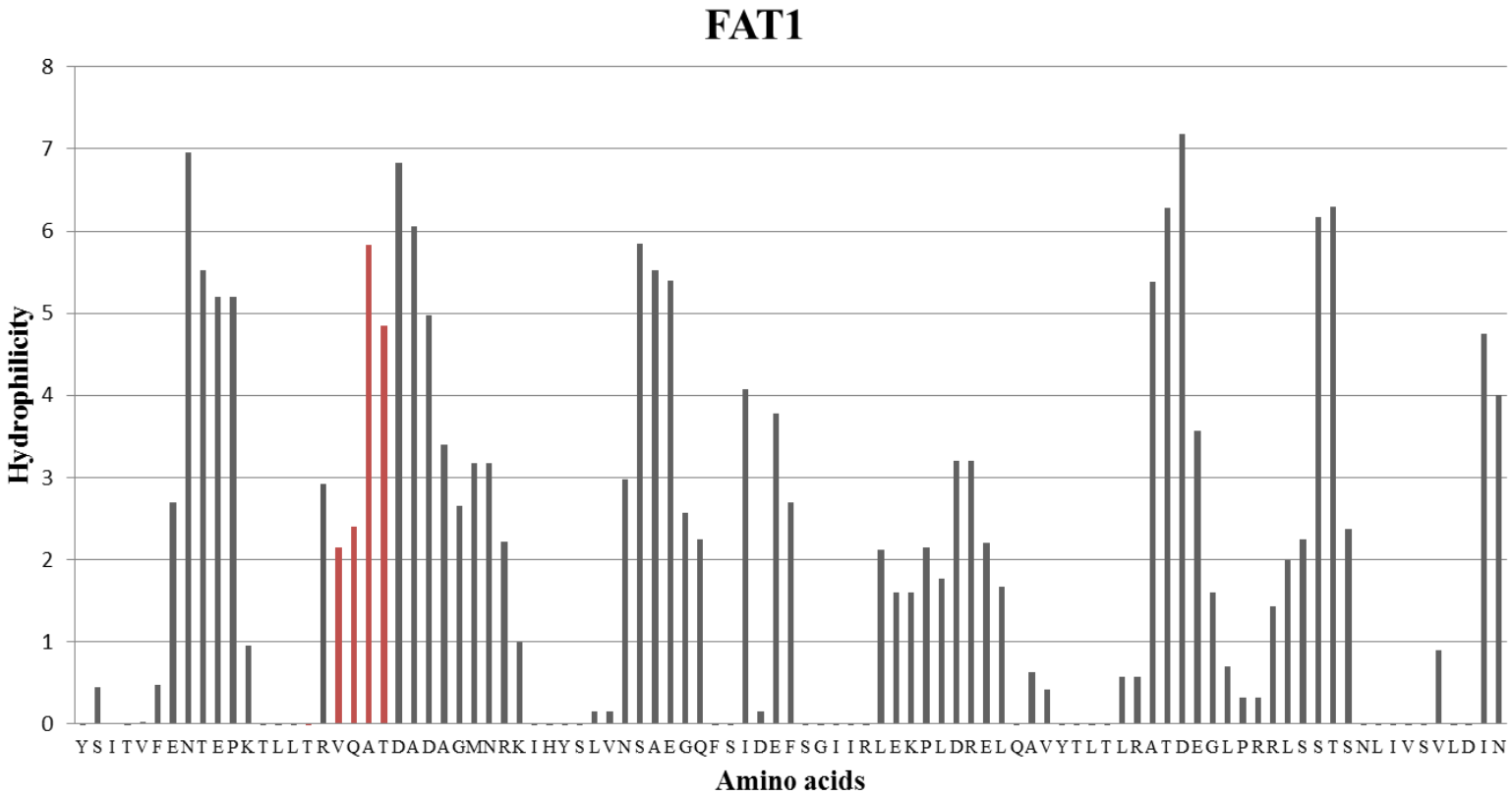

Figure 16. The hydrophilicity of predicted protein Fat1. The hydrophilicity of Fat1 was calculated using Parker hydrophilic prediction (http://tools.immuneepitope.org/tools/bcell/iedb_input). The bars highlighted in red indicate defined epitope by phage display library. Hydrophilicity score higher than 1 was considered as hydrophilic.

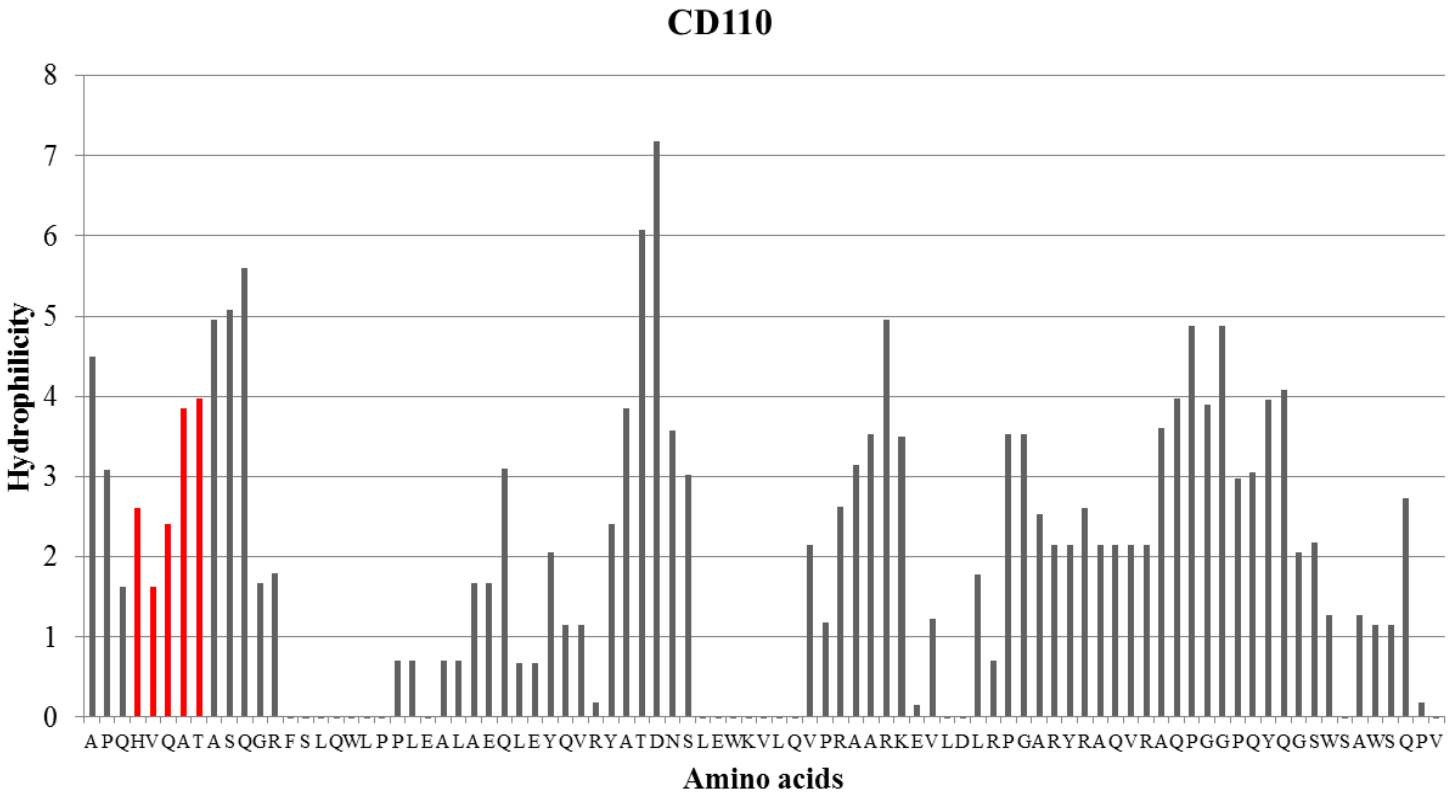

Figure 17. The hydrophilicity of predicted protein CD110. The hydrophilicity of CD110 was calculated using Parker hydrophilic prediction (http://tools.immuneepitope.org/tools/bcell/iedb_input). The bars highlighted in red indicate defined epitope by phage display library. Hydrophilicity score higher than 1 was considered as hydrophilic.

Discussion

A straightforward method to identify the specificity of a new Mab that does not require the availability of the original immunogen is to define the corresponding epitope by peptide phage display. A commercially obtained (New England Biolabs, Ipswich, MA) 7-mer random peptide phage display library displaying 1.28 x 10^9 unique heptapeptides was used for this purpose. However, the limitation of this approach is that such a library only simulates linear peptides, whereas 90% of B-cell epitopes are -at least partially- conformational (Freund *et al*., 2009). As a consequence, not all epitopes can be identified using this phage display library approach. After three rounds of biopanning, Mab 3F6 was shown to interact with an enriched clone of the phage library displaying the heptapeptide GTHVQAT.

Two candidate antigen molecules, CD110 (^{379}**HVQAT**^{383}) and protocadherin Fat1 (^{3146}**T**r**VQAT**^{3151}), were identified *in silico*. B-cell epitopes must be solvent-accessible, so they tend to be on the surface of the antigen, indicating a higher hydrophilicity is necessary. Algorithms designed to identify highly antigenic and hydrophilic properties based on protein primary structure indicated that the target motif GTHVQAT was indeed located in extracellular domains in both antigens. Protocadherin Fat 1 is mostly expressed on smooth muscle cells and plays an essential role in cellular polarization, cell migration, and modulation of cell-cell contact (Moeller *et al*., 2004; Tanoue and Takeichi, 2005). However, to our knowledge, the expression and function of Fat1 on chicken APCs have not been reported. On the other hand, CD110, also called myeloproliferative leukemia virus oncogene (c-Mpl), is a receptor for thrombopoietin

(TPO). Initially, it was thought to only be expressed on megakaryocytes and platelets. However, recent studies indicate that CD110 is also expressed on erythroid, granulocyte-macrophage progenitor cells (Segerer *et al*., 2013). Kawamoto *et al*. (2013) demonstrated that CD110 is expressed on blood-derived monocytes in the presence of TPO (Kawamoto *et al*., 2013). Finally, expression of CXCR4 mRNA (a homing receptor ligand in peripheral lymphoid tissue) has been shown to be up-regulated in the presence of TPO-CD110 ligation in mammals. So far, no literature evidence was published regarding CD110 expression and function in chicken APCs. Despite the high E-value and a partial mismatch in the result, the current study demonstrates that phage display of a random short peptide library is a powerful technique for epitope mapping.

Since Mabs 3A8 and 4A5 were unable interact with the phage display library, the combination of immunoprecipitation, mass spectrometry, and computer-based epitope prediction may be needed in future studies (Katz *et al*., 2007; Shevchenko *et al*., 2006). This will require a sufficiently large amount of S-PEMs as the source of protein. The availability of a consistent and relatively abundant source of antigen for immunoprecipitation is thus a concern, because the generation of primary S-PEMS is relatively complicated and cumbersome process.

Therefore, we have evaluated the possibility of using immortalized chicken macrophage cell lines as a surrogate antigen source. Our analysis has shown that such an approach may be prone to a number of problems.

The flow cytometric results indicated that both Mabs 3A8 and 4A5 stained a surprisingly small fraction of both HD11 and MQ-NCSU cells, and this situation could

not be ameliorated by prior stimulation with LPS. Macrophages frequently change their phenotypes based on the microenviroment from which they are exposed (Davis *et al*., 2013). In some cases, the *in vivo* functional phenotype of primary cells requires the synergy of multiple signals together, and this event cannot be replicated in an immortalized cell model *in vitro* (Chiang et al., 2008; Pan et al., 2009). The components in the peritoneal milieu are complicated, and next to C3b-bound particles, a number of synergizing agonists or antagonists may be involved in the *in vivo* activation of S-PEMs (Stout and Suttles, 2004). Thus, macrophage cell lines culture *in vitro* may not be able to mimic the microenviroment *in vivo.*

We can conclude that while MQ-NCSU may be a better substitute for S-PEMs than HD11 cells as the source of membrane proteins. However, fewer than 20% of the cells appeared stained by 3A8 and 4A5, which indicates that an *in vitro* macrophage cell line may not be a good choice as a substitute for S-PEMs.

CHAPTER VI

CONCLUSION

In our first study, we have demonstrated that a single parenteral (s.c.) or mucosal immunization with an anti-cCD40 Mab-guided antigen complex can induce not only a fast and long-lived systemic IgG immune response, but also a rapid local mucosal sIgA response. Specific IgG detected in circulation at an early stage post immunization indicates that the CD40 engagement mimics the biological role of $CD4^+$ T cells by targeting APCs, including B-cells, and further enhancing CD40 downstream signaling and subsequent immunoglobulin class-switching from IgM to IgG. Interestingly, we also observed that an anti-CD40 Mab 2C5-peptide complex was capable of inducing a specific sIgA immune response in tracheal mucosa extracts after a single s.c. injection. This result seems to indicate that a gateway similar as the one that has been described in the common mucosal immune system (CMIS) also exists between systemic (peripheral) and mucosal immunity. We hypothesize that this involves expression of mucosal homing receptor (CCR10) by CD40-activated memory B-cells, which provides capability to migrate to mucosal *effector* sites.

The concept of an anti-cCD40 Mab-guided immunogen complex has great potential as a targeting system for a broad variety of antigenic cargo which can be widely used for immunization of chickens through mucosal and/or parenteral administration when the systemic and mucosal immunity are both highly desirable.

In our second study, we functionally phenotyped the two most frequently used primary macrophage models in chicken: Sephadex-induced – and egg yolk-elicited

peritoneal exudate macrophages (S- and Y-PEMs), using functional phenotype assays and gene expression profiling. This study indicates that certain indicators are considered as "specific" M2 markers in mammals do not behave the same way in chicken. These include arginase activity, gene expression of the SOCS1/STAT3 axis, and SOCS1/SOCS3 ΔCt ratio. Thus, these markers cannot be used in chicken. Discrepancies could be the consequence of phylogenic separation of chickens from mammals about 300 million years ago, but could also be caused the fact that Y-PEMS have to be manipulated by a plastic adherence purification process prior to phenotypical characterization. Plastic adherence can be considered as a pro-inflammatory, M1-polarizing factor. . Our results clearly suggest Sephadex elicitation skews the phenotype of avian macrophages to the M1 phenotype. Despite the conflicting gene expression profiles mentioned above, we do support the view that egg yolk elicitation shifts the avian macrophage phenotype towards the M2 pole, especially when taking into account their low level of iNOS mRNA expression.

In the final study, three new Mabs against S-PEMs were generated. We have identified two candidate antigen molecules, CD110 (a receptor for thrombopoietin) and protocadherin Fat 1, recognized by Mab 3F6 by using a random 7-mer peptide phage display library. In mice, the expression of CXCR4 mRNA (a homing receptor ligand for peripheral lymphoid tissue) was shown to be up-regulated in the presence of Thrombopoietin-CD110 ligation. These results suggest that S-PEMs have the potential to migrate to peripheral lymphoid tissue as APCs in chicken. Despite the inability to delineate conformational epitopes, random 7-mer peptide phage display is a powerful

tool for epitope mapping. We further tested the cross-reactivity of the remaining two Mabs with immortalized chicken macrophage cell lines (HD11 and MQ-NCSU) in order to assess their potential to serve as a surrogate source of macrophage antigens for the further testing. However, only a surprisingly low level of HD11 and MQ-NCSU macrophages were stained with both Mabs, indicating chicken macrophage cell lines have a limited potential to substitute S-PEMs.

The poultry industry needs a new generation of vaccines for the induction of both mucosal and system immunity in a single immunization. The antibody-guided CD40-targeting concept described in this study may provide a new platform that can fit this need.

REFERENCES

Akaki, C., Simazu, M., Baba, T., Tsuji, S., Kodama, H., Mukamoto, M., and Kajikawa, T. (1997). Possible migration of harderian gland immunoglobulin A bearing lymphocytes into the caecal tonsil in chickens. Zentralblatt fur Veterinarmedizin. Reihe B. 44, 199-206.

Ash, D.E., Cox, J.D., and Christianson, D.W. (2000). Arginase: a binuclear manganese metalloenzyme. Metal Ions in Biological Systems 37, 407-428.

Barr, T., Carlring, J., Hatzifoti, C., and Heath, A.W. (2006). Antibodies against cell surface antigens as very potent immunological adjuvants. Vaccine 24 Suppl 2, S2-20-21.

Barr, T.A., Carlring, J., and Heath, A.W. (2005). CD40 antibody as a potent immunological adjuvant: CD40 antibody provides the CD40 signal to B cells, but does not substitute for T cell help in responses to TD antigens. Vaccine 23, 3477-3482.

Barr, T.A., and Heath, A.W. (1999). Enhanced in vivo immune responses to bacterial lipopolysaccharide by exogenous CD40 stimulation. Infection and Immunity 67, 3637-3640.

Barr, T.A., McCormick, A.L., Carlring, J., and Heath, A.W. (2003). A potent adjuvant effect of CD40 antibody attached to antigen. Immunology 109, 87-92.

Barron, L.G., Walzem, R.L., and Hansen, R.J. (1999). Plasma lipoprotein changes in hens (*Gallus domesticus*) during an induced molt. Comparative Biochemistry and Physiology. Part B, Biochemistry & Molecular Biology 123, 9-16.

Bartholdy, C., Kauffmann, S.O., Christensen, J.P., and Thomsen, A.R. (2007). Agonistic anti-CD40 antibody profoundly suppresses the immune response to infection with lymphocytic choriomeningitis virus. Journal of Immunology 178, 1662-1670.

Befus, A.D., Johnston, N., Leslie, G.A., and Bienenstock, J. (1980). Gut-associated lymphoid tissue in the chicken. I. Morphology, ontogeny, and some functional characteristics of Peyer's patches. Journal of Immunology 125, 2626-2632.

Bennett, S.R., Carbone, F.R., Karamalis, F., Flavell, R.A., Miller, J.F., and Heath, W.R. (1998). Help for cytotoxic-T-cell responses is mediated by CD40 signalling. Nature 393, 478-480.

Berghman, L.R., Grauwels, L., Vanhamme, L., Proudman, J.A., Foidart, A., Balthazart, J., and Vandesande, F. (1992). Immunocytochemistry and immunoblotting of avian prolactins using polyclonal and monoclonal antibodies toward a synthetic fragment of chicken prolactin. General and Comparative Endocrinology 85, 346-357.

Bernasconi, N.L., Traggiai, E., and Lanzavecchia, A. (2002). Maintenance of serological memory by polyclonal activation of human memory B cells. Science 298, 2199-2202.

Beug, H., von Kirchbach, A., Doderlein, G., Conscience, J.F., and Graf, T. (1979). Chicken hematopoietic cells transformed by seven strains of defective avian leukemia viruses display three distinct phenotypes of differentiation. Cell 18, 375-390.

Birkholz, K., Schwenkert, M., Kellner, C., Gross, S., Fey, G., Schuler-Thurner, B., Schuler, G., Schaft, N., and Dorrie, J. (2010). Targeting of DEC-205 on human dendritic cells results in efficient MHC class II-restricted antigen presentation. Blood 116, 2277-2285.

Bode, J.G., Nimmesgern, A., Schmitz, J., Schaper, F., Schmitt, M., Frisch, W., Haussinger, D., Heinrich, P.C., and Graeve, L. (1999). LPS and TNFalpha induce SOCS3 mRNA and inhibit IL-6-induced activation of STAT3 in macrophages. FEBS Letters 463, 365-370.

Bowersock, T.L., HogenEsch, H., Suckow, M., Guimond, P., Martin, S., Borie, D., Torregrosa, S., Park, H., and Park, K. (1999). Oral vaccination of animals with antigens encapsulated in alginate microspheres. Vaccine 17, 1804-1811.

Bowersock, T.L., and Martin, S. (1999). Vaccine delivery to animals. Advanced Drug Delivery Reviews 38, 167-194.

Briken, V., and Mosser, D.M. (2011). Editorial: switching on arginase in M2 macrophages. Journal of Leukocyte Biology 90, 839-841.

Callard, R.E., Armitage, R.J., Fanslow, W.C., and Spriggs, M.K. (1993). CD40 ligand and its role in X-linked hyper-IgM syndrome. Immunology Today 14, 559-564.

Canton, J., Neculai, D., and Grinstein, S. (2013). Scavenger receptors in homeostasis and immunity. Nature Reviews. Immunology 13,621-634.

Carlring, J., Altaher, H.M., Clark, S., Chen, X., Latimer, S.L., Jenner, T., Buckle, A.M., and Heath, A.W. (2011). CD154-CD40 interactions in the control of murine B cell hematopoiesis. Journal of Leukocyte Biology 89, 697-706.

Cecilio, C.A., Costa, E.H., Simioni, P.U., Gabriel, D.L., and Tamashiro, W.M. (2011). Aging alters the production of iNOS, arginase and cytokines in murine macrophages. Brazilian Journal of Medical and Biological Research 44, 671-681.

Chang, C.I., Liao, J.C., and Kuo, L. (1998). Arginase modulates nitric oxide production in activated macrophages. The American Journal of Physiology 274, H342-348.

Chen, C.H., Abi-Ghanem, D., Njongmeta, L., Bray, J., Mwangi, W., Waghela, S.D., McReynolds, J.L., Ing, N.H., and Berghman, L.R. (2010a). Production and characterization of agonistic monoclonal antibodies against chicken CD40. Developmental and Comparative Immunology 34, 1139-1143.

Chen, C.H., Abi-Ghanem, D., Waghela, S.D., Chou, W.K., Farnell, M.B., Mwangi, W., and Berghman, L.R. (2012). Immunization of chickens with an agonistic monoclonal anti-chicken CD40 antibody-hapten complex: rapid and robust IgG response induced by a single subcutaneous injection. Journal of Immunological Methods 378, 116-120.

Cheong, C., Choi, J.H., Vitale, L., He, L.Z., Trumpfheller, C., Bozzacco, L., Do, Y., Nchinda, G., Park, S.H., Dandamudi, D.B., et al. (2010). Improved cellular and humoral immune responses in vivo following targeting of HIV Gag to dendritic cells within human anti-human DEC205 monoclonal antibody. Blood 116, 3828-3838.

Chiang, C.S., Chen, F.H., Hong, J.H., Jiang, P.S., Huang, H.L., Wang, C.C., and McBride, W.H. (2008). Functional phenotype of macrophages depends on assay procedures. International Immunology 20, 215-222.

Classen, A., Lloberas, J., and Celada, A. (2009). Macrophage activation: classical versus alternative. Methods in Molecular Biology 531, 29-43.

Corna, G., Campana, L., Pignatti, E., Castiglioni, A., Tagliafico, E., Bosurgi, L., Campanella, A., Brunelli, S., Manfredi, A.A., Apostoli, P., et al. (2010). Polarization

dictates iron handling by inflammatory and alternatively activated macrophages. Haematologica 95, 1814-1822.

Cornax, I., Walzem, R.L., Larner, C., Macfarlane, R.D., and Klasing, K.C. (2013). Mobilization of ectopic yolk in *Gallus gallus domesticus*: a novel reverse lipid transport process. The Journal of Experimental Biology 216, 1949-1958.

Czerkinsky, C., and Holmgren, J. (2012). Mucosal delivery routes for optimal immunization: targeting immunity to the right tissues. Current Topics in Microbiology and Immunology 354, 1-18.

Davis, M.J., Tsang, T.M., Qiu, Y., Dayrit, J.K., Freij, J.B., Huffnagle, G.B., and Olszewski, M.A. (2013). Macrophage M1/M2 polarization dynamically adapts to changes in cytokine microenvironments in *Cryptococcus neoformans* infection. mBio 4, e00264-00213.

Dennehy, P.H., Reisinger, K.S., Blatter, M.M., and Veloudis, B.A. (1991). Immunogenicity of subcutaneous versus intramuscular Oka/Merck varicella vaccination in healthy children. Pediatrics 88, 604-607.

Desai, K.G., and Schwendeman, S.P. (2013). Active self-healing encapsulation of vaccine antigens in PLGA microspheres. Journal of Controlled Release 165, 62-74.

Dickensheets, H., Vazquez, N., Sheikh, F., Gingras, S., Murray, P.J., Ryan, J.J., and Djeraba, A., Musset, E., van Rooijen, N., and Quere, P. (2002). Resistance and susceptibility to Marek's disease: nitric oxide synthase/arginase activity balance. Veterinary Microbiology 86, 229-244.

Donnelly, R.P. (2007). Suppressor of cytokine signaling-1 is an IL-4-inducible gene in macrophages and feedback inhibits IL-4 signaling. Genes and Immunity 8, 21-27.

El Kasmi, K.C., Qualls, J.E., Pesce, J.T., Smith, A.M., Thompson, R.W., Henao-Tamayo, M., Basaraba, R.J., Konig, T., Schleicher, U., Koo, M.S., et al. (2008). Toll-like receptor-induced arginase 1 in macrophages thwarts effective immunity against intracellular pathogens. Nature Immunology 9, 1399-1406.

Fernandes, J.R., and Snider, D.P. (2010). Polymeric IgA-secreting and mucosal homing pre-plasma cells in normal human peripheral blood. International Immunology 22, 527-540.

Fingerut, E., Gutter, B., Meir, R., Eliahoo, D., and Pitcovski, J. (2005). Vaccine and adjuvant activity of recombinant subunit B of *E. coli* enterotoxin produced in yeast. Vaccine 23, 4685-4696.

French, R.R., Chan, H.T., Tutt, A.L., and Glennie, M.J. (1999). CD40 antibody evokes a cytotoxic T-cell response that eradicates lymphoma and bypasses T-cell help. Nature Medicine 5, 548-553.

Freund, N.T., Enshell-Seijffers, D., and Gershoni, J.M. (2009). Phage display selection, analysis, and prediction of B cell epitopes. Current Protocols in Immunology 9, 1-30.

Furlong, R.F. (2005). Insights into vertebrate evolution from the chicken genome sequence. Genome Biology 6, 207-210.

Gaetano, C., Massimo, L., and Alberto, M. (2010). Control of iron homeostasis as a key component of macrophage polarization. Haematologica 95, 1801-1803.

Gallardo-Soler, A., Gomez-Nieto, C., Campo, M.L., Marathe, C., Tontonoz, P., Castrillo, A., and Corraliza, I. (2008). Arginase I induction by modified lipoproteins in macrophages: a peroxisome proliferator-activated receptor-gamma/delta-mediated effect that links lipid metabolism and immunity. Molecular Endocrinology 22, 1394-1402.

Geissmann, F., Manz, M.G., Jung, S., Sieweke, M.H., Merad, M., and Ley, K. (2010). Development of monocytes, macrophages, and dendritic cells. Science 327, 656-661.

Ghosn, E.E., Cassado, A.A., Govoni, G.R., Fukuhara, T., Yang, Y., Monack, D.M., Bortoluci, K.R., Almeida, S.R., Herzenberg, L.A., and Herzenberg, L.A. (2010). Two physically, functionally, and developmentally distinct peritoneal macrophage subsets. Proceedings of the National Academy of Sciences of the United States of America 107, 2568-2573.

Girard, F., Pery, P., Naciri, M., and Quere, P. (1999). Adjuvant effect of cholera toxin on systemic and mucosal immune responses in chickens infected with *E. tenella* or given recombinant parasitic antigen *per os*. Vaccine 17, 1516-1524.

Golemboski, K.A., Whelan, J., Shaw, S., Kinsella, J.E., and Dietert, R.R. (1990). Avian inflammatory macrophage function: shifts in arachidonic acid metabolism, respiratory burst, and cell-surface phenotype during the response to Sephadex. Journal of Leukocyte Biology 48, 495-501.

Gordon, J., and Pound, J.D. (2000). Fortifying B cells with CD154: an engaging tale of many hues. Immunology 100, 269-280.

Gordon, S. (2003). Alternative activation of macrophages. Nature Reviews. Immunology 3, 23-35.

Grewal, I.S., and Flavell, R.A. (1996). A central role of CD40 ligand in the regulation of CD4+ T-cell responses. Immunology Today 17, 410-414.

Hamzah, J., Nelson, D., Moldenhauer, G., Arnold, B., Hammerling, G.J., and Ganss, R. (2008). Vascular targeting of anti-CD40 antibodies and IL-2 into autochthonous tumors enhances immunotherapy in mice. The Journal of Clinical Investigation 118, 1691-1699.

Hatzifoti, C., and Heath, A.W. (2007). CD40-mediated enhancement of immune responses against three forms of influenza vaccine. Immunology 122, 98-106.

He, H., Genovese, K.J., and Kogut, M.H. (2011). Modulation of chicken macrophage effector function by T(H)1/T(H)2 cytokines. Cytokine 53, 363-369.

Hernandez, M.G., Shen, L., and Rock, K.L. (2007). CD40-CD40 ligand interaction between dendritic cells and CD8+ T cells is needed to stimulate maximal T cell responses in the absence of CD4+ T cell help. Journal of Immunology 178, 2844-2852.

Holmgren, J., and Czerkinsky, C. (2005). Mucosal immunity and vaccines. Nature Medicine 11, S45-53.

Idoyaga, J., Lubkin, A., Fiorese, C., Lahoud, M.H., Caminschi, I., Huang, Y., Rodriguez, A., Clausen, B.E., Park, C.G., Trumpfheller, C., and Steinman, R.M. (2011). Comparable T helper 1 (Th1) and CD8 T-cell immunity by targeting HIV gag p24 to CD8 dendritic cells within antibodies to Langerin, DEC205, and Clec9A. Proceedings of the National Academy of Sciences of the United States of America 108, 2384-2389.

Iwasaki, A. (2007). Mucosal dendritic cells. Annual Review of Immunology 25, 381-418.

Jeurissen, S.H., Janse, E.M., Koch, G., and de Boer, G.F. (1988). The monoclonal antibody CVI-ChNL-68.1 recognizes cells of the monocyte-macrophage lineage in chickens. Developmental and Comparative Immunology 12, 855-864.

Kakhlon, O., and Cabantchik, Z.I. (2002). The labile iron pool: characterization, measurement, and participation in cellular processes (1). Free Radical Biology & Medicine 33, 1037-1046.

Kaspers, B., Lillehoj, H.S., and Lillehoj, E.P. (1993). Chicken macrophages and thrombocytes share a common cell surface antigen defined by a monoclonal antibody. Veterinary Immunology and Immunopathology 36, 333-346.

Katz, A., Waridel, P., Shevchenko, A., and Pick, U. (2007). Salt-induced changes in the plasma membrane proteome of the *halotolerant alga Dunaliella salina* as revealed by blue native gel electrophoresis and nano-LC-MS/MS analysis. Molecular & Cellular Proteomics 6, 1459-1472.

Kawamoto, T., Sasajima, J., Sugiyama, Y., Nakamura, K., Tanabe, H., Fujiya, M., Nata, T., Iuchi, Y., Ashida, T., Torimoto, Y., et al. (2013). *Ex vivo* activation of angiogenic property in human peripheral blood-derived monocytes by thrombopoietin. International Journal of Hematology 6, 111-122.

Khallou-Laschet, J., Varthaman, A., Fornasa, G., Compain, C., Gaston, A.T., Clement, M., Dussiot, M., Levillain, O., Graff-Dubois, S., Nicoletti, A., and Caligiuri, G. (2010). Macrophage plasticity in experimental atherosclerosis. PloS One 5, 1-10.

Khong, A., Nelson, D.J., Nowak, A.K., Lake, R.A., and Robinson, B.W. (2012). The use of agonistic anti-CD40 therapy in treatments for cancer. International Reviews of Immunology 31, 246-266.

Klasing, K.C. (1998). Avian macrophages: regulators of local and systemic immune responses. Poultry Science 77, 983-989.

Knuf, M., Zepp, F., Meyer, C.U., Habermehl, P., Maurer, L., Burow, H.M., Behre, U., Janssens, M., Willems, P., Bisanz, H., et al. (2010). Safety, immunogenicity and immediate pain of intramuscular versus subcutaneous administration of a measles-mumps-rubella-varicella vaccine to children aged 11-21 months. European Journal of Pediatrics 169, 925-933.

Kolaskar, A.S., and Tongaonkar, P.C. (1990). A semi-empirical method for prediction of antigenic determinants on protein antigens. FEBS Letters 276, 172-174.

Kothlow, S., Morgenroth, I., Tregaskes, C.A., Kaspers, B., and Young, J.R. (2008). CD40 ligand supports the long-term maintenance and differentiation of chicken B cells in culture. Developmental and Comparative Immunology 32, 1015-1026.

Krause, S.W., Kreutz, M., and Andreesen, R. (1996). Differential effects of cell adherence on LPS-stimulated cytokine production by human monocytes and macrophages. Immunobiology 196, 522-534.

Li, F., and Ravetch, J.V. (2011). Inhibitory Fcgamma receptor engagement drives adjuvant and anti-tumor activities of agonistic CD40 antibodies. Science 333, 1030-1034.

Linghua, Z., Xingshan, T., and Fengzhen, Z. (2007). Vaccination with Newcastle disease vaccine and CpG oligodeoxynucleotides induces specific immunity and protection against Newcastle disease virus in SPF chicken. Veterinary Immunology and Immunopathology 115, 216-222.

Liu, G., Xia, X.P., Gong, S.L., and Zhao, Y. (2006). The macrophage heterogeneity: difference between mouse peritoneal exudate and splenic F4/80+ macrophages. Journal of Cellular Physiology 209, 341-352.

Liu, Q., Zheng, J., Yin, D.D., Xiang, J., He, F., Wang, Y.C., Liang, L., Qin, H.Y., Liu, L., Liang, Y.M., and Han, H. (2012). Monocyte to macrophage differentiation-associated (MMD) positively regulates ERK and Akt activation and TNF-alpha and NO production in macrophages. Molecular Biology Reports 39, 5643-5650.

Louis, C.A., Reichner, J.S., Henry, W.L., Jr., Mastrofrancesco, B., Gotoh, T., Mori, M., and Albina, J.E. (1998). Distinct arginase isoforms expressed in primary and transformed macrophages: regulation by oxygen tension. The American Journal of Physiology 274, R775-782.

Macpherson, A.J., McCoy, K.D., Johansen, F.E., and Brandtzaeg, P. (2008). The immune geography of IgA induction and function. Mucosal Immunology 1, 11-22.

Mantovani, A., Biswas, S.K., Galdiero, M.R., Sica, A., and Locati, M. (2013). Macrophage plasticity and polarization in tissue repair and remodelling. The Journal of Pathology 229, 176-185.

Martinez, F.O., Helming, L., and Gordon, S. (2009). Alternative activation of macrophages: an immunologic functional perspective. Annual Review of Immunology 27, 451-483.

Mast, J., Goddeeris, B.M., Peeters, K., Vandesande, F., and Berghman, L.R. (1998). Characterisation of chicken monocytes, macrophages and interdigitating cells by the monoclonal antibody KUL01. Veterinary Immunology and Immunopathology 61, 343-357.

Mei, H.E., Yoshida, T., Sime, W., Hiepe, F., Thiele, K., Manz, R.A., Radbruch, A., and Dorner, T. (2009). Blood-borne human plasma cells in steady state are derived from mucosal immune responses. Blood 113, 2461-2469.

Mencacci, A., Cenci, E., Boelaert, J.R., Bucci, P., Mosci, P., Fe d'Ostiani, C., Bistoni, F., and Romani, L. (1997). Iron overload alters innate and T helper cell responses to Candida albicans in mice. The Journal of Infectious Diseases 175, 1467-1476.

Mestecky, J. (1987). The common mucosal immune system and current strategies for induction of immune responses in external secretions. Journal of Clinical Immunology 7, 265-276.

Moeller, M.J., Soofi, A., Braun, G.S., Li, X., Watzl, C., Kriz, W., and Holzman, L.B. (2004). Protocadherin FAT1 binds Ena/VASP proteins and is necessary for actin dynamics and cell polarization. The EMBO Journal 23, 3769-3779.

Monson, N.L., Foster, S.J., Brezinschek, H.P., Brezinschek, R.I., Dorner, T., and Lipsky, P.E. (2001). The role of CD40-CD40 ligand (CD154) interactions in immunoglobulin light chain repertoire generation and somatic mutation. Clinical Immunology 100, 71-81.

Mora, J.R., and von Andrian, U.H. (2008). Differentiation and homing of IgA-secreting cells. Mucosal Immunology 1, 96-109.

Morris, S.M., Jr., Kepka-Lenhart, D., and Chen, L.C. (1998). Differential regulation of arginases and inducible nitric oxide synthase in murine macrophage cells. The American Journal of Physiology 275, E740-747.

Muir, W.I., Bryden, W.L., and Husband, A.J. (2000). Immunity, vaccination and the avian intestinal tract. Developmental and Comparative Immunology 24, 325-342.

Mullner, N., Lazar, A., and Hrabak, A. (2002). Enhanced utilization and altered metabolism of arginine in inflammatory macrophages caused by raised nitric oxide synthesis. The International Journal of Biochemistry & Cell Biology 34, 1080-1090.

Munder, M. (2009). Arginase: an emerging key player in the mammalian immune system. British Journal of Pharmacology 158, 638-651.

Murray, P.J., and Wynn, T.A. (2011a). Obstacles and opportunities for understanding macrophage polarization. Journal of Leukocyte Biology 89, 557-563.

Murray, P.J., and Wynn, T.A. (2011b). Protective and pathogenic functions of macrophage subsets. Nature Reviews. Immunology 11, 723-737.

Neutra, M.R., and Kozlowski, P.A. (2006). Mucosal vaccines: the promise and the challenge. Nature reviews. Immunology 6, 148-158.

Nili, H., and Kelly, W.R. (1996). In vitro responses of avian monocytes to homologous yolk. The Anatomical Record 246, 458-464.

Noelle, R.J. (1996). CD40 and its ligand in host defense. Immunity 4, 415-419.

Omara, F.O., and Blakley, B.R. (1994). The effects of iron deficiency and iron overload on cell-mediated immunity in the mouse. The British Journal of Nutrition 72, 899-909.

Pan, C., Kumar, C., Bohl, S., Klingmueller, U., and Mann, M. (2009). Comparative proteomic phenotyping of cell lines and primary cells to assess preservation of cell type-specific functions. Molecular & Cellular Proteomics 8, 443-450.

Parker, J.M., Guo, D., and Hodges, R.S. (1986). New hydrophilicity scale derived from high-performance liquid chromatography peptide retention data: correlation of predicted surface residues with antigenicity and X-ray-derived accessible sites. Biochemistry 25, 5425-5432.

Platt, N., and Gordon, S. (2001). Is the class A macrophage scavenger receptor (SR-A) multifunctional? - The mouse's tale. The Journal of Clinical Investigation 108, 649-654.

Qin, H., Yeh, W.I., De Sarno, P., Holdbrooks, A.T., Liu, Y., Muldowney, M.T., Reynolds, S.L., Yanagisawa, L.L., Fox, T.H., 3rd, Park, K., et al. (2012). Signal transducer and activator of transcription-3/suppressor of cytokine signaling-3 (STAT3/SOCS3) axis in myeloid cells regulates neuroinflammation. Proceedings of the National Academy of Sciences of the United States of America 109, 5004-5009.

Qureshi, M.A., Heggen, C.L., and Hussain, I. (2000). Avian macrophage: effector functions in health and disease. Developmental and Comparative Immunology 24, 103-119.

Qureshi, M.A., and Miller, L. (1991). Signal requirements for the acquisition of tumoricidal competence by chicken peritoneal macrophages. Poultry Science 70, 530-538.

Qureshi, M.A., Miller, L., Lillehoj, H.S., and Ficken, M.D. (1990). Establishment and characterization of a chicken mononuclear cell line. Veterinary Immunology and Immunopathology 26, 237-250.

Qureshi, N., Perera, P.Y., Shen, J., Zhang, G., Lenschat, A., Splitter, G., Morrison, D.C., and Vogel, S.N. (2003). The proteasome as a lipopolysaccharide-binding protein in macrophages: differential effects of proteasome inhibition on lipopolysaccharide-induced signaling events. Journal of Immunology 171, 1515-1525.

Rauw, F., Gardin, Y., Palya, V., Anbari, S., Gonze, M., Lemaire, S., van den Berg, T., and Lambrecht, B. (2010). The positive adjuvant effect of chitosan on antigen-specific cell-mediated immunity after chickens vaccination with live Newcastle disease vaccine. Veterinary Immunology and Immunopathology 134, 249-258.

Ravn, P., Stahn, R., Danielczyk, A., Faulstich, D., Karsten, U., and Goletz, S. (2007). The Thomsen-Friedenreich disaccharide as antigen for in vivo tumor targeting with multivalent scFvs. Cancer Immunology, Immunotherapy 56, 1345-1357.

Recalcati, S., Locati, M., Marini, A., Santambrogio, P., Zaninotto, F., De Pizzol, M., Zammataro, L., Girelli, D., and Cairo, G. (2010). Differential regulation of iron homeostasis during human macrophage polarized activation. European Journal of Immunology 40, 824-835.

Sabet, T., Wen-Cheng, H., Stanisz, M., El-Domeiri, A., and Van Alten, P. (1977). A simple method for obtaining peritoneal macrophages from chickens. Journal of Immunological Methods 14, 103-110.

Sachithanandan, N., Graham, K.L., Galic, S., Honeyman, J.E., Fynch, S.L., Hewitt, K.A., Steinberg, G.R., and Kay, T.W. (2011). Macrophage deletion of SOCS1 increases sensitivity to LPS and palmitic acid and results in systemic inflammation and hepatic insulin resistance. Diabetes 60, 2023-2031.

Segerer, S.E., Martignoni, F., Bogdan, A., Muller, N., Kapp, M., Dietl, J., Rieger, L., and Kammerer, U. (2013). Thrombopoietin modulates the proliferation, migration and cytokine profile of decidual cell subsets during early gestation. Molecular Human Reproduction 19, 361-368.

Selvarajan, K., Moldovan, L., Chandrakala, A.N., Litvinov, D., and Parthasarathy, S. (2011). Peritoneal macrophages are distinct from monocytes and adherent macrophages. Atherosclerosis 219, 475-483.

Shevchenko, A., Tomas, H., Havlis, J., Olsen, J.V., and Mann, M. (2006). In-gel digestion for mass spectrometric characterization of proteins and proteomes. Nature Protocols 1, 2856-2860.

Sica, A., and Mantovani, A. (2012). Macrophage plasticity and polarization: in vivo veritas. The Journal of Clinical Investigation 122, 787-795.

Singh, H., Ansari, H.R., and Raghava, G.P. (2013). Improved method for linear B-cell epitope prediction using antigen's primary sequence. PloS One 8, 1-8.

Smialek, M., Tykalowski, B., Stenzel, T., and Koncicki, A. (2011). Local immunity of the respiratory mucosal system in chickens and turkeys. Polish Journal of Veterinary Sciences 14, 291-297.

Smith, C.K., Kaiser, P., Rothwell, L., Humphrey, T., Barrow, P.A., and Jones, M.A. (2005). *Campylobacter jejuni*-induced cytokine responses in avian cells. Infection and Immunity 73, 2094-2100.

Stempin, C.C., Dulgerian, L.R., Garrido, V.V., and Cerban, F.M. (2010). Arginase in parasitic infections: macrophage activation, immunosuppression, and intracellular signals. Journal of Biomedicine & Biotechnology 2010, 683485.

Stout, R.D., Jiang, C., Matta, B., Tietzel, I., Watkins, S.K., and Suttles, J. (2005). Macrophages sequentially change their functional phenotype in response to changes in microenvironmental influences. Journal of Immunology 175, 342-349.

Stout, R.D., and Suttles, J. (2004). Functional plasticity of macrophages: reversible adaptation to changing microenvironments. Journal of Leukocyte Biology 76, 509-513.

Tacke, F., and Randolph, G.J. (2006). Migratory fate and differentiation of blood monocyte subsets. Immunobiology 211, 609-618.

Tanoue, T., and Takeichi, M. (2005). New insights into Fat cadherins. Journal of Cell Science 118, 2347-2353.

Tel, J., Benitez-Ribas, D., Hoosemans, S., Cambi, A., Adema, G.J., Figdor, C.G., Tacken, P.J., and de Vries, I.J. (2011). DEC-205 mediates antigen uptake and presentation by both resting and activated human plasmacytoid dendritic cells. European Journal of Immunology 41, 1014-1023.

Tenbusch, M., Nchinda, G., Storcksdieck genannt Bonsmann, M., Temchura, V., and Uberla, K. (2013). Targeting the antigen encoded by adenoviral vectors to the DEC205

receptor modulates the cellular and humoral immune response. International Immunology 25, 247-258.

Trembicki, K.A., Qureshi, M.A., and Dietert, R.R. (1986). Monoclonal antibodies reactive with chicken peritoneal macrophages: identification of macrophage heterogeneity. Proceedings of the Society for Experimental Biology and Medicine. Society for Experimental Biology and Medicine 183, 28-41.

Turchyn, L.R., Baginski, T.J., Renkiewicz, R.R., Lesch, C.A., and Mobley, J.L. (2007). Phenotypic and functional analysis of murine resident and induced peritoneal macrophages. Comparative Medicine 57, 574-580.

van Kooten, C., and Banchereau, J. (2000). CD40-CD40 ligand. Journal of Leukocyte Biology 67, 2-17.

von Bergwelt-Baildon, M., Shimabukuro-Vornhagen, A., Popov, A., Klein-Gonzalez, N., Fiore, F., Debey, S., Draube, A., Maecker, B., Menezes, I., Nadler, L.M., and Schultze, J.L. (2006). CD40-activated B cells express full lymph node homing triad and induce T-cell chemotaxis: potential as cellular adjuvants. Blood 107, 2786-2789.

Vonderheide, R.H., and Glennie, M.J. (2013). Agonistic CD40 antibodies and cancer therapy. Clinical Cancer Research 19, 1035-1043.

Walzem, R.L., Davis, P.A., and Hansen, R.J. (1994). Overfeeding increases very low density lipoprotein diameter and causes the appearance of a unique lipoprotein particle in association with failed yolk deposition. Journal of Lipid Research 35, 1354-1366.

Weiss, G., Bogdan, C., and Hentze, M.W. (1997). Pathways for the regulation of macrophage iron metabolism by the anti-inflammatory cytokines IL-4 and IL-13. Journal of Immunology 158, 420-425.

Whyte, C.S., Bishop, E.T., Ruckerl, D., Gaspar-Pereira, S., Barker, R.N., Allen, J.E., Rees, A.J., and Wilson, H.M. (2011). Suppressor of cytokine signaling (SOCS)1 is a key determinant of differential macrophage activation and function. Journal of Leukocyte Biology 90, 845-854.

Woodrow, K.A., Bennett, K.M., and Lo, D.D. (2012). Mucosal vaccine design and delivery. Annual Review of Biomedical Engineering 14, 17-46.